Scholars' Mine

Doctoral Dissertations

Student Theses and Dissertations

1971

A measurement of complex viscosity with large amplitudes

Kuo-Shein Shen

Recommended Citation

A MEASUREMENT OF COMPLEX VISCOSITY

WITH LARGE AMPLITUDES

by

KUO-SHEIN SHEN, 1939-

A DISSERTATION

Presented to the Faculty of the Graduate School of the

UNIVERSITY OF MISSOURI-ROLLA

In Partial Fulfillment of the Requirements for the Degree
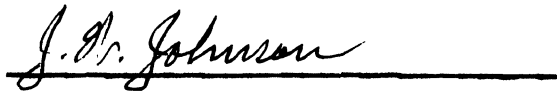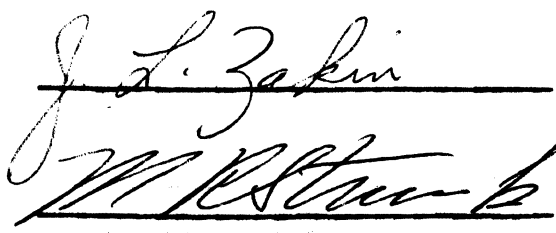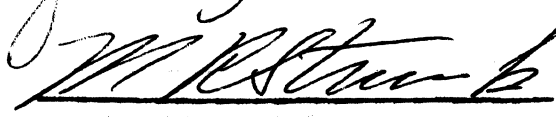
DOCTOR OF PHILOSOPHY

in

CHEMICAL ENGINEERING

1971
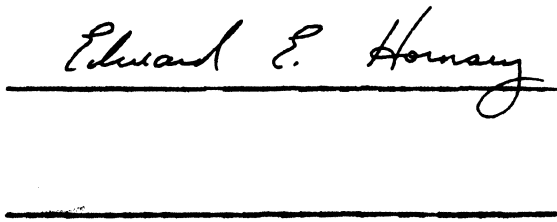
Advisor

ABSTRACT

In order to study the viscoelastic properties of polymer solutions and greases, a dynamic apparatus was built for making measurements of complex viscosity. Characteristic impedance was measured by a force transducer, an accelerometer and a phase meter. Large amplitudes to 0.5 inch can be obtained with this apparatus. The largest amplitude used was 1.27×10^{-1} cm. The frequency range was 30 Hz - 1500 Hz. The lowest dynamic viscosity to be measured was 0.5 poise.

In order to determine the capabilities of the instrument, complex viscosities of polymer solutions and greases were measured. The polymer solutions studied were polyisobutylene (PIB) L-80*, PIB L-200*, and polydimethyl siloxane (SR) 130**. Comparisons of results for NLGI System A grease and Mobilgrease 24 showed that at the same level of dynamic viscosity the NLGI grease had twice the elastic response of Mobilgrease. For NLGI grease about 60% of the total energy input was dissipated under the experimental conditions. About 80% of the total energy input was dissipated for Mobilgrease 24.

---

* Enjay Vistanex

** General Electric

Comparing the shapes of curves for the steady shear viscosity vs. shear rate with the dynamic viscosity vs. frequency for PIB L-80 (3 g/dl and 5 g/dl), there was a trend toward agreement of η and η' at vanishingly small values of γ and ω. For 17% solution of NLGI grease and a 25% solution of Mobilgrease 24, η' and η only have similar shapes. η' and η can be shifted into coincidence along the γ - ω axis with shift factor of 2.

The dependence of complex viscosity on amplitude was investigated for the 5 g/dl PIB L-80 solution. Both η' and η'' decrease with increasing amplitude when amplitude is beyond a limit; the η'' was more sensitive to amplitude. That means the dynamic storage modulus data are more critical than dynamic viscosity data in determining the limitation on amplitude for linear viscoelasticity. For instance, when shear wave length equaled 1.5 cm, the limitation on shear strain for linear viscoelasticity was 9.5% for the PIB L-80 solution.

ACKNOWLEDGEMENTS

TABLE OF CONTENTS

Table of Contents (continued)   Page

LIST OF FIGURES

List of Figures (continued)

List of Figures (continued)

List of Figures (continued)

LIST OF TABLES

I. INTRODUCTION

From the measurements of viscoelastic properties of polymers, information can be obtained about the nature and the rates of the configurational rearrangements. It also has practical importance in application of rubbers, plastics, and fibers.

Much work has been done in the development of instruments that measure complex moduli of viscolastic materials at infinitesimal shear strains. There is a need for more measurements at finite shear strains. According to the theory of linear viscoelasticity, the complex viscosity is dependent only on frequency when strain is small. It is important, both from theoretical considerations and from a practical standpoint, to determine the limitation of the strain, below which linear viscoelasticity is valid.

II. REVIEW OF LITERATURE

A. Viscoelastic Phenomena

A viscoelastic material exhibits behavior which combines liquidlike and solidlike characteristics. When such a body is constrained at constant deformation, the stress required to hold it diminishes gradually (relaxation). Also, it does not maintain a constant deformation under constant stress but goes on slowly deforming with time (creeping). If a sinusoidally oscillating stress is imposed on such material, the strain is neither exactly in phase with the stress (as it would be for a perfectly elastic solid) or 90° out of phase (as it would be for a perfectly viscous liquid), but is somewhere in between. Some of the energy input is stored and recovered in each cycle, and some is dissipated as heat.

1. Concept of the complex modulus[1]

If a linear viscoelastic material is subjected to sinusoidally varing stress of a given frequency, its response will be a sinusoidal strain of the same frequency which lags the stress by a phase angle, $\emptyset$. In such a case, the strain is related to the stress by a complex number which is a function of frequency and which may be called the complex modulus of the material. The absolute value of this complex number is given by the ratio of amplitude of the

stress to that of the strain, while its phase is given by the angle by which the stress leads the strain.

If the stress is divided into two components, one in-phase with the strain and one 90 degrees out-of phase, then the ratio of the amplitude of the in-phase component of the stress to the amplitude of the strain gives the real part of the complex modulus, and the other gives the imaginary part of the modulus. Since the response of an elastic element is completely in-phase with the stress, and since the response of a viscous element is 90 degrees out-of-phase with the stress, the real part of the complex modulus is a measure of the elasticity of the material, while the imaginary part is a measure of its viscosity.

Let an alternating stress $\gamma = \gamma_0 \sin \omega t$ be applied to a linear viscoelastic material whose complex modulus is denoted by G^*. The response of the material will be an alternating strain $\gamma = \gamma_0 \sin (\omega t - \phi)$, where γ_0 and ϕ are determined uniquely by γ and G^*. Let $G^* = G' + iG''$. Then, by definition

$$|G^*| = \gamma_0/\gamma_0 \tag{1}$$

$$G' = (\gamma_0/\gamma_0)\cos \phi \tag{2}$$

$$G'' = (\gamma_0/\gamma_0)\sin \phi \tag{3}$$

$$\phi = \tan^{-1} \frac{G''}{G'} \tag{4}$$

The important consideration is that, given the complex modulus of a material as a function of frequency, the material's response to sinusoidal stress of a given frequency is completely determined, since both its amplitude and its phase angle at the frequency are easily found. The material is considered to be linearly viscoelastic if G^* is not a function of γ.

2. Molecular theories

Most treatments have dealt with very dilute solutions in which the polymer molecules are supposed to be isolated. Such a molecule, surrounded and pervaded by solvent, is continually rearranging its configuration by random motions. The driving force for these Brownian motions is the thermal energy. They are opposed by viscous forces involving the hydrodynamic resistance to the solvent and intramolecular steric effects which are usually referred to as internal viscosity. The assortment of configurations and the rates or configurational change are only slightly disturbed by the application of an external shear stress if the latter is small enough to correspond to the usual restrictions of linear viscoelastic behavior : the Brownian motion goes on just the same.

The complete specification of configuration requires a more detailed knowledge of the dimensions and shapes of the monomeric units, local packing effects, and interactions

with the solvent molecules than can in practice be available - and at the same time be tractable. A valuable simplification can be made if one is willing to sacrifice consideration of short-range relationships and attendant behavior at the very highest frequencies. One utilizes the prediction from polymer chain statistics that any two points on the chain backbone separated by 50 or more chain atoms will be related to each other in space in accordance with a Gaussian distribution of vectors[2,3]. In the absence of external forces, the form of this distribution holds regardless of the bond distances and angles, local packing effects, interaction with solvents, and other hindrances to free rotation, all of which enter only into a proportionality constant with dimensions of length[4]. Thus the root-mean-square distance between two points separated by N chain bonds ($N>50$) is $r = a\sqrt{N}$, where a depends on local geometric parameters and is generally of the order of several times the length of a single chain bond[2].

The statistical theory of rubberlike elasticity shows that the fluctuations in length of such a chain segment cause it to act like a Hooke's spring with spring constant $3KT/Na^2$. When a dilute polymer solution is subjected to a shearing stress, the flowing solvent distorts the molecules so that the assortment of vectors between two chain atoms N units apart is slightly perturbed from a Gaussian distribution. The Brownian motion will result in a diffusion back

to approach this distribution, however, and the visco-
elastic behavior is determined by the interaction between
these two effects.

In both Rouse's theory and Zimm's theory the above
model was used. For Rouse's treatment, the hydrodynamic
interaction between the motions of submolecule junctions
was ignored. A velocity gradient in a solution of linear
polymer produced motions of the polymer molecules which were
resolved into two components: (1) a motion of the atom at
each junction between two submolecules with a velocity equal
to that of surrounding liquid, and (2) the coordinated
Brownian motions of the segments of each polymer molecule by
which the configurations drift toward their equilibrium
Gaussian distribution. Based on the change in free energy
associated with the entropy decrease for non-random con-
figurations and the tendency of the system to diffuse toward
a random state, the energy dissipation and storage in sinu-
soidally oscillating deformations were calculated, and the
complex viscosity can be obtained as

$$\eta' = \eta_s + \frac{6(\eta_0 - \eta_s)}{\pi^2} \sum_{p=1}^{N} \frac{1}{p^2 + \omega^2 \gamma_1^2} \tag{5}$$

$$\eta'' = \frac{6(\eta_0 - \eta_s)}{\pi^2} \sum_{p=1}^{N} \frac{\omega}{p^2 + \omega^2 \gamma_1^2} \tag{6}$$

where

η_s = viscosity of the solvent

η_o = steady state viscosity of the solution

$$\mathcal{T}_1 = \frac{6\,(\eta_o - \eta_s)M}{\pi^2\,CRT}$$

M = molecular weight of polymer

C = concentration in g/cc

In the theory of Zimm, the force on each bead is calculated as the sum of the hydrodynamic drag force by the solvent, the force associated with the Brownian motion, and the Hookean spring-like forces exerted by the two neighboring submolecules. Inertial forces are neglected. The contribution of the solute to the shear stress for oscillation deformations was derived. He examined two limiting cases, one corresponding to vanishing hydrodynamic interaction (the freely drained coil) and one corresponding to dominant hydrodynamic interaction. For vanishing hydrodynamic interaction Zimm found the same result as Rouse's theory. For the dominant hydrodynamic interaction case, he got

$$\mathcal{T}_1 = \frac{M(\eta_o - \eta_s)}{2.369\,CRT} \tag{7}$$

A solution for partial hydrodynamic interaction was obtained by Tschoegl[7]. He used a parameter h for varying the degree of hydrodynamic interaction. Then, with h = 0, the relaxation times of the Rouse theory were obtained; with h = ∞, the relaxation time of the Zimm theory was obtained.

3. Constitutive equations for viscoelastic fluids

The central problem in engineering rheology is that of finding explicit constitutive equations, for non-linear as well as linear behavior, with a small number of constants to correlate the variety of viscous and elastic phenomena. These equations could be based either on molecular or continuum theories. Two general classes of equations have met with some success. The first is the "rate equation", which is a constitutive equation in which time rates of change of stress and deformation appear. The second class of constitutive equations is the "integral equation".

a. Rate equations

One of the more successful rate type equations was due to Spriggs[8], which was motivated by the generalized Maxwell model, Oldroyd's studies of convected derivatives[9,10], and the results of certain molecular theories[5,6]. The following equations were obtained.

$$\overline{\overline{\tau}} = \sum_{p=1}^{\infty} \overline{\overline{\tau}}_p \tag{8}$$

$$\overline{\overline{\tau}}_p + \lambda_p \overline{\overline{\tau}}_{\frac{p}{2}} = \frac{y_o}{p\, Z(\alpha)}\, \overline{\overline{\gamma}} \tag{9}$$

where

$\overline{\overline{\gamma}}$ is the rate of deformation tensor

$\overline{\overline{\tau}}$ is the stress tensor

$\overline{\tau}$ is a convected derivative given by Spriggs as

$$\mathcal{H} \, \mathcal{T}_{ik} = \frac{\mathcal{D} \mathcal{T}_{ik}}{\mathcal{D} t} + \frac{1 + \varepsilon}{2} \left(\mathcal{T}_{ij} \, \gamma_{jk} + \mathcal{T}_{ik} \, \gamma_{ij} + \frac{1}{3} \mathcal{T}_{jm} \, \gamma_{jm} \, \delta_{ik} \right) \tag{10}$$

and $\mathcal{D}/\mathcal{D}t$ is the Jauman derivative, ε is an adjustable constant, and λ_p are relaxation times.

$$Z(\alpha) = \sum_{p=1}^{\infty} p^{-\alpha}$$

Instead of an infinite set of unknown relaxation times, λ_p, molecular theory was used to suggest an empirical expression for the λ_p in terms of only two adjustable constants, with the result

$$\lambda_p = \lambda \, p^{-\alpha} \tag{11}$$

where p is an integer.

From the work of Spriggs the dynamic viscosity can be obtained,

$$\frac{\eta'}{\eta_0} = \frac{1}{Z(\alpha)} \sum_{p=1}^{\infty} \frac{p^{\alpha}}{p^2 + (\lambda \omega)^2} \tag{12}$$

$$\frac{\eta''}{\eta_0} = \frac{\lambda \omega}{Z(\alpha)} \sum_{p=1}^{\infty} \frac{1}{p^2 + (\lambda \omega)^2} \tag{13}$$

One way to test the constitutive equation is to compare calculated values of η' and η'' with experimental results.

b. **Integral equations**

As yet it is not apparent that constitutive equations written as integral representations offer any better

description of real material response than rate equations. The major advantage of integral theories is that they are explicit in stress; if the deformation history is given, the stress follows immediately upon an integration of the form

$$\text{Stress} = \int_{-\infty}^{t} (\text{relaxation function})(\text{strain history})dt'$$

(14)

This proceducer is simpler to perform than that which would be required with rate theories, the more realistic of which often require solution of simultaneous differential equations.

Bernstein, Kearsley, and Zapas[11] have developed an elastic fluid integral theory. The BKZ theory takes the form

$$\overline{\overline{\tau}} = \int_{-\infty}^{t} \left[\mu_1 (t-t') \overline{\overline{C}} + \mu_2 (t-t') \overline{\overline{C}}^{-1} \right] dt'$$

(15)

where μ_1 and μ_2 are unspecified scalar functions of time, and possibly of the invariants of $\overline{\overline{C}}$ and $\overline{\overline{C}}^{-1}$, and play the role of a relaxation function. The deformation tensors $\overline{\overline{C}}$ and $\overline{\overline{C}}^{-1}$ are taken with respect to the present time as the reference configuration. Since μ_1 and μ_2 are generally empirical in nature, the BKZ theory is a continuum theory.

The BKZ theory is illustrated best by the study of

Zapas and Craft[12]. It seems to be quite successful in describing both the behavior of rubbery elastomers in creep and elongation experiments, and the non-Newtonian viscosity of polymer solutions. More complete experimental studies will be required, such as dynamic viscosity, normal stress difference, etc., before it is possible to argue in favor of the BKZ theory as a constitutive equation applicable to polymer solutions and melts over a wide range of shear rates.

Since the BKZ theory is not easy to use, Tanner[13] developed the network rupture hypotheses based on Lodge's[14,15] theory. He adopted the following simple criterion for network rupture in flowing solutions. Rupture was supposed to occur when

$$\text{tr } \bar{\bar{S}} = (1 + 2\beta)B^2 \tag{16}$$

where tr $\bar{\bar{S}}$ is the sum of the principal strains, B is a number expected to be of order 10 and which is probably temperature and rate dependent, and β is a constant which equals normal stress ratio in simple shearing.

The following equation was obtained after the rupture criterion was applied to the Lodge constitutive equation:

$$\bar{\bar{\mathcal{T}}} = \int_{t-\mathcal{T}_R}^{t} N(t - t')\bar{\bar{S}}(t')dt' \tag{17}$$

where $\mathcal{T}_R = B/\gamma$ and $\bar{\bar{S}} = (1 + \beta)\bar{\bar{C}}^{-1} + \beta\bar{\bar{C}}$
The function $N(t - t')$ governs the response to a small sinusoidal shear strain, from such tests $N(t - t')$ can easily be

found[16]. Usually a sum of exponentials is considered to be a sufficiently accurate approximation for N. With discrete time constants, λ_n, the form

$$N(\tau) = \Sigma \frac{a_n}{\lambda_n} e^{-\tau/\lambda_n} + \eta_\infty \delta'(\tau) \tag{18}$$

may be used. The a_n and λ_n may be assigned in terms of the Rouse or Zimm theory if desired[17]. η_∞ is the limiting viscosity at very high shear rates. $\delta'(\tau)$ is the formal derivative of the delta function[18].

For polyisobutylene-cetane solutions very good prediction of steady shearing viscosity was obtained starting from the measured dynamical response to small sinusoidal strains up to the critical strain magnitude. Normal stress effects were also well represented. The dynamic viscosity takes the well known form

$$\eta' = \eta_\infty + \Sigma_n \frac{a_n}{(1 + \lambda_n^2 \omega^2)} \tag{19}$$

The network rupture theory is based on molecular considerations which may give more confidence in predictions for complex flows. More complete reviews of constitutive equations were given by Bogue and Doughty[19], and by Spriggs, Huppler and Bird[20].

4. **Relationship of steady shear to dynamic properties**

Philippoff[21] made a comparison of steady-flow measure-

ments. He found the steady-state value determined by the flow curve at the same rate of shear always has a higher shear stress than any of the dynamic curves. This means that the steady-shear viscosity is always larger than the dynamic viscosity at same rate of shear.

Some continuum theories predict relationships among the steady and dynamic coefficients. The general Coleman-Noll[22,23] theory predicted the following relationships between steady shear and dynamic coefficients:

$$\eta_0 = \lim_{\omega \to 0} \frac{G''}{\omega} = \lim_{\omega \to 0} \eta' \tag{20}$$

$$\psi_{12}^{(o)} = \lim_{\omega \to 0} 2G'/\omega^2 = \lim_{\omega \to 0} 2\eta''/\omega \tag{21}$$

where η_0 is the zero shear viscosity

$\psi_{12}^{(o)}$ is the zero shear normal stress coefficient

Other predictions were made by the continuum theory of Spriggs[8], which suggests that

$$\eta(\dot{\gamma}) = \eta'(c\omega) = G''(c\omega)/c\omega \tag{22}$$

$$\psi_{12}(\dot{\gamma}) = 2\eta''(c\omega)/c\omega = 2G'(c\omega)/(c\omega)^2 \tag{23}$$

without any restriction to vanishingly small values of $\dot{\gamma}$ or ω. c is a "shift factor", and equation 22 states that η and η' have the same shape but are shifted with respect

to each other, along the $\gamma - \omega$ axis by the factor c.

Osaki[24] has made some comparisons between steady shear and dynamic shear behavior of a solution of polybutadiene. The agreement with Sprigg's prediction was excellent for both sets of functions. No shift factor was required. A similar comparison of data for polymethyl methacrylate solution was made also by Osaki. The curves cannot be shifted into coincidence, and equations 22 and 23 are clearly refuted. The trend of data, as γ and ω decrease, was toward agreement with equations 20 and 21, but insufficient low shear data are availiable for firm confirmation.

Lamb[25] also obtained a relation between the steady and dynamic properties from the Maxwell model. The results were the same as equations 22 and 23. Good agreement was found for concentrated solutions of polyvinyl alcohol with $c \approx 1$ for values of η'/η_0 from unity down to 0.2. For solutions of polyisobutylene[27] in decalin agreement was obtained with $c \approx 0.7$ for same range of η'/η_0, but at lower values of the viscosity ratio deviations occurred, with the viscosity in continuous shear being higher than oscillating shear.

Comparisons of normal stress values in continuous shear with the real part of the complex shear modulus, G', given by oscillatory experiments for solutions of polyisobutylene showed good agreement with $c \approx 0.7$ up to a certain stress

value. But at higher shear rates the normal stress difference exceeded the corresponding G' values[28,29]. There is therefore a strong suggestion that the comparison in question holds only up to a certain limiting value of shear stress.

5. Viscoelastic behavior and the lubrication properties of liquids

A substantial body of qualitative information concerning highly viscoelastic materials suggests they may be much superior to Newtonian fluids in some lubrication applications. Metzner[30] analysed the behavior of viscoelastic lubricants in squeeze films. Appeldoorn[31] has suggested this mode of deformation to be fo relevance to the behavior of connecting rod bearings of internal combustion engines. It is also a good first approximation to the deformational modes to which the lubricant is subjected in gears, and depicts the qualitative test in which biological and aqueous polymeric fluids exhibit such markedly superior slipperiness. He analysed the elongational flow for a sheet first and obtained the following result:

$$(\tau_{11}) = \frac{4\mu\dot{\gamma}}{(1 + 2\theta\gamma)(1 - 2\theta\gamma)} \tag{24}$$

where μ is the viscosity function of fluid

θ is the relaxation time function of fluid

$\dot{\gamma}$ is the deformation rate

For viscoelastic media the relaxation time function λ is a finite value; the deformational stress may reach much higher levels than a Newtonian fluid which has relaxation time $\lambda = 0$. This prediction was qualitatively proven by experimental work[32]. Then, this result was applied in the squeeze film problem and the total force per unit area opposing the squeezing of the the plates was obtained as

$$\frac{F}{A} = \frac{4\mu V_o/h}{(1 + 2\theta V_o/h)(1 - 2\theta V_o/h)} \qquad (25)$$

This resistance to the removal of the lubricant by squeezing the plates may by compared to that for a Newtonian fluid given as[33]:

$$\frac{F}{A} = \frac{V_o L^2}{h^3} \qquad (26)$$

Hence for the case in which the Newtonian and viscoelastic fluids possess identical viscosity levels:

$$\frac{(F/A) \text{ viscoelastic}}{(F/A) \text{ Newtonian}} = \frac{4(h/L)^2}{(1 + 2\theta V_o/h)(1 - 2\theta V_o/h)} \qquad (27)$$

where h = half thickness of deforming fluid film

L = dimension of apparatus

V_o = imposed velocity

The derivation of equation 24 assumed that the elastic stresses would be large in comparison to the shearing stresses. Under these conditions the ratio expressed by equation 27 is always much greater than unity. At the

opposite asymptotic extreme of very low deformation rates, the ratio will just be unity for the fluid model chosen, a material exhibiting a constant viscosity. It is possible that in the case of shear-thinning fluids ($\mu \neq$ constant) an intermediate region may exist in which the non-Newtonian lubricant is inferior, but this is largely an artifact dependent on the shear rate levels chosen for the "equal viscosity level" comparison and the bearing design (whether h/L is small or not). Much more important is the fact that if the bearing is grossly overloaded ($F/A \rightarrow \infty$) the squeeze rate V_o/h does not need to increase without limit to carry the overload, as in the Newtonian case. Viscoelastic lubrications would thus, at this level of approximation, be predicted to be especially effective under extreme conditions.

Philippoff[34], using an eccentric cylinder geometry, measured the pressure distribution around 360 degrees with liquid manometers. This mode of flow is related to sleeve bearings. When a viscoelastic solution of polyisobutylene in oil was used, he found the pressure profile was shifted toward smaller angles and the sharp peaks were flatter than when Newtonian fluid was used. Simultaneously, the integral under the curve, which is the load bearing capacity of bearings, diminished from the one calculated for the Newtonian liquid of the same initial viscosity due to the well-known decrease in viscosity with shear rate of the visco-

elastic liquid. The result showed that a non-Newtonian viscosity definitely is detrimental, decreasing the load-carrying capacity, but the viscoelasticity brings a small improvement against a Newtonian liquid of the same viscosity as the viscoelastic liquid at the given rate of shear. These measurements were done at very low rates of shear, but much higher rates of shear occur in sleeve bearings.

In plain bearings, in ball-and-socket joints and especially in rolling-contact bearings, greases are subjected to sinusoidal shearing action. Under these conditions the viscoelastic properties are of paramount importance. Forster and Kolfenbach[35] studied two greases having fiber length-to-diameter ratios of 1000 to 1 and 10 to 1, over a range of frequencies from 10^{-4} to 10 cps and of temperature from -17 to 50°C.

They found that the elastic and loss moduli changed relatively little with frequency (by a factor of 10 over a range of frequencies that changed by a factor of 10,000). For both greases the elastic and loss moduli are nearly equal over the range of frequencies covered. Curves of moduli of the short-fiber grease crossed each other so that the viscous response was greater than the elastic response at high frequencies. This may be due to the higher soap content of this grease (22% as compared to 12%). Two yield stresses were found in this work. The first was the minimum

stress required to produce movement of the grease. For both greases this was 30 dynes/cm^2. The second occurred in the region between 550-710 dynes/cm^2 and was attributed to a change in the type of flow from creep flow to plastic flow. Of the total work done in deforming the grease, from 40 to 80% was dissipated and from 60 to 20% was recoverable under the experimental conditions used.

B. <u>Experimental Methods for Dynamic Measurments of Visco-elasticity in Liquids</u>

In simple shear, the experimental determination is usually a complex ratio of force to displacement (or torque to angular displacement) measured at a surface in contact with the sample; or a force measured at one surface and a displacement at another with a gap between, in which the sample is contained. In the second case sample thickness must be smaller than the wavelength of a shear wave propagated through the medium; and the shear disturbance must experience negligible attenuation within the gap. The states of stress and strain are then uniform across the gap. If, on the other hand, the sample thickness is large compared with wavelength of a shear wave, the shear wave decays in amplitude as it progresses from the driving surface to the opposite side. In some cases, the amplitude vanishes within an extremely short distance of the driving surface.

1. <u>Direct measurments of sinusoidally varying stress and</u>
   <u>strain</u>

The simplest oscillatory experiment is based on driving one surface with a known periodic displacement and measuring the periodic force at the surface on the other side of a gap with a sensing device of negligible motion. The phase angle between force and displacement is the same as that between stress and strain. The components of the complex shear modulus can then be calculated. Miles[36,37] apparatus has this conceptual simplicity; force and displacement are read as voltage outputs of transducers with appropriate calibration, and the phase angle is measured on a dual beam oscilloscope. The liquid must be held in the gap by capillary forces. This limits the apparatus to very small strains only. A range of frequencies from 20 to 1000 cps can be covered.

The Weissenberg[38] rheogoniometer can be used for oscillatory measurements in this manner with either parallel plate or cone and plate geometery. A sinusoidally varying angular displacement is imposed on one surface by a mechanical drive and the resulting torque on the other surface is measured with a strain gage transducer. From maximum values of torque and anglular displacement, G' and G'' can be calculated. The sample must be sufficiently compliant so that the displacement due to its deformation is large compared with that of the force-sensing element, which cannot be zero,

or other parts of the apparatus structure. This requirement
sets the high-frequency limit of operation.

2. <u>Measurement involving the mechanical impedance of a
moving element</u>

In some types of apparatus, the force and displacement
are measured at the same surface, so motion of a part of the
apparatus must be specifically taken into account.

The Birnboim[39] apparatus employs an annular pumping
geometry, in which a viscoelastic liquid is subjected to
small oscillating deformations by a rod moving axially in a
cylindrical container closed at one end. The total impedance
Z of such a system has been calculated by Markovitz[40],
taking into account the inertia of the sample as a first
approximation. It is

$$Z = AG''/\omega + i \left[\omega(M + \rho \beta A) - S_M/\omega - AG'/\omega \right]$$

(28)

where

$A = 2 \pi L / \left[\ln \sigma - (\sigma^2 - 1)/(\sigma^2 + 1) \right]$

$\sigma = R_2/R_1$

$\beta = -(R_1^2/2)$

R_1 = radius of driving rod

R_2 = radius of cylinder

L = length of annular gap

Z = total impedance

$G'' =$ loss shear modulus of sample

$G' =$ storage shear modulus of sample

$S_M =$ the elastance of the supporting spring

$\omega =$ circular frequency of oscillation

$M =$ mass of moving system

and $\rho =$ density of sample

The term in β is adequate only if $\omega^2 \rho B / |G*|$ is small compared with 1, where $G* = G' + iG''$, as is usually the case. From equation 28 after Z has been determined by either impedance or phase-shift measurement, the frequency-dependent viscoelastic quantities G' and G'' can be calculated.

For the impedance measurement mode, the electrical impedance ($Z_e = R_e + iX_e$) of the driving coil is measured while in motion, subjecting the sample to periodic deformations, and again when the coil is firmly clamped to prevent motion ($Z_o = R_o + iX_o$). Here the R's are the resistances and the X's the reactances. From these four quantities, the components of the total impedance Z can be calculated as follows,

$$R = \frac{(BL)^2 (R_e - R_o)}{(R_e - R_o)^2 + (X_e - X_o)^2} \quad (29)$$

$$X = \frac{-(BL)^2 (X_e - X_o)}{(R_e - R_o)^2 + (X_e - X_o)^2} \quad (30)$$

where   B is the flux density of the magnetic field

L is the length of wire in the coil.

The frequency range in this mode is 2.5 to 400 cps.

For the phase shift measurement, the essential measurements are the ratio between maximum amplitudes of the driving force (f_o) and displacement (X_o) and the phase difference θ between them, from which the total impedance can be obtained by the relation

$$Z = (f_o/ \omega X_o) (\sin \theta - i \cos \theta) \tag{31}$$

The force is measured by the magnitude of the alternating current passing through the driving coil, which is in the field of a permanent magnet; the displacement is measured by a linear variable differential transformer. The frequency range obtained in this mode is from 0.05 to 5 cps.

Philippoff[41,42] also designed a sinusoidally driven vibrator for complex modulus measurements. It employs annular pumping geometry for liquid samples. The force and displacement are measured by strain gauge transducers. The frequency range is from 3×10^{-5} to 10 cps, the apparatus being especially suitable for extremely low frequencies, and large forces and displacements can be used.

In rotational instruments, Morrison, Zapas and DeWitt[43] proposed a coaxial cylinder instrument. Dynamic torques and

angular displacements can be measured simultaneously on the same surface in contact with the sample. The equation of motion must be reformulated with torsional stiffness con- stants substituted for elastances and moment of inertia substituted for mass. A less direct method has been used by Horio and Onogi[44]; the outer cylinder is oscillated through a small angle. The inner cylinder, suspended from a torsion wire of suitable stiffness, responds with an angular os- cillation whose amplitude and phase depend on the visco- elastic properties of the material in the gap as well as the moment of inertia of the inner cylinder and the stiffness of its support. From the ratio of amplitudes and the phase difference between the two motions, the viscoelastic pro- perties can be calculated by some rather complicated equa- tions.

3. Measurements of characteristic impedance

If the gap is large enough that shear waves from the driving surface dissipate before they reach the opposite surface, the driving surface is oblivious of the latter and feels only surface loading. In curved geometries the radius of curvature is usually large compared with the wavelength and the only dimension that matters is the area of the driving surface. In experiments, the quantities measured are the components of the complex characteristic impedance, or impedance per unit area of driving surface, $R_r + iX_r$, due to contact with the sample. Whereas in gap loading R is

related only to G" and X only to G', in surface loading G'
and G" each depend on both impendance components, as fol-
lows[45]:

$$R_r = (f/2)^{\frac{1}{2}} (\sqrt{G'^2 + G''^2} + G')^{\frac{1}{2}} \qquad (32)$$

$$X_r = (f/2)^{\frac{1}{2}} (\sqrt{G'^2 + G''^2} - G')^{\frac{1}{2}} \qquad (33)$$

and so G' and G" can be obtained by rearrangement in the
form

$$G' = (R_r^2 - X_r^2)/f \qquad (34)$$

$$G'' = 2 R_r X_r/f \qquad (35)$$

The total impedance R + iX is $(R_r + iX_r)$ times the area of
contact plus the contribution from whatever inertia,
elasticity, and friction must be attributed to the apparatus
itself.

Most characteristic impedance devices are operated at a
system resonance frequency where X is zero, to achieve high
sensitivity. This feature has the disadvantage that measur-
ments can be made only at a single frequency, or a few dis-
crete frequencies.

A very sensitive device operating at about 100 cps has
been described by Konno, Makino, and Kaneko[46], shown in
figure 1. A very thin microscope slide immersed in the
viscoelastic liquid to be measured is oscillated by a coil
moving in a magnetic field. The resonance frequency is
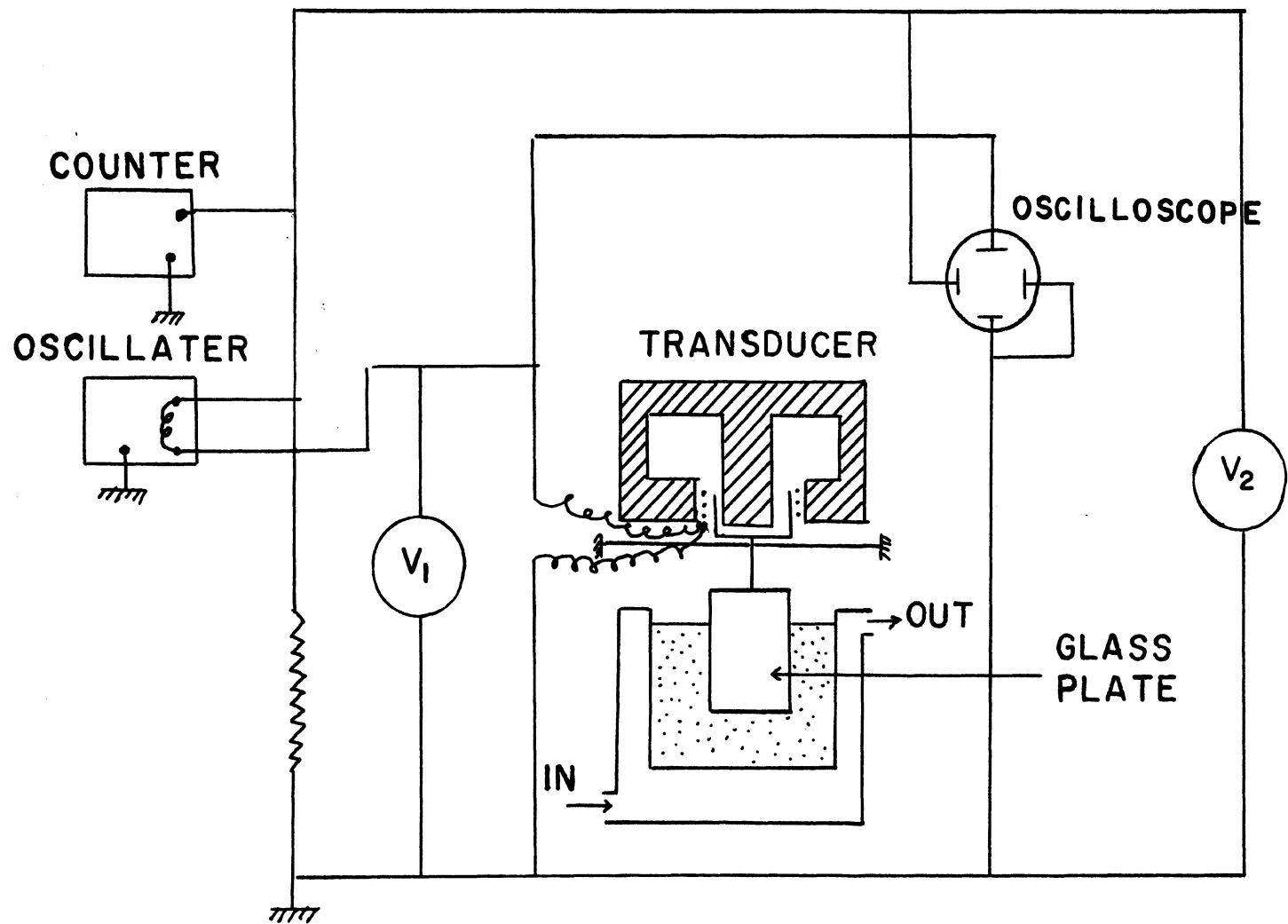
Figure 1. Schematic Diagram of Apparatus of Konno, Makio and Kaneko[46]

determined with and without sample present; the resonance frequencies, ω_o and ω_o' respectively, are identified by an oscilloscope pattern and measured to many significant figures by a frequency counter. The relation can be obtained,

$$X_r = -2 \triangle \omega_o M/A \tag{35}$$

where   A is the area of contact

M is the mass of moving element

$\triangle \omega_o$ is the difference between ω_o and ω_o'

The characteristic resistance R_r can be obtained from equation 29 noting that when the apparatus is driven at resonance

$$X_e = X_o$$

so, $R_r = (BL)^2/(R_e - R_o)A - R^o \tag{37}$

where R^o is a frictional correction for the apparatus itself. Finally G' and G" can be obtained. Measurements can be made on liquids with viscosities as low as one centipoise and rigidities (at 100 cps) as low as 1 dyne/cm^2.

A hollow torsion pendulum designed by Sittel, Rouse and Bailey[47] has been used for higher frequencies. The test liquid is contained in a hollow oscillating disk. The shear stress which is exerted at the liquid-metal interface alters the frequency and the rate of decay of the free oscillations of the pendulum. The frequency and the rate of decay of the resulting alternating voltage are measured electronically.

The characteristic impedance can be calculated and then the G' and G" are determined. It is necessary to use a different torsion rod for each frequency desired.

Birnboim[48] used a somewhat similar principle in the multiple lumped resonator. The viscoelastic liquid is in contact with the outside of a torsionally oscillating cylinder, and a stack of cylinders with torsion rods of different stiffnesses can be oscillated in five different modes so that measurements can be made at five frequencies without changes in apparatus.

C. Measurements of Viscoelasticity of Polymer Solutions

In order to make comparison of the Rouse[5] theory of viscoelasticity with that of Zimm[6], which takes hydrodynamic interaction into account, DeMallie[49], et al. measured storage (G') and loss (G") shear moduli for dilute solutions of polystyrenes with sharp molecular weight distributions in a chlorinated diphenyl solvent. The concentration range was 0.5 to 4% and the temperature range was from $0^{\circ}C$ to $40^{\circ}C$. An essential difference between the prediction of the two theories is illustrated in figure 2, where the dimensionless reduced shear modulus components were plotted against a dimensionless frequency

$$\omega_R = \omega \tau_1$$

here

$$G_R' = G'M/CRT \tag{38}$$
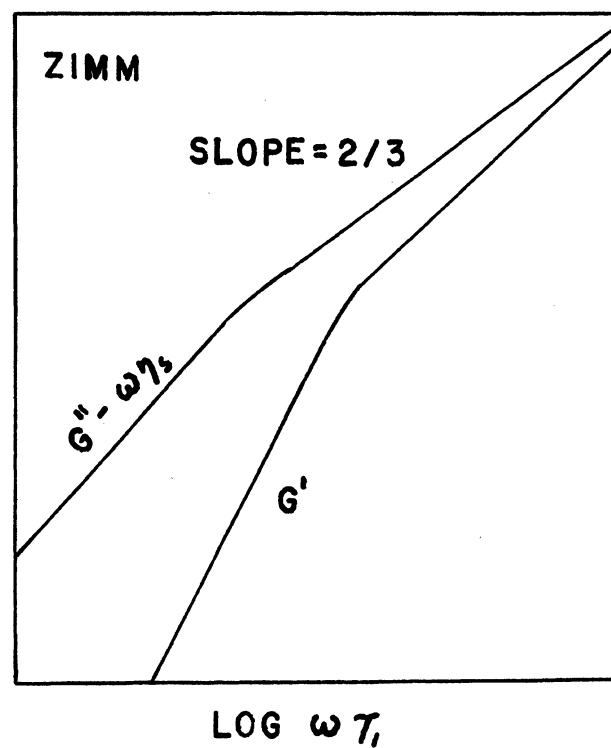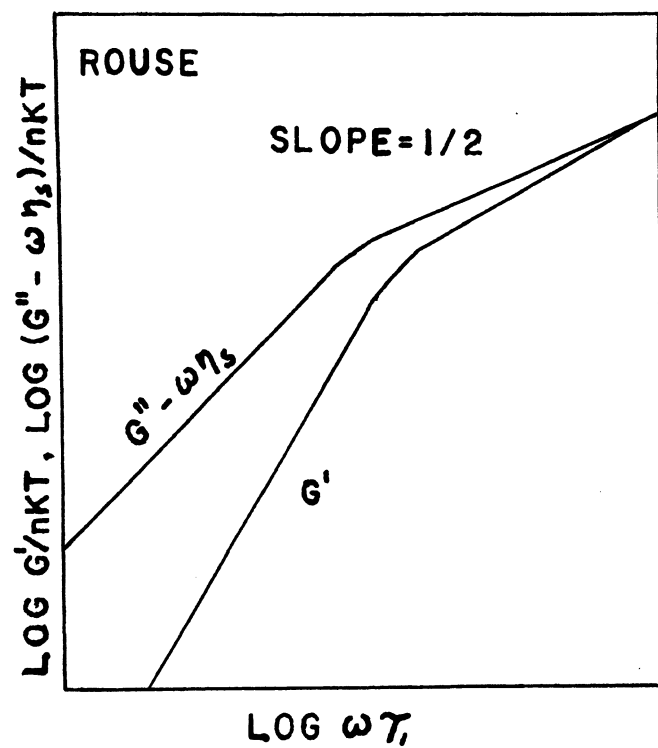
Figure 2. Contribution of a Polymer in Dilute Solution to the Storage and Loss
Shear Moduli, as Predicted by the Theories of Rouse and Zimm

and $G_R{}'' = (G'' - \omega \eta_s)M/CRT$ (39)

M is the molecular weight, C the polymer concentration in g/ml, ω the circular frequency, and η_s the solvent viscosity; τ_1 is the terminal or longest relaxation time in each theory.

At high frequencies according to the Rouse theory, $G_R{}' = G_R{}''$ and both are proportional to $\omega^{\frac{1}{2}}$; according to the Zimm theory, the ratio $G_R{}''/G_R{}'$ is not 1 but 1.73, and both quanitites are proportional to $\omega^{\frac{2}{3}}$. They found results in close accord with the theory of Zimm, as follows: (a) the ratio $G_R{}''/G_R{}'$ agrees with the theoretical value; (b) $G_R{}''$ and $G_R{}'$ are proportioanl to $\omega^{\frac{2}{3}}$; (c) the experimentally determined terminal relaxation times agree with those calculated from the solution viscosity; (d) the molecular weights calculated from the Zimm theory are correct at low concentrations, though somewhat too high at the higher concentrations.

Frederick[50], et al. also measured the storage (G') and loss (G") shear moduli for dilute solutions of several polystyrenes with sharp molecular weight distributions in three chlorinated diphenyls (Aroclors) and in di-2-ethylhexyl phthalate at the θ-temperature. The molecular weights ranged from 8.2 x 10^4 to 1.7 x 10^6 and the concentration from 0.5 to 4% polymer. They found the data changed gradually from Zimm-like to Rouse-like behavior with increasing molecular

weight or concentration but close to Zimm-like in θ-solvents regardless of the polymer molecular weight. At low concentration, they point out the shapes of the frequency dependence data were intermediate between the Rouse and Zimm predictions. It could be described by the Tschoegl[51] extension of the Zimm theory using a parameter ϵ calculated from intrinsic viscosities and a parameter h, representing the strength of the hydrodyramic interaction, chosen empirically.

Quartz crystals, resonant in the fundamental torsional mode at frequencies of 38 and 73 Kc/sec, have been used to measure the viscoelastic properties of dilute solutions of polystyrene in toluene by Harrison[52]. Seven narrow molecular weights from 4.8×10^4 to 1.2×10^6 were employed. The results for both the dynamic viscosity and shear rigidity modulus for polystyrenes of molecular weight up to 2.39×10^5 show good agreement with the predictions of Zimm theory but do not agree with curves calculated from the Rouse theory. But the results for the higher molecular weight deviate from the curves calculated from the Zimm theory. Measurements on more dilute solutions of these polymers show similar behavior, suggesting that the deviation from Zimm theory was not due to the solutions being too concentrated. They concluded that a different mechanism was operative above a molecular weight of about 3×10^5. They also found that it gave good fit to experimental data for higher molecular

weight solutions by increasing γ_1 or M in the Zimm theory by a factor of two for the first mode only.

Sakanishi[53] introduced the ideas of intrinsic rigidity, dynamic intrinsic viscosity, and limiting relaxation time, which were obtained by extrapolation of measured values at finite concentration to zero concentration. The dimensionless functions of the above quantities have been used to compare the experimental results with the theoretical conclusions of Rouse and Zimm. Measurements were made of complex rigidity G* of very dilute polyisobutylene solutions using the torsional crystal method in the range of 19.6 to 117.7 KHz. In benzene at the theta temperature, he found that curves based upon the Zimm theory excellently represent the experimental plots of log (G*) M/RT vs log $M\eta_s$ ω (η)/RT. In cyclohexane at 15° and 30°C, the results were intermediate between the Rouse and Zimm theories.

O'Reilly[54] measured some rheological properties of polymer melts by cone and plate viscometer. In figure 3 is shown the rheological properties of polystyrene (styron-666) at 192°C. Simmons[55] has performed some experiments with 5.4% polyisobutylene cetane solution obtaining dynamic viscosities (η') and elastic moduli (G') not only in the fluid at rest but also when the sample was undergoing shearing.
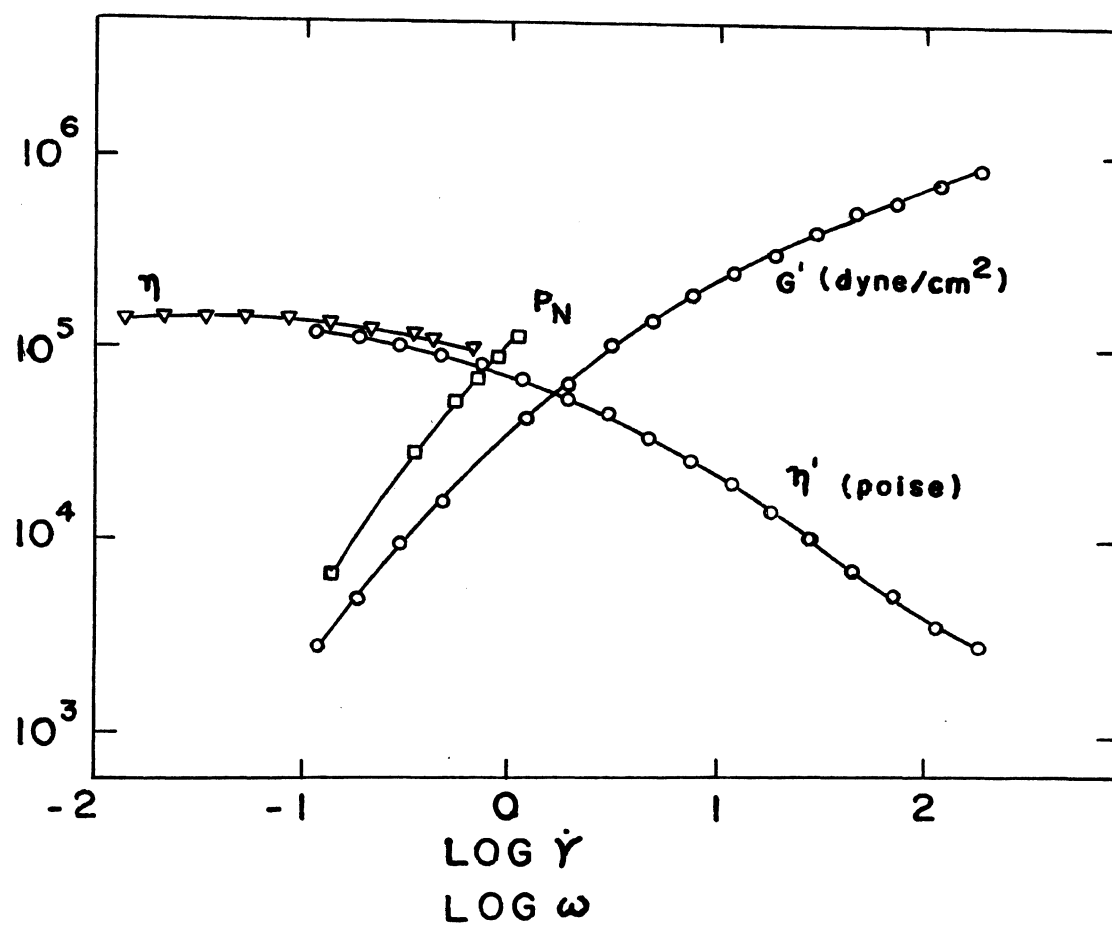
Figure 3. Rheological Properties of Polystyrene at 192°C [54]

III. APPARATUS

A. Objective

The aim was to design and construct a high shear strain instrument for measuring the complex viscosity of liquids by measuring the characteristic impedance. A thin plate immersed in the viscoelastic liquid to be measured was to be oscillated by a speaker. The shear stress on the plate was to be determined by a piezoelectric crystal; the strain was to be measured by an accelerometer and a phase meter was to be used to determine the phase angle between stress and strain. From this it was hoped that an instrument capable of large shear stains could be demonstrated.

B. Principles of Measurement

The viscoelastic properties of a liquid may be studied by bringing the liquid into contact with a plane surface which executes a simple harmonic motion in its own plane with the angular frequency $\omega = 2\pi f$. A shearing wave is propagated in the liquid. It will be assumed that the liquid extends to infinity in the direction of Z-positive and that the plane surface is infinite in extent. When a steady state has been established, the transverse velocity of the liquid at the distance Z from the surface is[31]

$$V = V_0 \, e^{-\beta' Z} \, e^{i\omega t}$$

$$\beta' = \left(\frac{i \, \omega \, \rho}{\eta} \right)^{\frac{1}{2}} \tag{40}$$

where $i^2 = -1$, V_o is the maximum velocity of the oscillating surface, and η and ρ are the viscosity and the density of the liquid, respectively. If the liquid is viscoelastic the gradient of velocity is not in phase with the shearing stress. Under steady-state conditions, the phase difference can be taken into account by use in equation 40 of a complex viscosity, η^*.

In a liquid of low viscosity, the amplitude of the wave described by equation 40 decreases rapidly with increasing value of Z. At a frequency of 100 cps the transverse velocity in a liquid with a viscosity of ten centipoise and a density of one gram per cubic centimeter is reduced by a factor of 10^{-3} in approimately 1.2 mm, the attenuation becomes even more rapid with increasing frequency or decreasing viscosity.

The rapid attenuation of the wave generated in the liquid prevents direct measurements of the phase and amplitude of the transmitted wave. The alternating shearing stress exerted by the liquid on the oscillating surface is

$$\mathcal{T}_s = - \quad \eta^* \left(\frac{\partial V}{\partial Z}\right)_{Z=0}$$

$$= \eta^* \beta' V_o \, e^{i \omega t}$$

$$= (i \omega \rho \eta^*)^{\frac{1}{2}} V_{Z=0} \tag{41}$$

The complex radiation impedance per unit area, Z, of the liquid is defined as the ratio of the shearing stress to the

velocity;

$$Z = \frac{\mathcal{T}_s}{V_s} = \frac{\eta^* V_o \beta e^{it\omega}}{V_o e^{it\omega}} = \eta^* \beta$$

$$= (i\omega \rho \eta^*)^{\frac{1}{2}} \tag{42}$$

The impedance has a real component R_r and an imaginary component X_r, the resistance and reactance, respectively.

$$Z_r = R_r + i X_r = (i\omega \rho \eta^*)^{\frac{1}{2}} \tag{43}$$

The components η' and η'' of the complex viscosity can be solved as

$$\eta' = \frac{2 R_r X_r}{\omega \rho} \tag{44}$$

$$\eta'' = (R_r^2 - X_r^2)/\omega \rho \tag{45}$$

The resistance R_r and reactance X_r can be measured and then converted to the desired quantities η' and η''.

C. Equipment and Detailed Description of the Apparatus

1. The frame

In order to achieve structural stability, a stand was built with three 0.75-inch diameter steel poles and four 10-inch diameter plates, each 1-inch thick. All plates were ring shaped except the bottom one. The three poles were completely threaded in order to be able to adjust and fix the plates at suitable levels. The driving speaker was fixed to the top plate by three steel bolts and some vibration damping material was used between the speaker and the plate. The height of the stand was 2 feet and the inside diameter of the top plate was 7 inches.

The second plate was 1-inch thick with 3-inch inside diameter. A triangle plate was bolted to the lower side of it by three steel bolts. This triangle plate served as the stationary part of the capacitive displacement transducer and it had to be completely rigid for precise measurements. The tempering vessel was placed on the third plate and fixed by three screws as shown in figure 4. The hole diameter of this plate was 3 inches. This space served as the entrance of the sample beaker. The bottom plate was used as the base of the whole stand. A diagram of the frame is shown in figure 5.

2. Transducer support

Different methods were tested to keep the force transducer centered and confine the motion of the driving plate to axial oscillation. First, a diaphragm was fixed at the center of the main plate, damping material was used to connect the diaphragm and the main plate. The result was not satisfactory. Then three brackets were welded on the top of the tempering vessel and six nylon strings were attached to stabilize the transducer. This design did not give satisfactory results either. Finally, three nylon strings were attached at the top of the plastic connection rod and another three at the top of the force transducer (see figure 5). Each string was connected to a support pole by one screw as shown in figure 6. The tension of the string was adjusted by turning the nut on the screw. This design proved to be
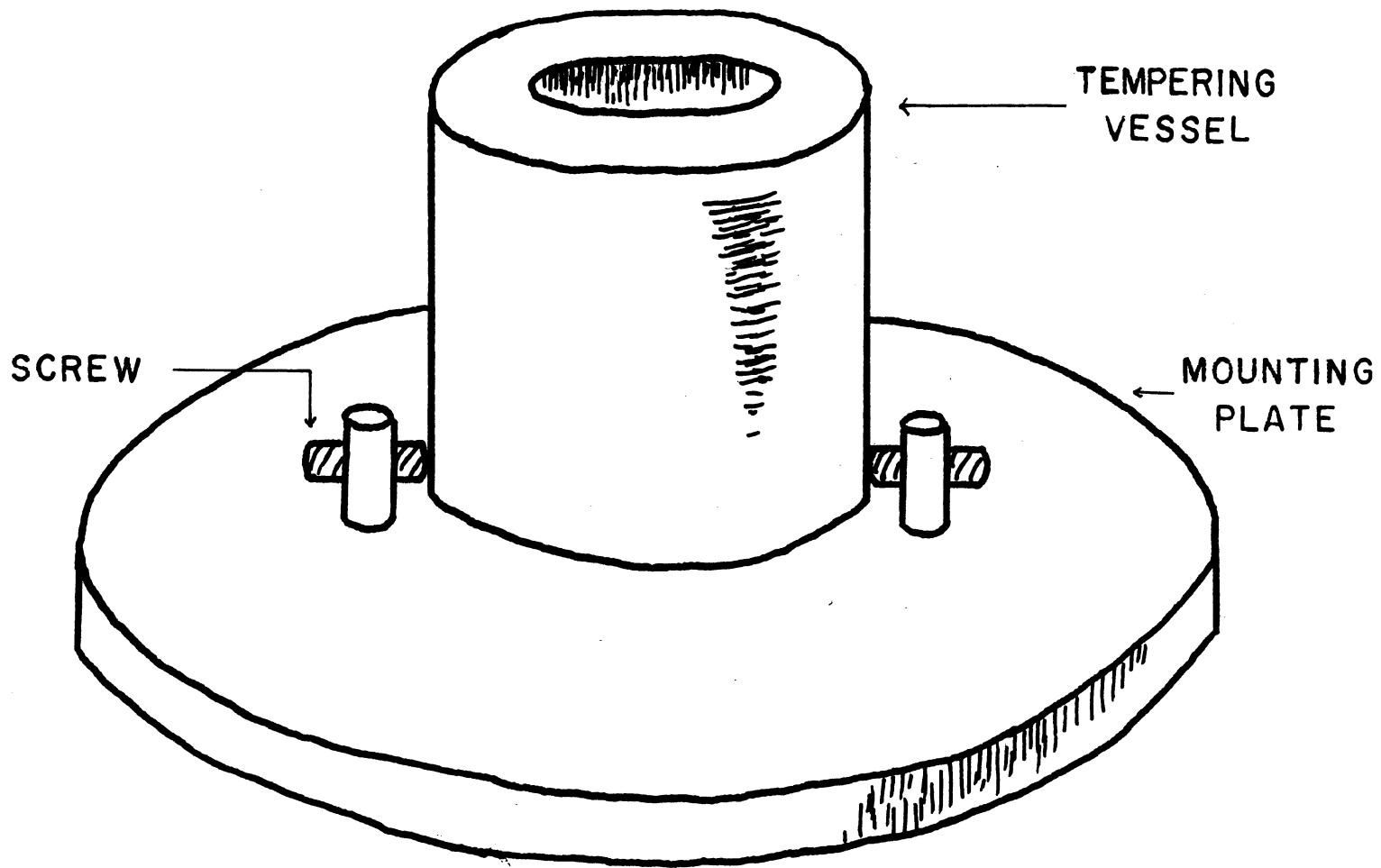
Figure 4. Tempering Vessel Mounting Method

A. Speaker

B. Tension adjust screw

C. Capacitive transducer output

D. Force transducer output

E. Sample beaker

F. Vibrating damping table

G. Supporting string

H. Plastic connection rod

I. Stationary plate of capacitive transducer

J. Accelerometer output

K. Driving plate

L. Sand bath
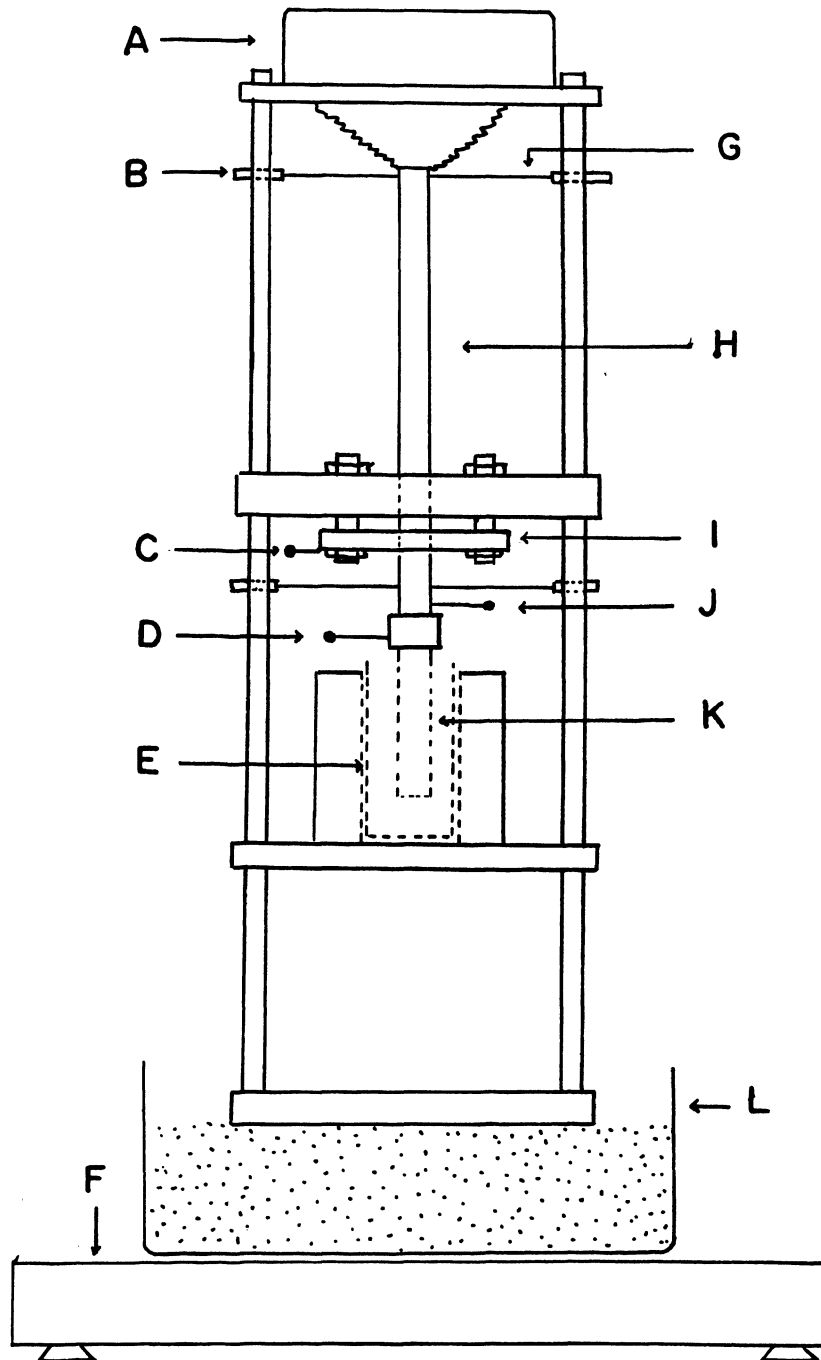
Figure 5. The Frame of the Dynamic Apparatus
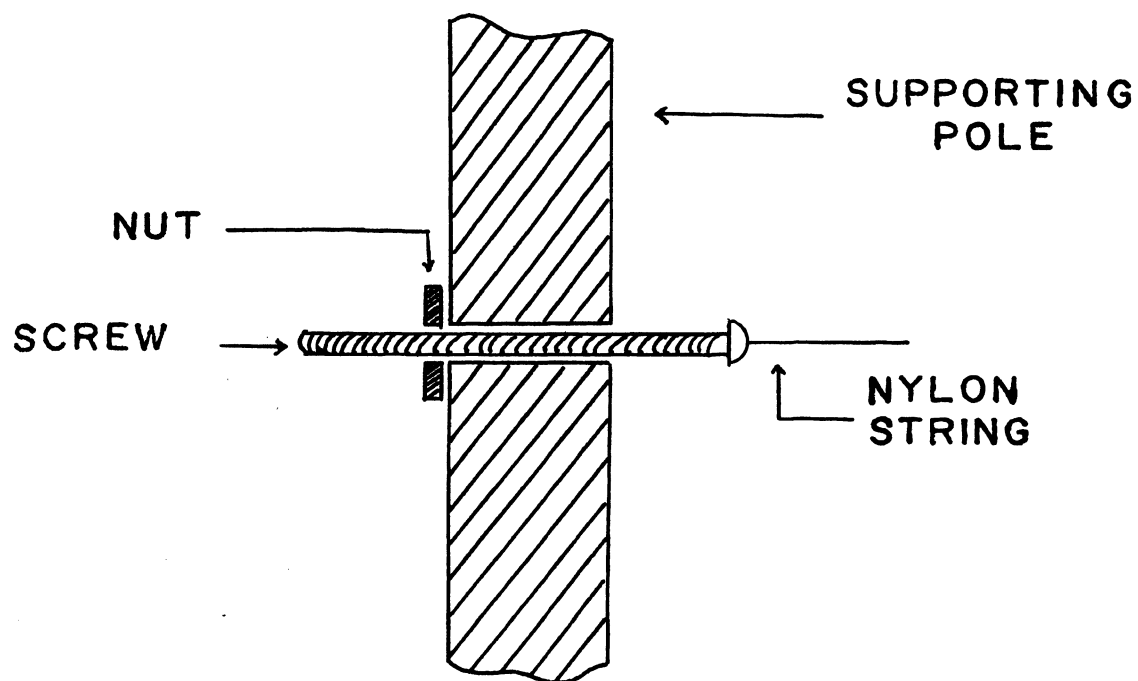
Figure 6. The Connection of Supporting Strings

satisfactory in limiting the lateral movement of the trans-
ducer and in its adjustablility. The strings used were
guitar size E.

3. Force transducer

For the purpose of better rigidity and large contact
area, a stainless steel cylinder was first made with a
piezoelectric crystal cemented on the top. Two very fine
wires were used to connect the crystal to the amplifier as
shown in figure 7. Since the stainless steel cylinder was
not light enough, the cylinder impedance was too great to
compare with the solution impedance. This made the measure-
ments imprecise, four different cylinders with 0.001-0.003-
inch thick walls were made and tested. A brass cylinder
with 0.003-inch thick wall gave the best result. The diam-
eter of the cylinder was 0.5 inch; this limited the measure-
ments for high viscosity solutions to high frequencies only.
(The reason will be discussed in a later section.)

In order to obtain a better operational frequency range,
a slightly curved plate was substituted for the cylinder.
An exploded view of the new force transducer is shown in
figure 8. The driving plate is 0.003-inch thick, 0.88-inch
wide, and 3.00 inches in length. The material must be light
enough to give low mechanical impedance yet stiff enough to
maintain complete rigidity. For this purpose, a 0.003-inch
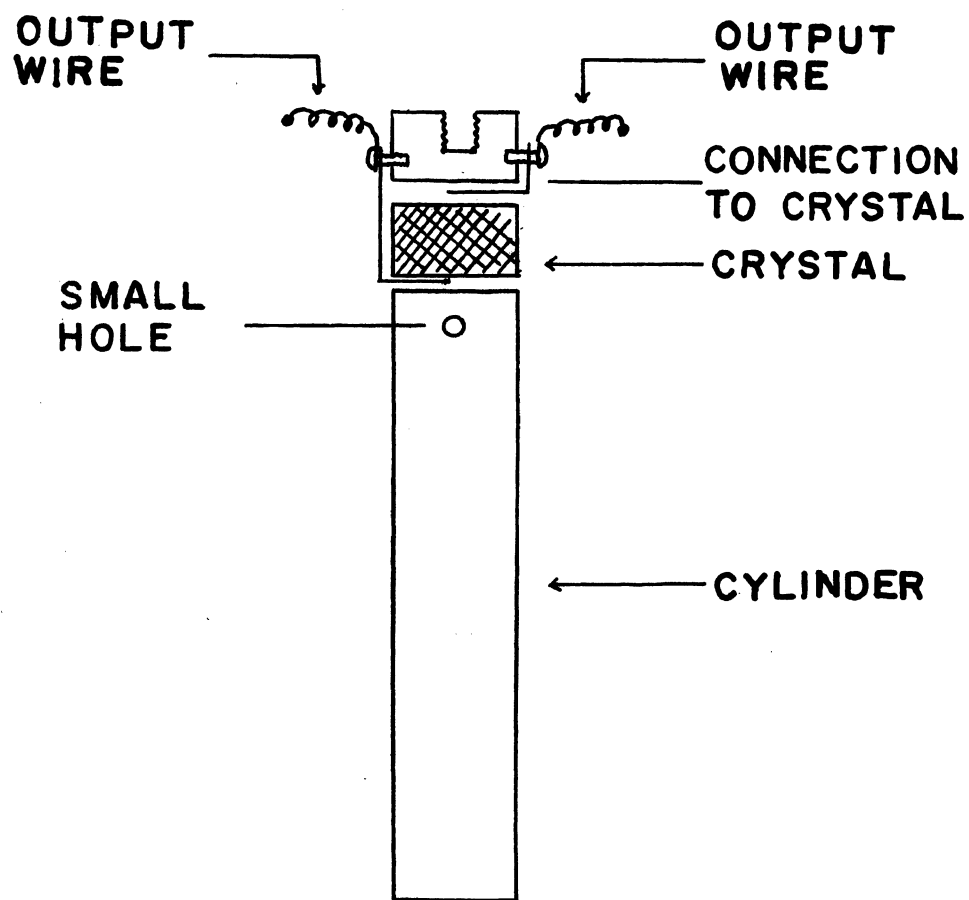
Figure 7.   Force Transducer with Cylinder
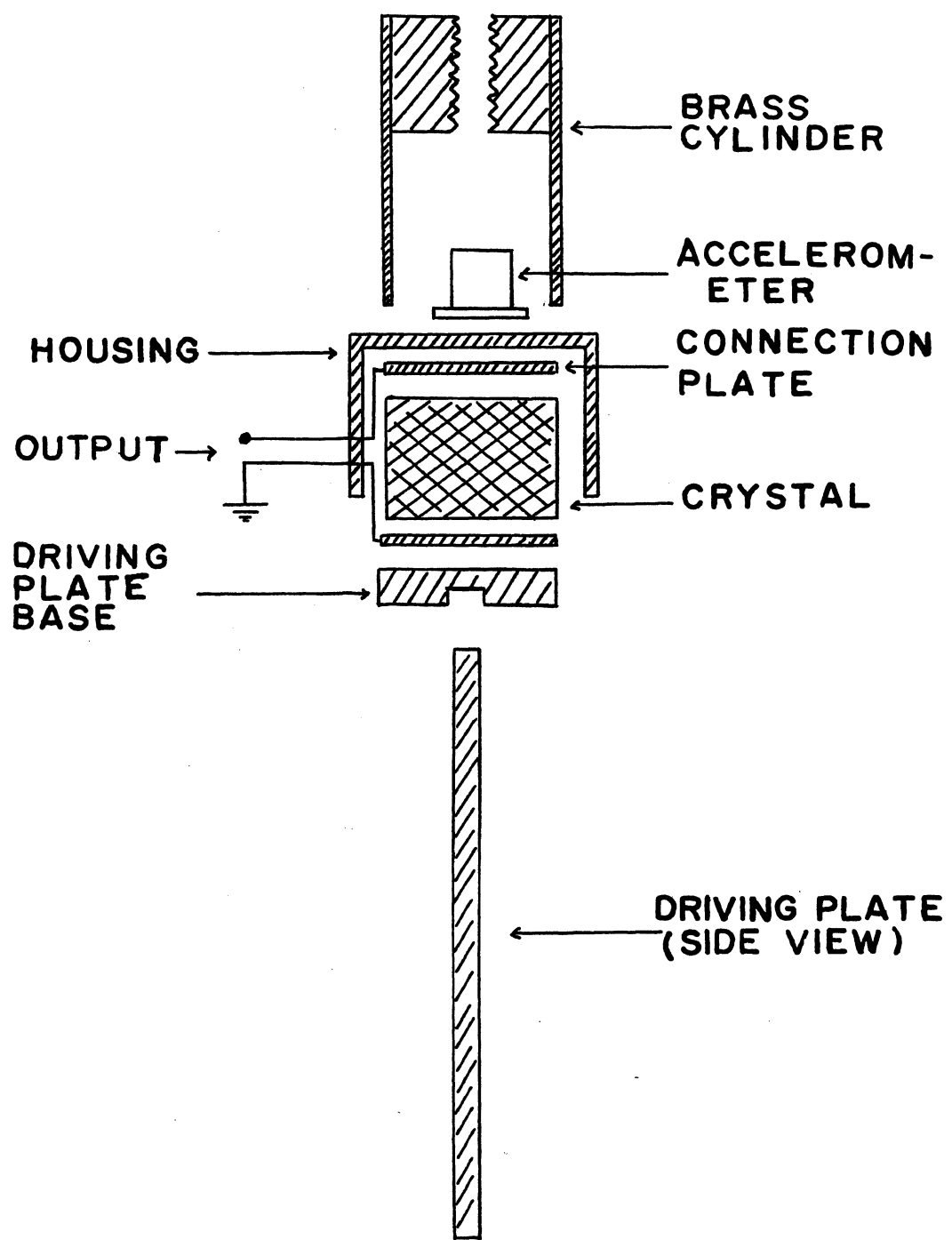
Figure 8. Force Transducer with Plate

thick steel sheet was used and a curvature of one and half inches was applied to obtain enough rigidity.

The quartz piezoelectric crystal was 0.3 inch thick and 0.5 inch in diameter. It was cemented between the upper end of the driving plate and a connecting brass cylinder, which offered enough room for the accelerometer to be placed inside. Since the connections of piezoelectric crystal were on each end, one brass plate with 0.5 inch diameter was cemented on each end of the crystal as a connection plate. This assured even force on both ends of the crystal. A small hole was made at the center of each plate and silver paint was applied in the small hole to obtain good connections. A metal cover was used to fix the connection cable and to minimize environmental effects on the crystal (temperature variations, static electricity fields, magnetic fields, etc.).

When the transducer was subjected to sinusoidal vibration in solution, the solution and the mass of the plate exerted a variable force on the piezoelectric crystal. Due to the piezoelectric effect a variable potential was developed across the crystal, which was proportional to the force. This potential was measured using a very high impedance amplifier and used for determination of the force.

4. **Capacitive transducer**

For calibration of the displacement, a capacitive trans-

ducer was used in conjuction with a Disa Model 55B02 react-
ance converter. The transducer was connected to the input
of an oscillator which converted the measured reactance of
the transducer into a frequency. The frequency detector
converted frequency into a D. C. voltage. This voltage was
displayed by the oscilloscope and used to establish the
calibration curve of voltage versus plate displacement.

The capacitance between two surfaces is given by

$$C = \frac{\epsilon A}{a} \qquad (46)$$

where ϵ is the dielectric constant of the medium between
the two surfaces, A is the area of the surfaces, and a is
the distance between them. The capacitance is inversely
proportional to the separation between the surfaces. This
response is non-linear with respect to a. If C_o and a_o are
reference values, C and a are values at any position, then;

$$C = C_o + C' \qquad (47)$$

$$a = a_o + a' \qquad (48)$$

and

$$\frac{C'}{C_o} = \frac{-a'/a_o}{1 + a'/a_o} \qquad (49)$$

If a_o is very large, the ratio C'/C_o will be proportional to
displacement and a linear relationship will result. However,
the sensitivity will be small. If a_o is small, the opposite
is true; there will be large sensitivity, but a non-linear

relationship between capacitance and displacement will be obtained.

In order to avoid the difficulties stated above, the transducer was designed with variable overlap area instead of separation distance and then the displacement was correlated with overlap area. Since the original design of the force transducer was a cylinder instead of plate to obtain best rigidity and larger contact area with solution, the capacitance transducer was constructed with a steel rod inserted into the cylinder as shown in figure 9. When the cylinder was vibrated along its longitudinal axis, the displacement was proportional to the change in overlap area between the rod and the cylinder. By the same token, if C_o and A_o are reference values, and C and A are values at any position, then:

$$C = C_o + C' \qquad (50)$$

$$A = A_o + A' \qquad (51)$$

and

$$\frac{C'}{C_o} = \frac{A'}{A_o} \qquad (52)$$

so a linear relationship between capacitance and displacement will be obtained. However, the clearance must be very small between the cylinder and the rod to achieve high sensitivity. In this case, the alignment and the stability of the cylinder is very important. The dielectric constant,
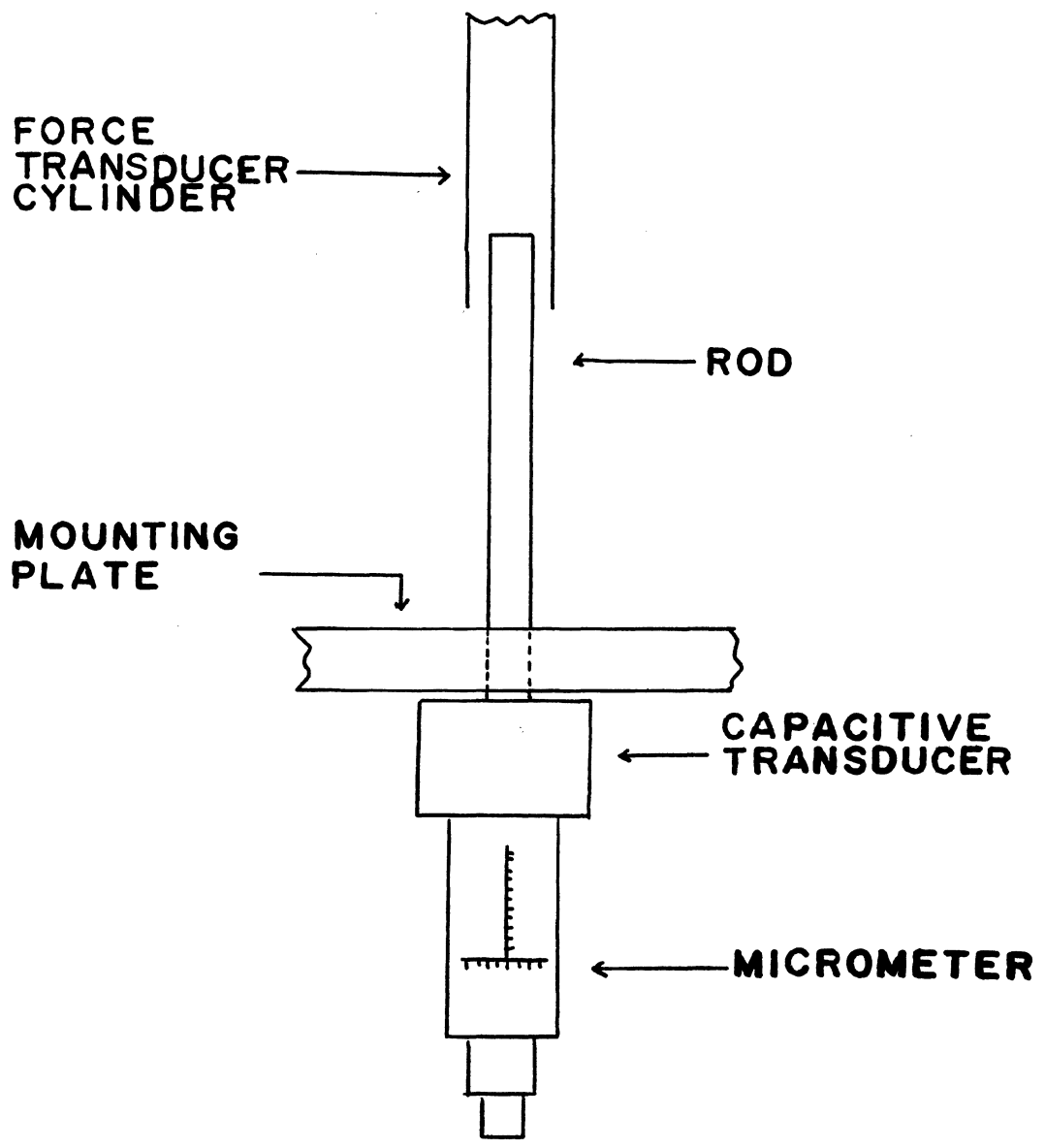
Figure 9. Capacitance Transducer with Micrometer

ϵ , was different for each sample, thus requring one calibration curve for each sample. This may introduce extra errors when comparing two different samples. To eliminate this problem, the capacitive transducer was moved to the top of the force transducer as shown in figure 10. Then, only one calibration curve was needed. The capacitive transducer can be used up to a frequency of 400 cps. Above that frequency the displacements are too small for the sensitivity achieved.

5. Connection rod

A 10-inch plastic rod was used as a connection between the driving speaker and the force transducer. The purpose of this connection rod was to separate the driving speaker and the force transducer. Since the driving speaker had a very strong magnetic field, this caused some extra signal in the force transducer. The rod was covered by alumium foil and grounded to eliminate build up of the static electricity. The force transducer was very sensitive to static electricity fields, sometimes causing spurious voltage signals larger than the force signal when unshielded.

6. Sample beaker

The sample beaker and the tempering vessel are shown in figure 11. The sample beaker was 1.6 inches inside diameter and 5.0 inches in length. The outside diameter just fit into the tempering vessel. After filling, but before introducing

VIBRATION ROD

STATIONARY PLATE

CAPACITIVE TRANSDUCER OUTPUT

ACCELEROM- ETER OUTPUT

FORCE TRANSDUCER OUTPUT
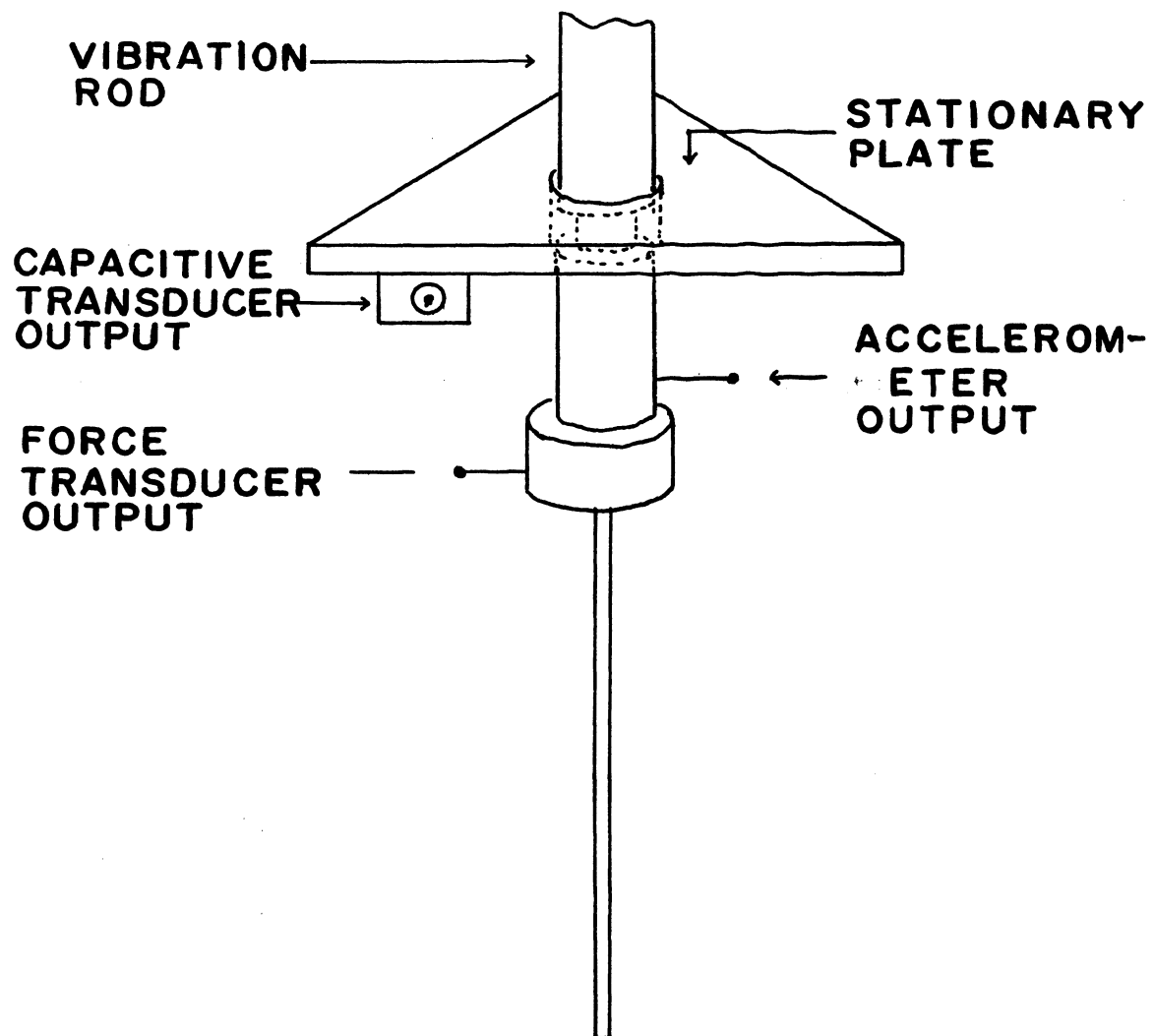
Figure 10.   New Design of Capacitance Transducer
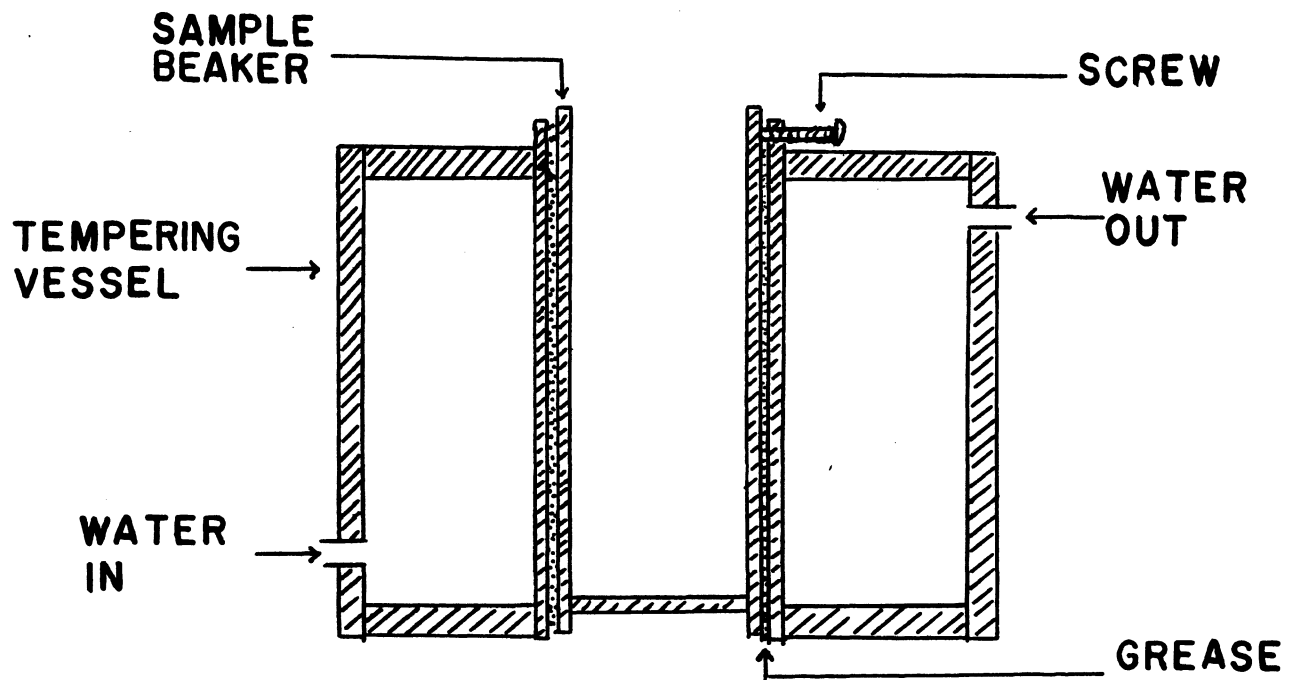
Figure 11.   Tempering Vessel and Sample Beaker

the beaker into the tempering vessel, the outside of the beaker was coated with glycerin to improve the heat transfer. A screw on the top of the tempering vessel was used to fix the sample beaker.

7. Tempering vessel

The tempering vessel was water jacketed for circulation of temperature control water. It was constructed from two different sizes of pipe. The outside diameter of the outer pipe was 4.5 inches and the inside diameter of the inner pipe was 1.5 inches. One ring-type plate was glued on each end. The height of the tempering vessel was 5 inches. The water outlet and inlet are shown in figure 11. The whole vessel was rigidly attached to the mounting plate of the stand.

8. Mechanical isolation

The whole apparatus was very senstive to outside vibration. Perhaps the single most important factor in the ability to make precise measurements is the prevention of external mechanical vibrations from reaching and exciting the system. A sand bath was found to give some attenuation to external vibration. The entire apparatus was set on the sand bath and then the whole system was placed on a vibration damping table. The constant temperature water bath and the circulation pump was set on another bench to eliminate the vibration effect to the system.

9. Accelerometer

Since the capacitive transducer could only be used to 400 cps, an accelerometer was used to measure displacement. It could be applied to a much higher frequency range, but the capacitive transducer was necessary for calibration. The construction of the accelerometer is shown in figure 12. It was made by Buel & Kjaer company. The transducing element consists of two piezoelectric discs on which a heavy mass is resting. The mass is preloaded by a stiff spring and the whole assembly is mounted in a metal housing with a thick base. When the accelerometer is subjected to vibration, the mass will exert a variable force on the piezoelectric discs. This force is exactly proportional to the acceleration of the mass. Therefore, the acceleration can be obtained by measuring the potential generated by the accelerometer. The output voltage of the accelerometer at constant displacement amplitude is proportional to the frequency squared, just as for the force transducer voltage.

After the output voltage from the accelerometer was adjusted to a similar amplitude to the signal from the force transducer at one frequency, it gave the same result for all frequencies. This made the readout from one voltmeter easier and the phase measurements more accurate at higher frequencies. The accelerometer was mounted inside of the brass cylinder and the connection cable was in the opposite direction of the force transducer cable to balance the vibration
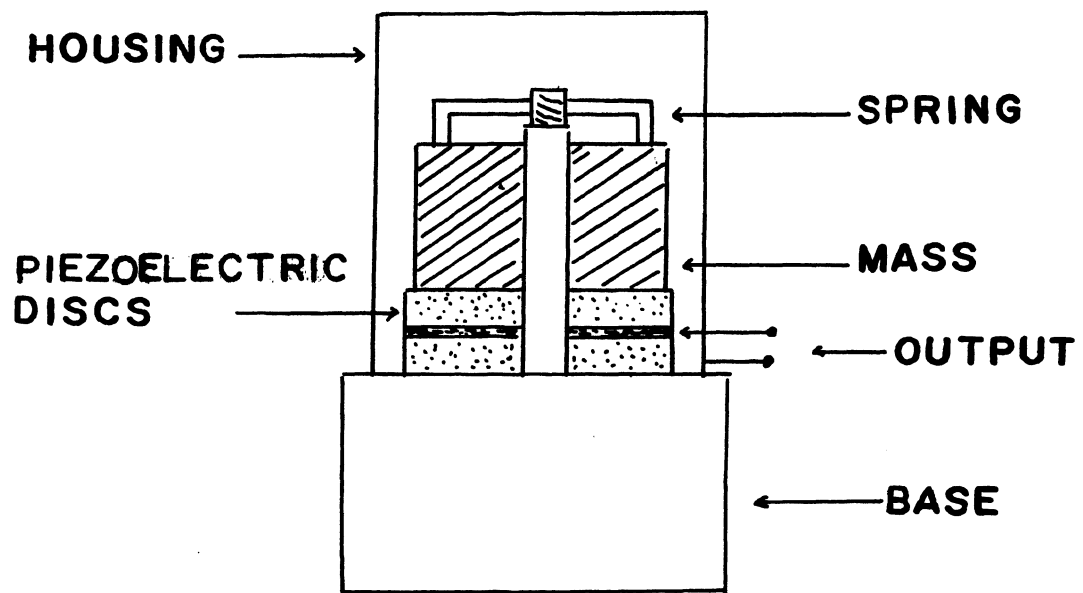
Figure 12. Piezoelectric Accelerometer

effect. The outer coating of the cable was removed for
10 cm to reduce weight and stiffness. Then, it was fixed on
the pole of the stand. Coaxial cable must be used for all
connections. Improper cables and connections between the
transducer and amplifier caused high noise inputs, erratic
inputs, and sometimes no input. Damaged or worn connectors
were also responsible for erratic signals or loss of sensi-
tivity.

10. Driving speaker

The modified loudspeaker drive was mounted on the top
of the stand. It had an extra support diaphragm to stablize
the voice coil and to prevent the attached moving assembly
from vibrating perpendicularly to its axis. Vibration
amplitudes up to 0.5 inch were possible at low frequencies
(below 50 cps), but maximum amplitude decreased approximate-
ly proportionally to the frequency square for higher
frequencies.

11. Phase meter

The Wiltron model 351 Differential Input Phase Meter
was used to measure the phase angle between force and
acceleration. It measures phase angle to high accuracy at
any frequency in the range of 10 Hz to 2 MHz and with either
input voltage at any amplitude within a 100 db range from 1
millivolt to 100 volts rms. Readout is direct in degrees on
a precision 4-inch zero center meter. Because the phase

meter makes its phase measurement by measuring the fraction of a cycle between the negative-going zero axis crossings of the two test signals, if the waveform of either test signal is distorted so as to change its zero axis crossing, the phase reading will change accordingly. To ensure that the waveform was not distorted, both signals were shown on the dual-trace oscilloscope. The shape is shown in figure 13.

12. Voltmeter

The rms voltage of the signal from the force transducer or accelerometer was read out from a vacuum tube voltmeter. A three-way switch was used to connect both signals to the voltmeter. This permited reading the rms voltages one at a time by operation of the switch. The Hewlett-Packard 400 D vacuum tube voltmeter was used. It measures AC voltages from 0.001 to 300 volts, with a frequency bandwidth covering 10 Hz - 4 MHz. More detailed specifications are given in the instruction manual.

13. Oscilloscope

The Hewlett-Packard Model 122 A/AR dual-trace cathode-ray oscilloscope was used to show the waveform of the signals from the force transducer and accelerometer. Dual trace operation is obtained with an electronic switch. That permits observation of two signals at the same time. The oscilloscope was also used to read the D. C. voltages from the capacitive transducer during the calibration of displace-
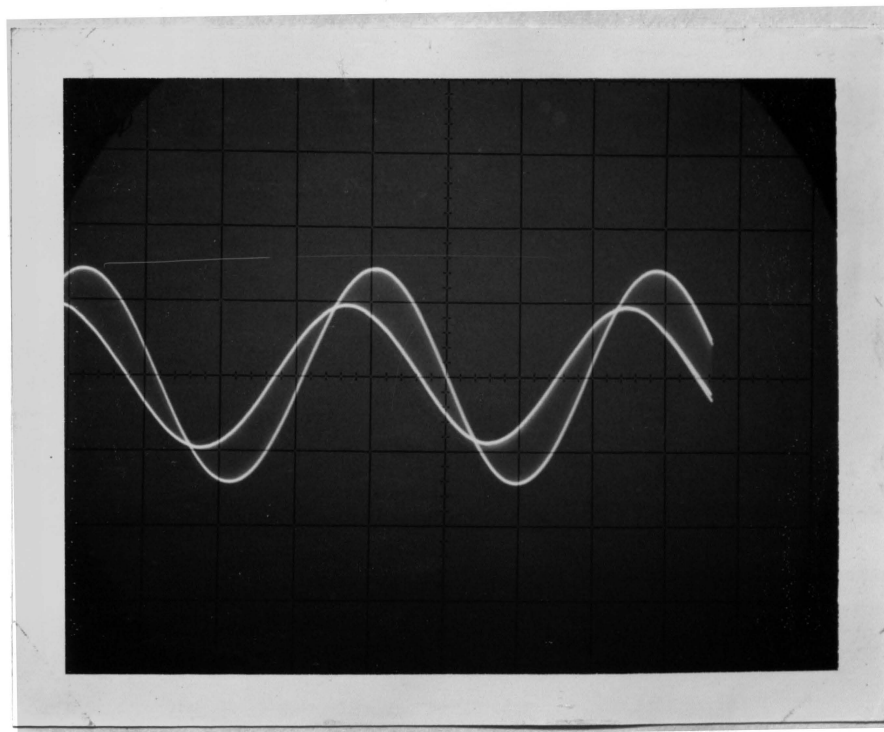
Figure 13.   The Shapes of Force and Displacement
Signals

ment.

14. Electrometer amplifier

A Keithley M603 electrometer was used to amplify the signals from the force transducer. It is a high gain amplifier and has a remote probe which contains the first stage electrometer tubes. The remote probe allows the input grids to be located as far as 24 feet from the main amplifier. By employing this feature the input capacitance may be kept to a minimum so that it is possible to achieve fast voltage measurements in high impedance circuits. The probe had two input connections. It was desired to use the instrument only as a single ended device, so the other connection was shorted to ground.

15. Electrostatic charge amplifier

The signal from the accelerometer was first amplified by a Kistler Model 566 multi-range electrostatic charge amplifier.

16. Amplifier

A Hewlett-Packard Model 465 A amplifier was used as a preamplifier and impedance adapter for the signal output from the charge amplifier. The purpose of the amplifier was to stablize the output signal and improve the phase measurements. This amplifier has selectable gain of 20 dB or 40 dB stable over a continuous frequency range of 5 Hz to 1 MHz.

The 20 dB gain was used for this work.

17. Oscillator

The driving speaker was energized by a Hwelett-Packard Model 201 C Audio oscillator. It contained a built-in stabilized amplifier stage delivering 3 watts of power into a 600-ohm resistive load with distortion held to $\frac{1}{2}$ per cent at frequencies above 50 KHz. The output level is adjustable. A transformer was used to adapt the output impedance of the oscillator to the 16-ohm impedance of the speaker.

18. Viscometer

The steady viscosities of the sample were measured by a Haake Rotovisco which is a rotaional viscometer. The substance to be measured was introduced into a gap between a rotating and a fixed cylinder. The viscosity was determined from the resistance to rotation caused by the sample material. The factor actually measured is torque; the measuring heads convert the torque into an electrical value which is proportional to the angle of diaplacement. Conversion was accomplished through torsion dynamometers which consist of two coaxial shafts, coupled machanically by a creep-resistant torsion spring. The angle of displacement of the spring was a measure of transmitted torque. The conversion of the torque angle into an electrical resistance value was effected by a potentiometer mounted on the upper shaft of the dynamometer. The measuring bob can be rotated at 10 different

shear rates. Since only one measuring head was available, the shear rate range was not wide. For most of the higher speeds, the resistance (torque) was in excess of permissible tolerance of the measuring head. This limited the range of shear rate that could be measured.

D. Measuring System and Operation

A block diagram of electric instruments is shown in figure 14. After more than half an hour warm up of the instruments, the loudspeaker driver was energized by the audio oscillator. The loudspeaker generated a sinusoidal vibration on the force transducer and the accelerometer. Signals from the transducer and the accelerometer were observed on the oscilliscope. Both waveforms should be of sinusoidal form and the phase angle between them should be nearly zero. This was checked every time before sample was introduced, because some unknown environmental effect sometimes introduced noise and changed the phase angle. The choice of amplitude of the vibration was arbitary within the linear limitation of the displacement transducer. (The limitation will be discussed in later a section.) The essential measurments were the amplitudes of the force from the force transducer, the acceleration of the accelerometer, and the phase angle between them, from which the complex impedance were obtained and than converted to the desired quantities G' and G" or η' and η''.
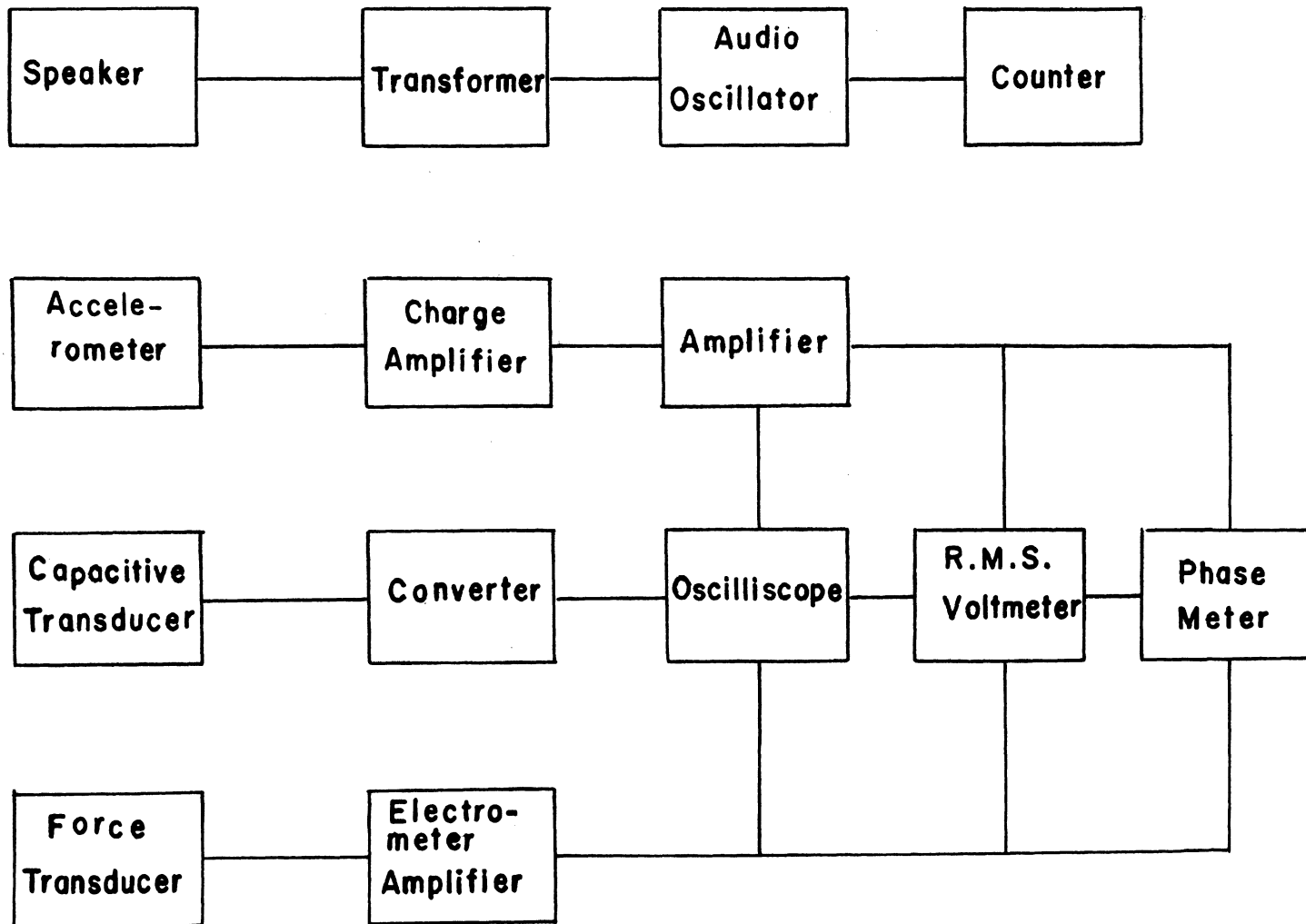
Figure 14. Measuring System

To measure the complex viscosity of a sample, the sample was first introduced to the sample beaker to a low level, then it was inserted into the tempering vessel with the end of driving plate just touching the surface of the sample. The length of the driving plate from the top of the temper- ing vessel was premeasured, this made it possible to establish the necessary sample level with a scale measuring the same length from the top of the beaker. At this level, the data for phase angle at each frquency was taken as a reference. Then, two higher levels of sample were introduced into the sample beaker by the same method. For each level, the data of force amplitude and acceleration amplitrde were taken using the voltmeter, the phase angles using the phase meter, and the frquencies using the counter. To insure temperature equilibrium between the tempering vessel and the sample, the sample beaker was inserted into the tempering vessel at least half an hour before the data was taken. The tempera- ture of this system was controlled to T $\pm$ 0.1° C.

IV. CALIBRATION

A. Phase Difference

In order to adjust the zero point of the phase meter, a sinusoidal signal from the audio oscillator was introduced to both channels, E 1 and E 2. Then, the zero control was used to obtain zero reading. In the experimental frequency range, the zero did not change with frequency. If the zero reading changes with frequency, this reading must be subtracted from the phase reading in solution to obtain the true phase difference. One 0.001 μ f capacitor was added to each input terminal to ground for stable phase measurements.

When the driving plate vibrates in air, the phase difference, θ, between the force and acceleration should be nearly 180 degrees for all frequencies. By throwing the 0 + 180° switch to 180° on the phase meter the reading should be nearly zero. This was tested and the results are shown in Table 1. The grounding of the whole system and the alignment of the force transducer were very important factors for all the measurements.

B. Displacement

A micrometer was set under the driving plate as shown in figure 15. The relative position of the moving part and the stationary plate of the capacitive transducer can be changed by turning the micrometer. At normal position, the

TABLE I

Phase Angle in Air

Freq. cps	$\emptyset$ degrees	Freq. cps	$\emptyset$ degrees
30	3.5	250	0.7
40	-1.0	300	-0.9
50	-2.5	400	1.0
60	-0.9	500	-1.0
70	-2.0	600	-0.4
80	-1.3	700	0.0
90	-2.0	800	2.0
110	-1.9	900	2.0
130	-2.0	1000	-2.8
150	-1.9	1500	-1.9
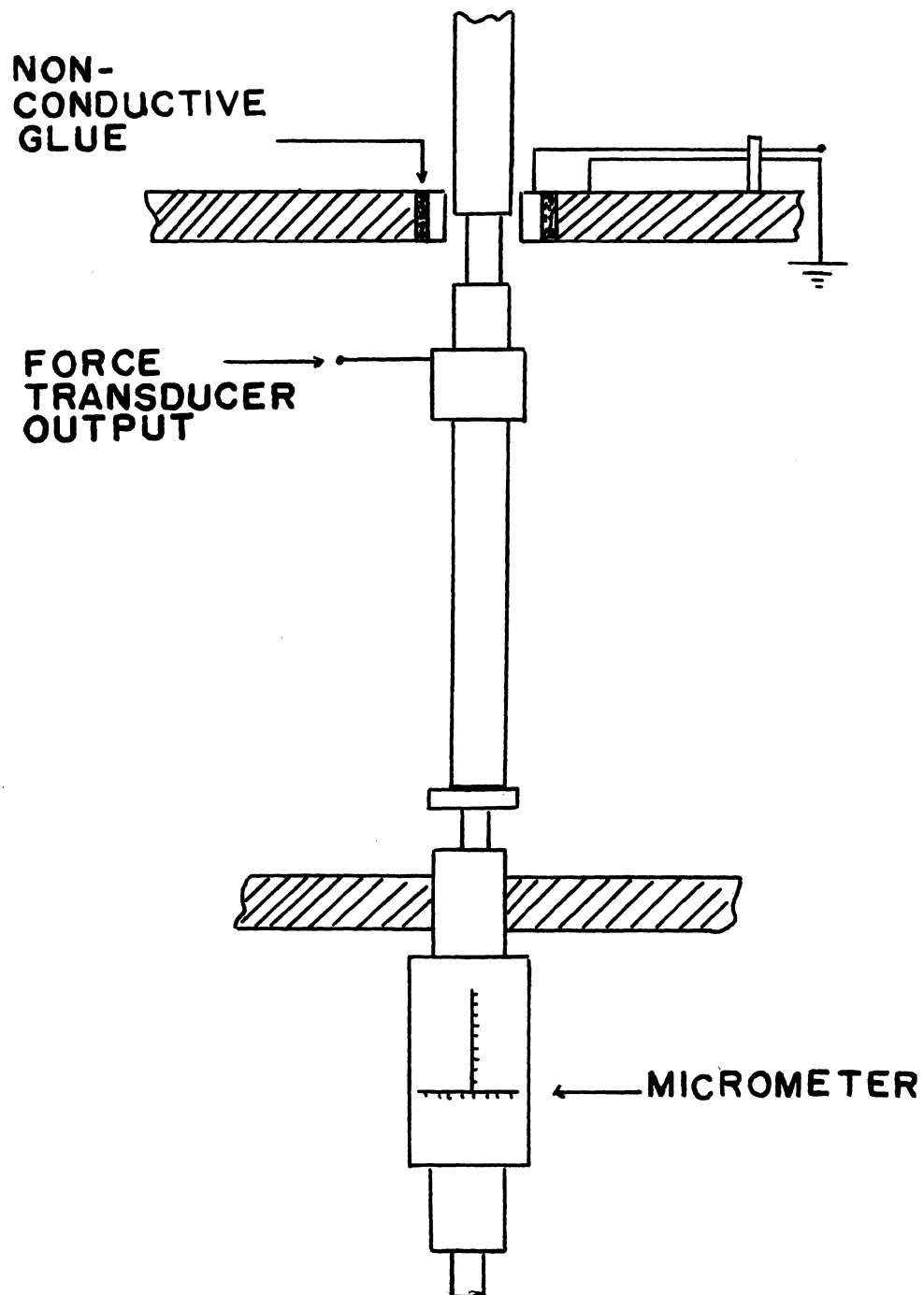
igure 15. Arrangement for Displacement Calibration

output voltage of the capacitive transducer was adjusted to zero by turning the converter tuning control. This means that the converter was tuned to the oscillator frequency. Then, the micrometer was turned to push up the driving plate. This changed the relative position of the two parts of the capacitive transducer and the capacitance between them. By recording the voltage variation measured by the oscilloscope and the reading of the micrometer, a calibration curve can be obtained as shown in figure 16. The relation was linear and a constant was obtained to convert the voltage reading to displacement as follows:

$$X = V_d \cdot K_d$$

$$K_d = \frac{1}{0.035 \times 10^3} cm/volt \tag{53}$$

where X = displacement of the driving plate

V_d = output voltage from the capacitive transducer

K_d = calibration constant for the capacitive transducer

In order to calibrate the accelerometer, a sinusoidal signal was applied to the moving assembly. The frequencies and the voltage output from the accelerometer and the capacitive transducer were recorded as shown in Table 2. For the accelerometer

$$m \, \omega^2 \, X_o = K_a \, V_a \tag{54}$$

where X_o = maximum amplitude of the displacement
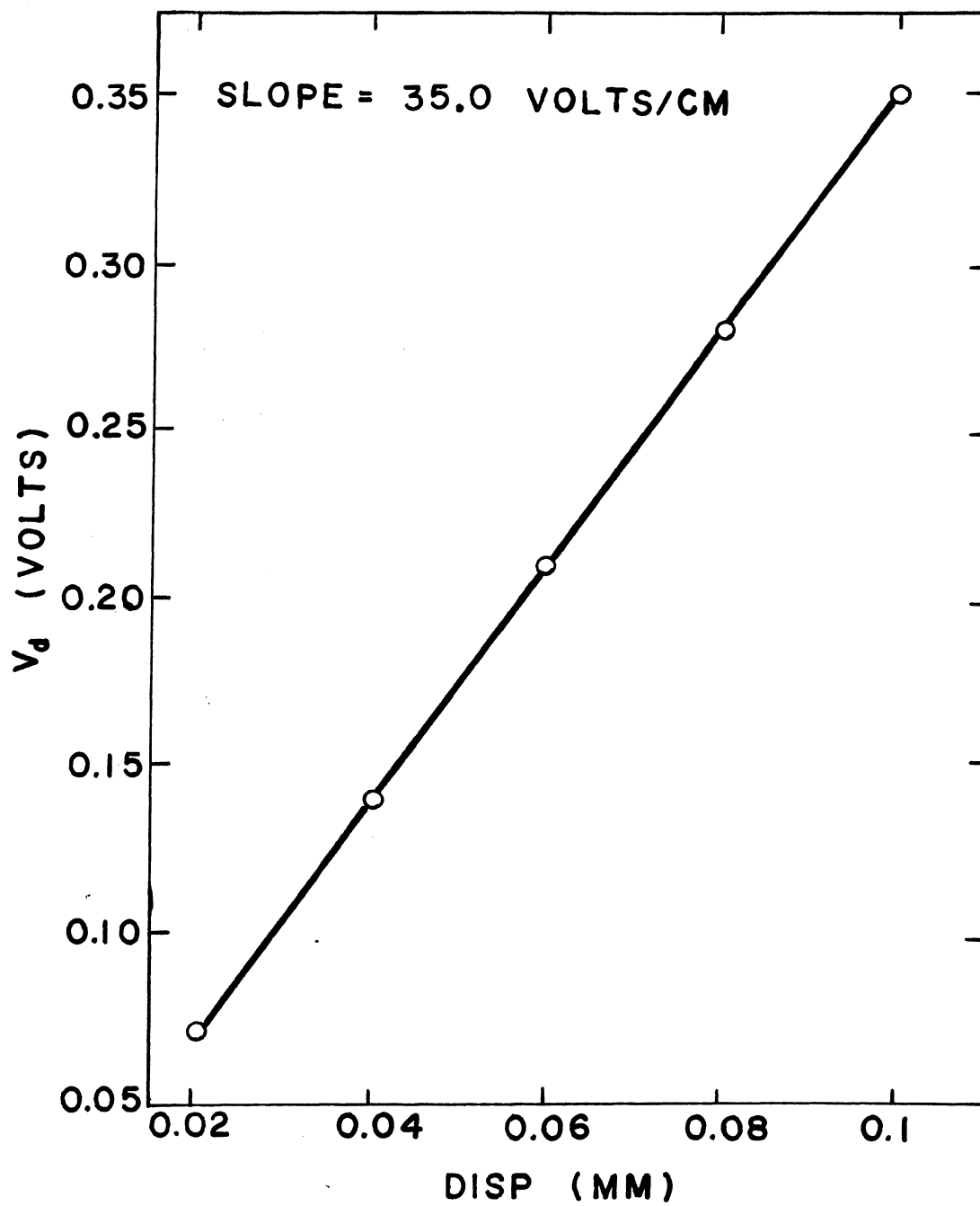
Figure 16. Capacitance Transducer Calibration Curve

TABLE 2

Calibration Constant of Accelerometer

Freq. cps	V_d volts	V_a volts	K cm/volts - sec^{-2}
70	0.325	0.2	8.98×10^3
80	0.250	0.2	9.03×10^3
90	0.199	0.2	9.08×10^3
300	0.027	0.3	9.10×10^3
400	0.020	0.4	9.03×10^3
500	0.016	0.5	9.03×10^3

ω = circular frequency, $2\pi f$

f = frequency of vibration

m = mass in the accelerometer

V_a = maximum output voltage of accelerometer

K_a = calibration constant for accelerometer

Since,

$$X_o = V_d K_d \tag{55}$$

$$K = \frac{K_a}{m} = \frac{V_d(2\pi f)^2}{V_a \times 0.035 \times 10^3} \tag{56}$$

The results for determinations of K are tabulated in Table 2. This constant K can be applied to convert the output voltage of the accelerometer to acceleration or displacement.

C. Force Calibration

A known viscosity Newtonian fluid was used to calibrate the force transducer. If a driving force acts on the force transducer causing it to oscillate sinusoidally with a displacement X as

$$X = X_o e^{i\omega t} \tag{57}$$

then

$$V = dX/dt = i\omega X_o e^{i\omega t} \tag{58}$$

The force due to the mass of the plate and the viscosity of the fluid will be

$$F = F_o e^{i(\omega t + \theta)}$$

where θ is the phase angle by which X lags F. By the definition of impedance

$$Z = \frac{F}{V} = \frac{F_o\, e^{i\theta}}{i\omega X_o} = \frac{F_o(\cos\theta + i\sin\theta)}{i\, X_o\, \omega}$$

$$= \frac{F_o(\sin\theta - i\cos\theta)}{X_o\, \omega} = \frac{F_o\, \omega}{\omega^2\, X_o}(\sin\theta - i\cos\theta)$$

$$\tag{60}$$

Since

$$F_o = V_f\, K_f \tag{61}$$

and $\theta = \pi - \phi$

where ϕ is the phase angle read out from the phase meter

V_f is the output voltage from the force transducer

K_f is the calibration constant for the force transducer

$$Z = \frac{V_f\, K_f}{V_a\, K}(\sin\phi + i\cos\phi) \tag{62}$$

The total impedance, Z, is the sum of the mechanical impedance of plate and the radiation impedance of fluid.

$$Z = Z_M + A\, Z_r \tag{63}$$

where A is the contact area between the driving plate and the fluid.

In order to eliminate the Z_M from equation 63 from which the complex viscosity of the liquid is calculated, measurement was made for different height of liquid in the sample beaker.

$$Z_1 = Z_M + A_1\, Z_r \tag{64}$$

$$Z_2 = Z_M + A_2 Z_r \tag{65}$$

substract equation 64 from equation 65

$$Z_2 - Z_1 = (A_2 - A_1)Z_r$$

$$= (h_1 - h_2)W Z_r \tag{66}$$

where h_1, h_2 are two contact lengths of the driving plate

W is the width of the driving plate

The linear relationship between the contact length and impedance was verified experimently. The result is shown in figure 17 and figure 18. The other advantage of this method is elimination of the end effect at the same time.

For a Newtonian fluid

$$Z = \frac{K_f}{K}(\frac{V_{f2}}{V_{a2}} \sin \phi_2 - \frac{V_{f1}}{V_{a1}} \sin \phi_1)$$

$$+ i (\frac{V_{f2}}{V_{a2}} \cos \phi_2 - \frac{V_{f1}}{V_{a1}} \cos \phi_1)$$

$$= (h_2 - h_1)W(1 + i) \sqrt{\frac{\omega \rho \eta}{2}} \tag{67}$$

so,

$$K_f = \frac{K(h_2 - h_1)W \sqrt{\pi f \rho \eta}}{(\frac{V_{f2}}{V_{a2}} \sin \phi_2 - \frac{V_{f1}}{V_{a1}} \sin \phi_1)}$$

$$= \frac{K(h_2 - h_1)W \sqrt{\pi f \rho \eta}}{(\frac{V_{f2}}{V_{a2}} \cos \phi_2 - \frac{V_{f1}}{V_{a1}} \cos \phi_1)} \tag{68}$$
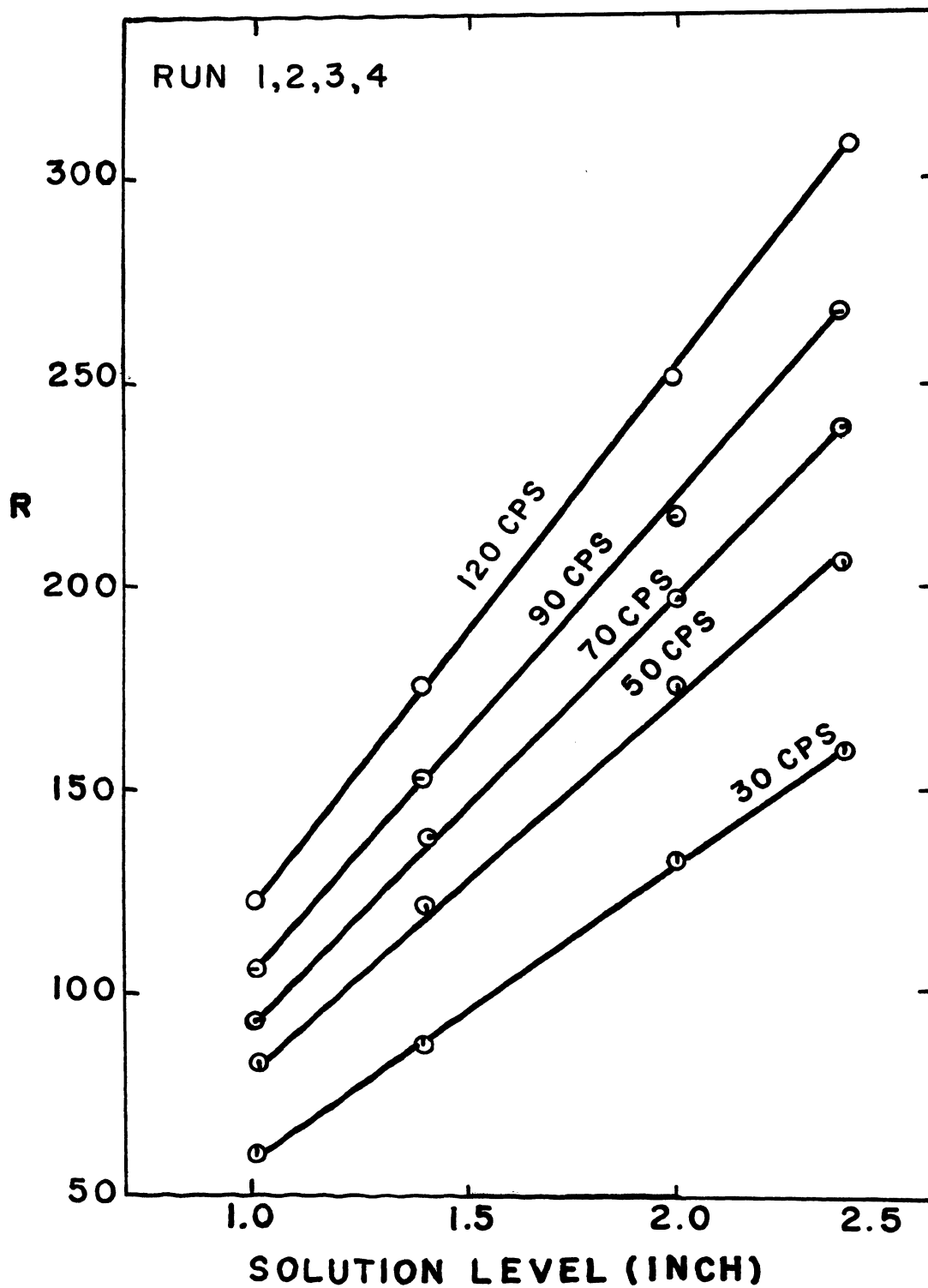
Figure 17. Resistance of Complex Impedance vs. Solution
Level for Castor Oil at 25°C
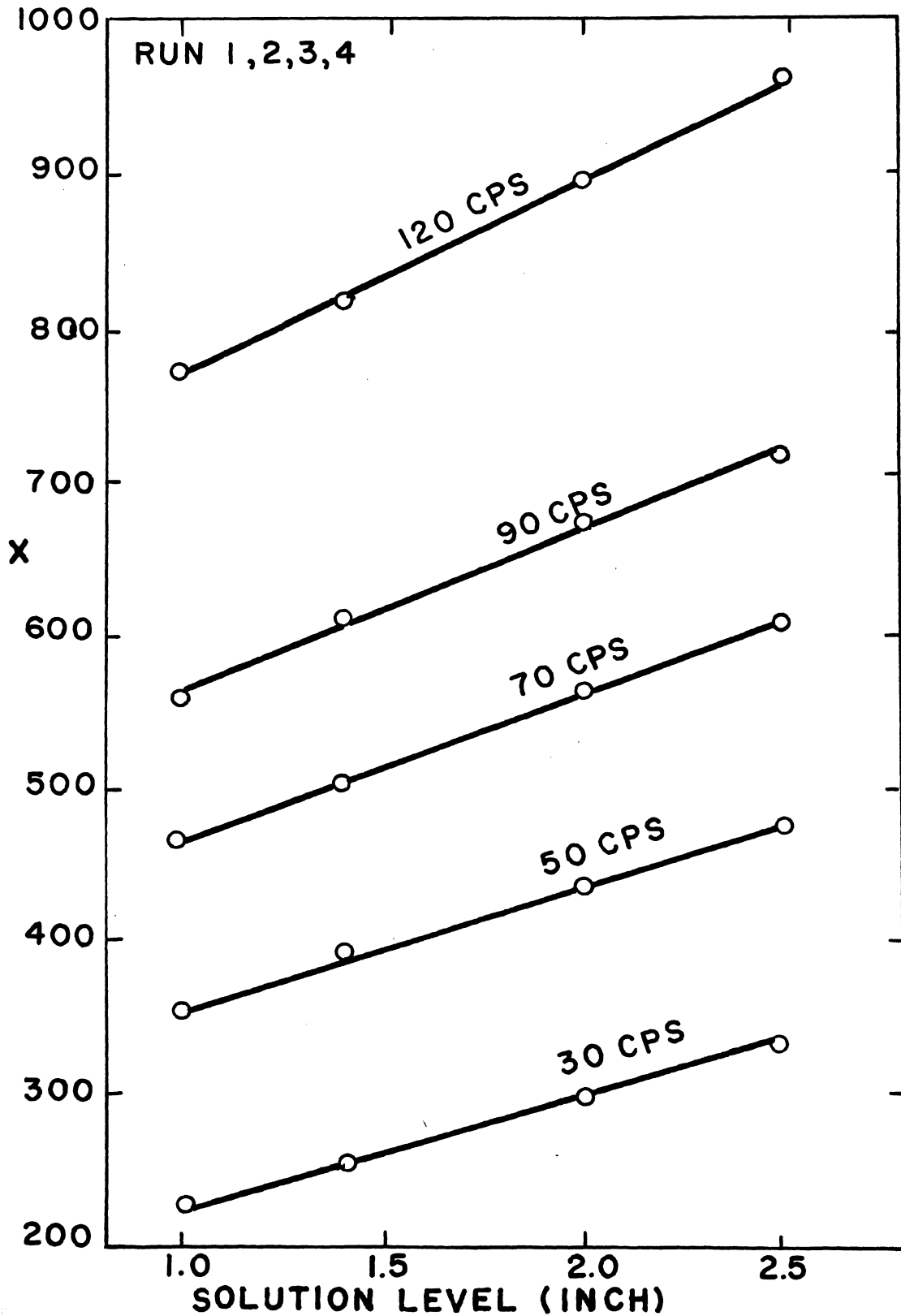
Figure 18. Reactance of Complex Impedance vs. Solution Level for Castor Oil at 25°C

This is the basic equation for calibration of the force transducer and calculation of the constant K_f. In this work, castor oil was used as the Newtonian fluid to calibrate the force transducer. The data is tabulated in Appendix B and the results are shown in Table 3. The steady viscosity was measured by the Haake Rotovisco. While taking readings, paired values for the speed factor "U" and the scale reading "S" were obtained. From these values, the viscosity (η) was obtained in centipoise.

$$\eta = U \times S \times 0.746 \tag{69}$$

The rate of shear D (sec^{-1}) on the rotor surface is given by the relationship.

$$D = \frac{B}{U} (sec^{-1}) \tag{70}$$

where B is the rate of shear factor

The results for castor oil at $22^{\circ}C$ and $31^{\circ}C$ are tabulated in Table 4. The castor oil at $31^{\circ}C$ was used to check the calibration constant K_f. The data is tabulated in Appendix B and the results are shown in figure 19.

TABLE 3

Calibration Constant of Force Transducer

Freq. cps	R x 1000	X x 1000	K_f
30.0	0.0332	0.0334	875.33
40.0	0.0367	0.0364	920.61
50.0	0.0403	0.0387	953.46
60.0	0.0416	0.0449	954.22
70.0	0.0474	0.0463	950.89
80.0	0.0494	0.0477	980.12
90.0	0.0528	0.0509	973.64
100.0	0.0578	0.0613	894.24
120.0	0.0630	0.0601	946.92
140.0	0.0645	0.0621	995.58
250.0	0.0910	0.0935	912.07
300.0	0.0973	0.1000	934.15
400.0	0.1168	0.1281	871.0
600.0	0.1394	0.1243	991.6
800.0	0.1574	0.1661	931.19

Mean Value = 939.00

Deviation

from Mean = 7%

TABLE 4

Steady Shear Viscosity of Castor Oil

Temperature °C	R	S	η (cp)
22°C	81	15.2	922
	54	22.9	925
	27	46.0	926
	18	69.2	930
31°C	81	8.1	486
	54	12.0	484
	27	24.0	484
	18	35.9	484
	9	72.0	485
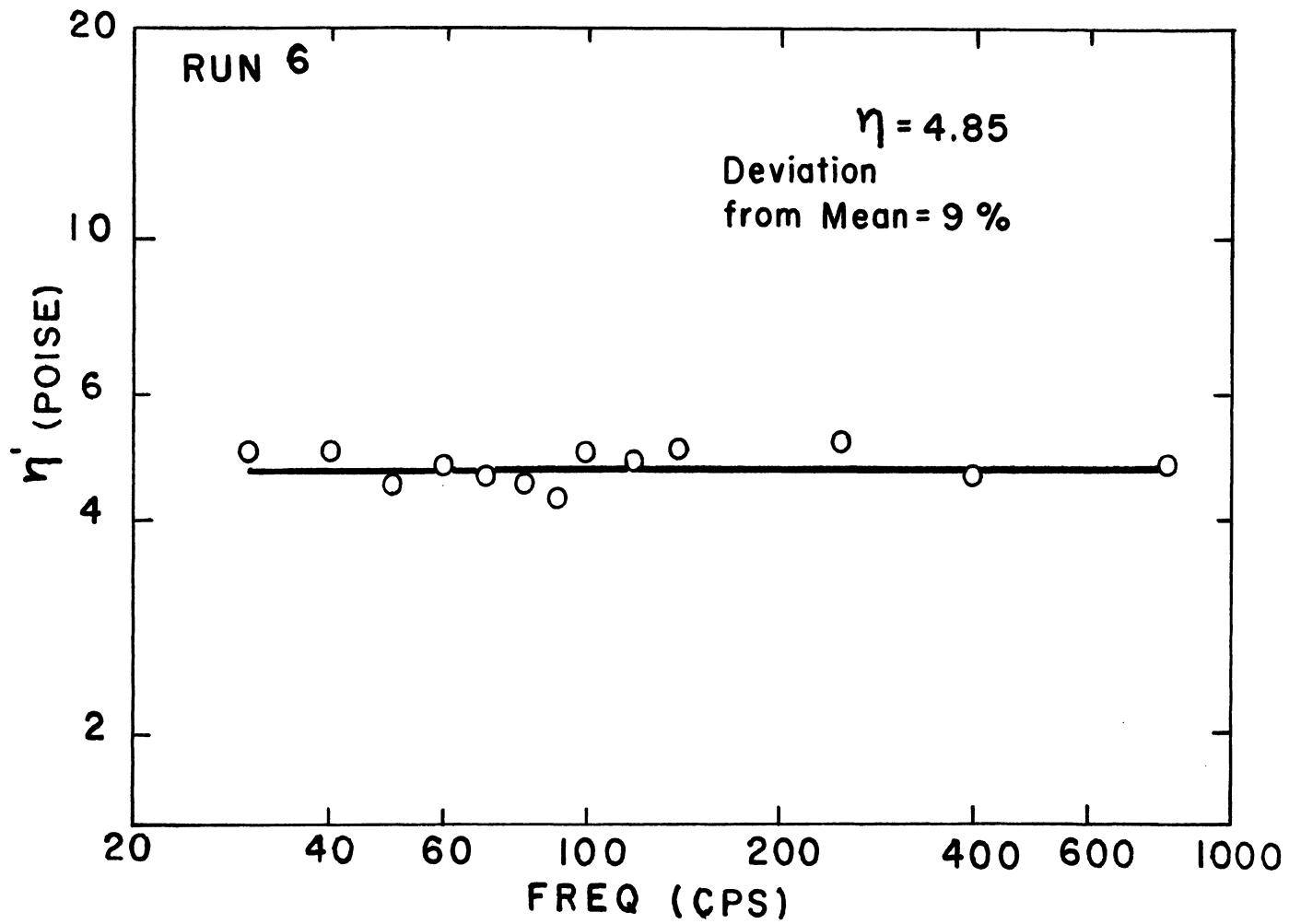
Figure 19. Complex Viscosity Measurements; Castor Oil at 31°C

V. MATERIALS

Two types of material were used in this study. The first type was polymer solutions which included polyiso-butylene (PIB) L-80, PIB L-200, and polydimethyl siloxane (SR) 130. The solution of the polymers in the solvents was accomplished by using a magnetic stirrer in bottles. The most concentrated solutions were first prepared, then these stock solutions were then added to solvent in the proper amount to produce the desired concentrations. Since high concentrations were required, three weeks or longer time were needed to insure the complete dissolution of the solute. The specifications of solvents and polymers are given in Appendix A.

The second type of material was greases which included the NLGI Grease A and Mobilgrease 24. The properties of these greases are given in Table 5.

TABLE 5

Grease Properties

	NLGI System A	Mobilgrease 24
Color	Brown, Transparent	Red, Opaque
Penetration, Unworked	301	295
60 x Worked	297	295
Thickener Type	Li Hydroxysterarate	Organic Pigment
Fluid Type	Naphthenic M. O.	Silicone
K.V., @ 100°F	68.7	77.5
@ 210°F	7.00	30.0
Viscosity Index(D567)	48	155
Additives	Antioxidant	Antioxidant
		Corrosion
		Inhibitor

VI. RESULTS

A. Steady Shear Measurements

The results of steady shear measurements are shown in figures 20-25. Each figure indicates solution concentration, solvent, steady shear viscosity and steady shear rate. The data are tabulated in Tables 6-10.

B. Dynamic Measurements

For a viscoelastic liquid, the impedance is $(i \omega \rho \eta^*)^{\frac{1}{2}}$ (see equation 42). When combined with equation 66, the complex viscosity was obtained as:

$$\eta' = \frac{2 \, \Delta X \times \Delta R}{\omega \, \rho} \tag{71}$$

$$\eta'' = \frac{\Delta R^2 - \Delta X^2}{\omega \, \rho} \tag{72}$$

$$\text{where } \Delta R = \frac{K_f \, \omega}{(h_2 - h_1) W \, K} \left(\frac{V_{f2}}{V_{a2}} \sin \phi_2 - \frac{V_{f1}}{V_{a1}} \sin \phi_1 \right)$$

$$\Delta X = \frac{\omega \, K_f}{(h_2 - h_1) W \, K} \left(\frac{V_{f2}}{V_{a2}} \cos \phi_2 - \frac{V_{f1}}{V_{a1}} \cos \phi_1 \right)$$

The results of the dynamic measurements are shown in figures 26-36. Computer printouts of the data and the numerical results for complex viscosity and the complex modulus are listed in Appendix B.
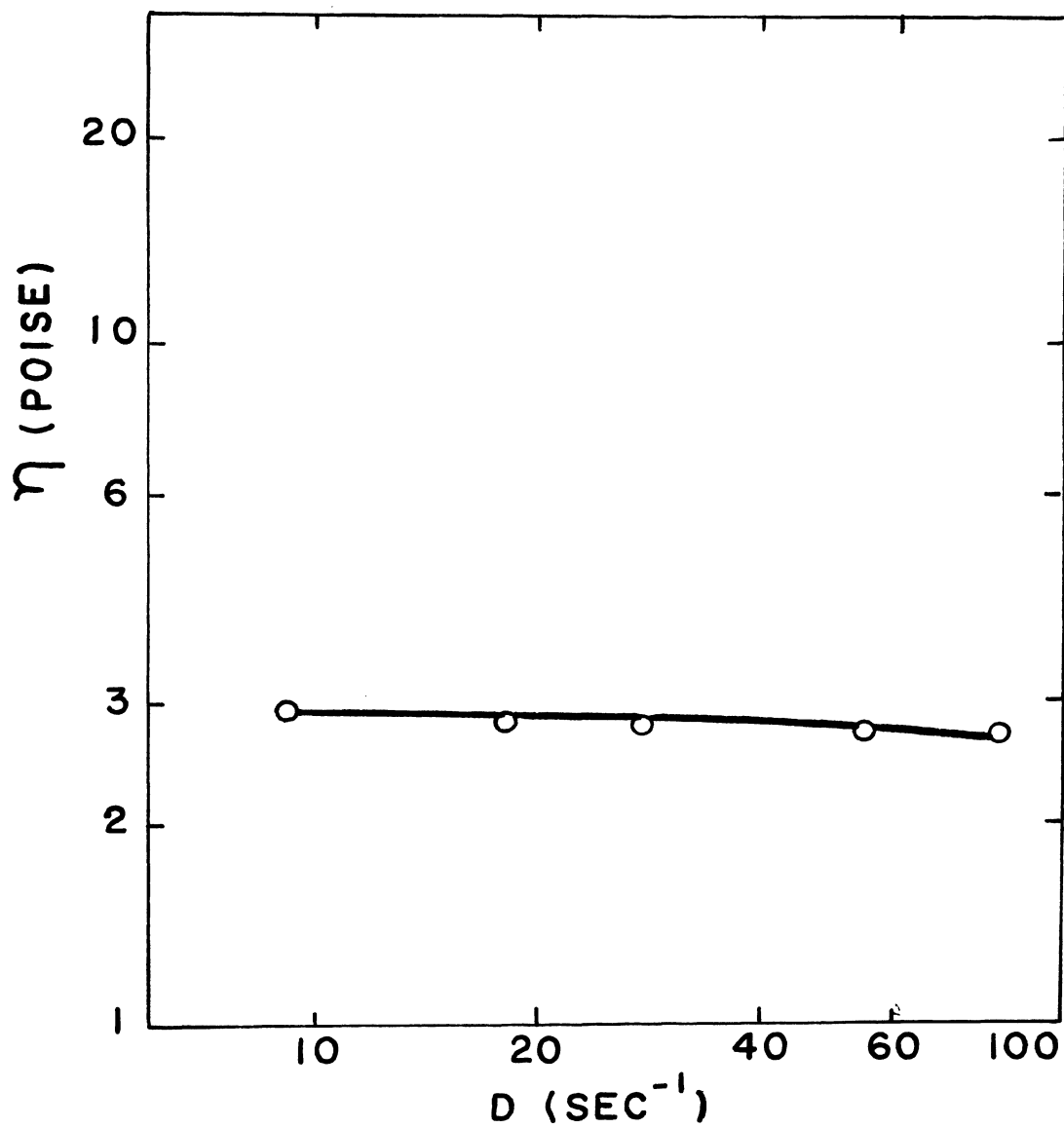
Figure 20. Steady Shear Viscosity Measurements;
3 g/Dl PIB L-80 at 25°C
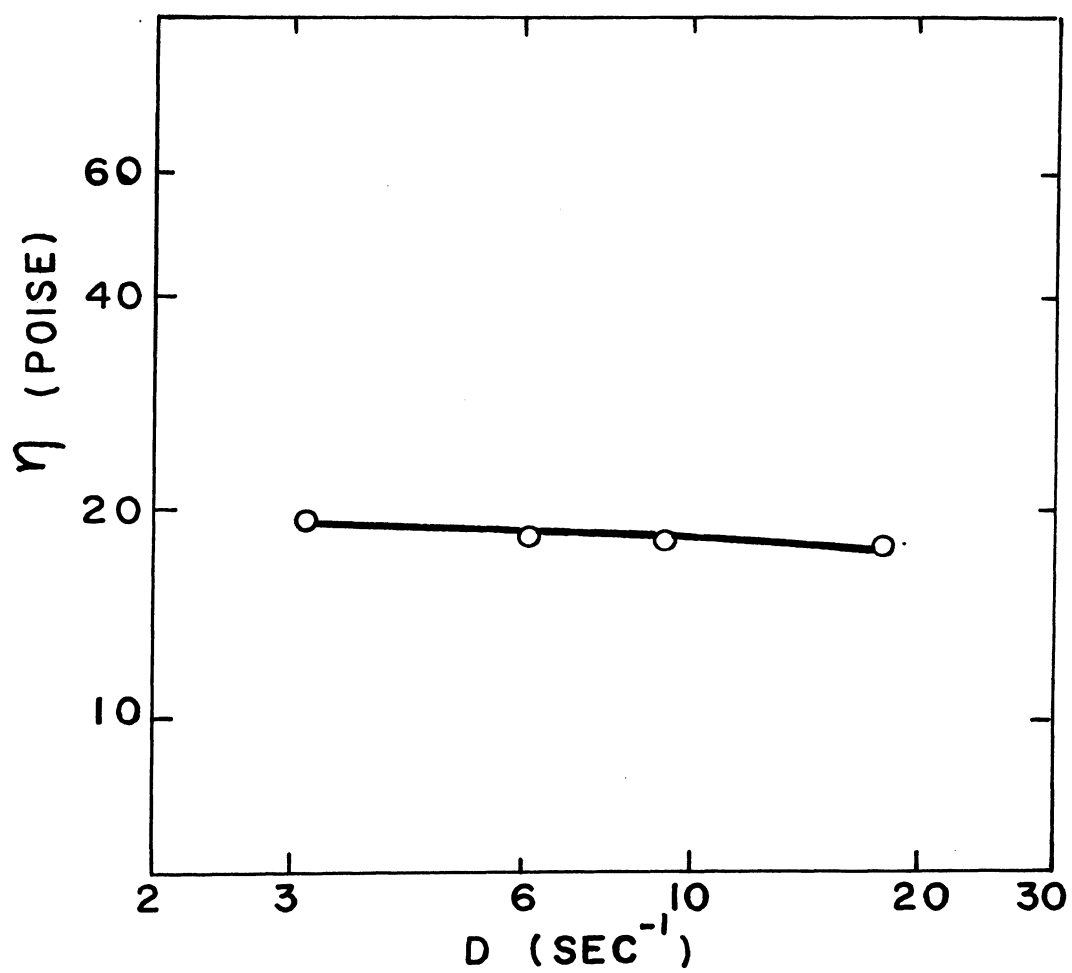
Figure 21. Steady Shear Viscosity Measurements;
5 g/Dl PIB L-80 at 25°C
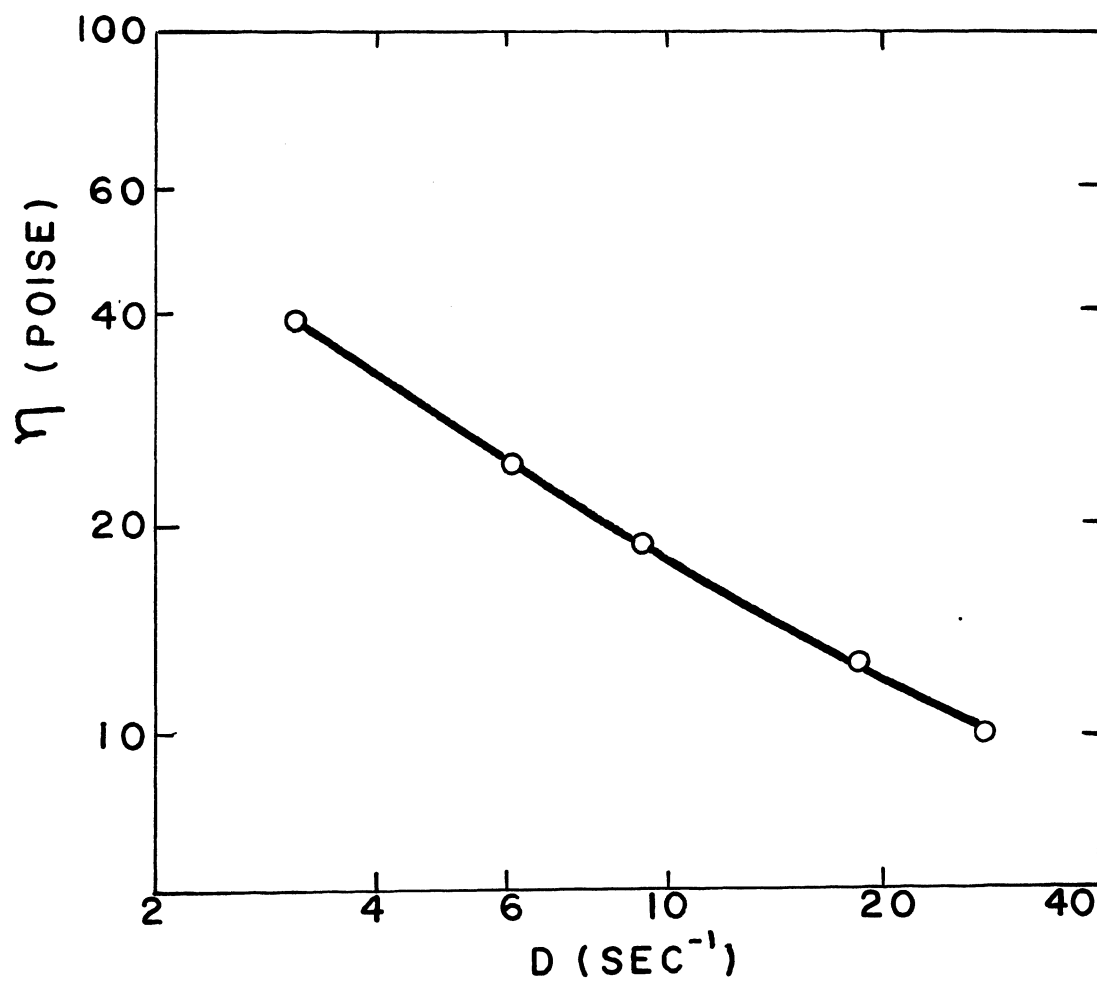
Figure 22. Steady Shear Viscosity Measurements;
17% NLGI Grease at 25°C
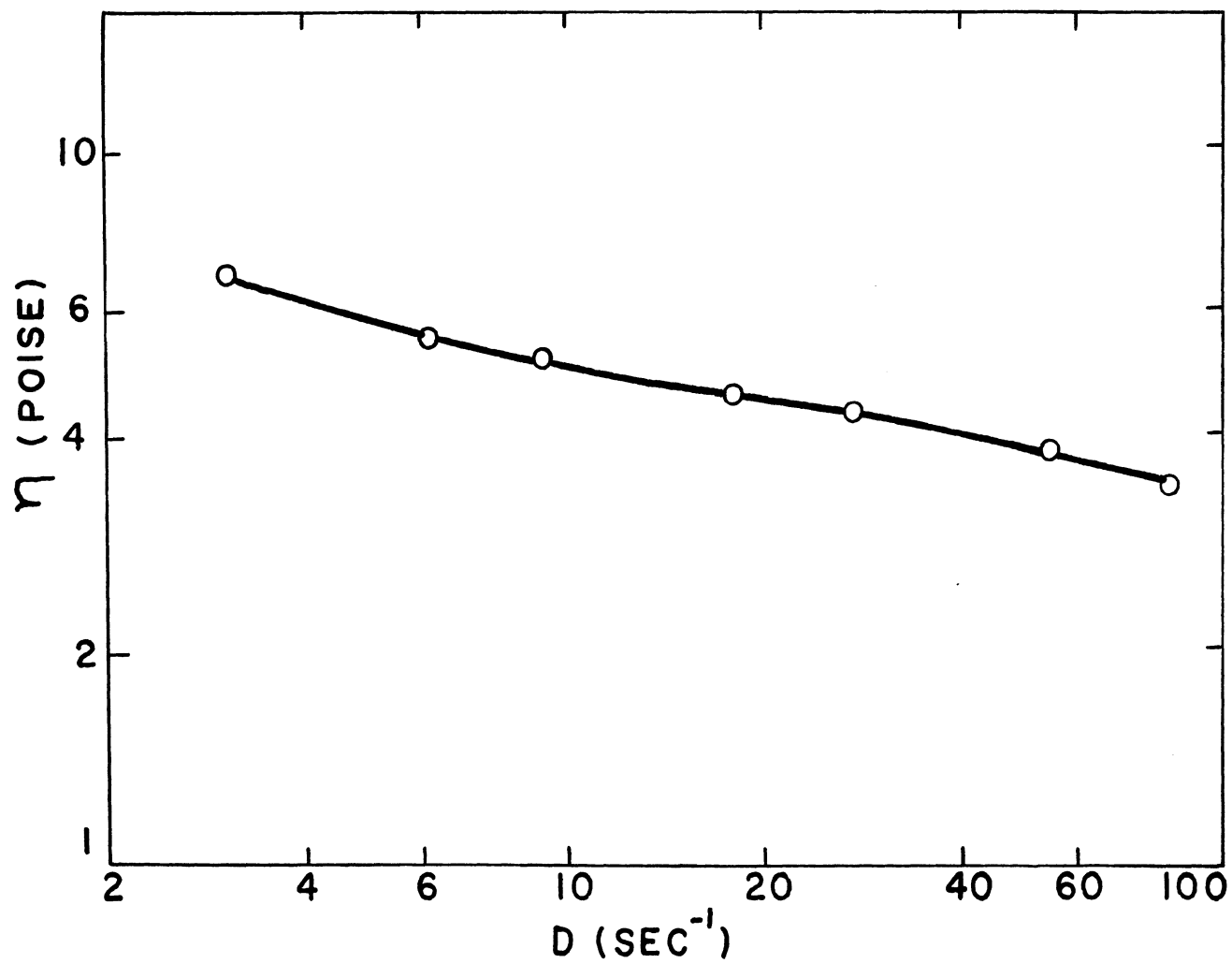
Figure 23. Steady Shear Viscosity Measurements; 25% Mobilgrease 24 at 25°C
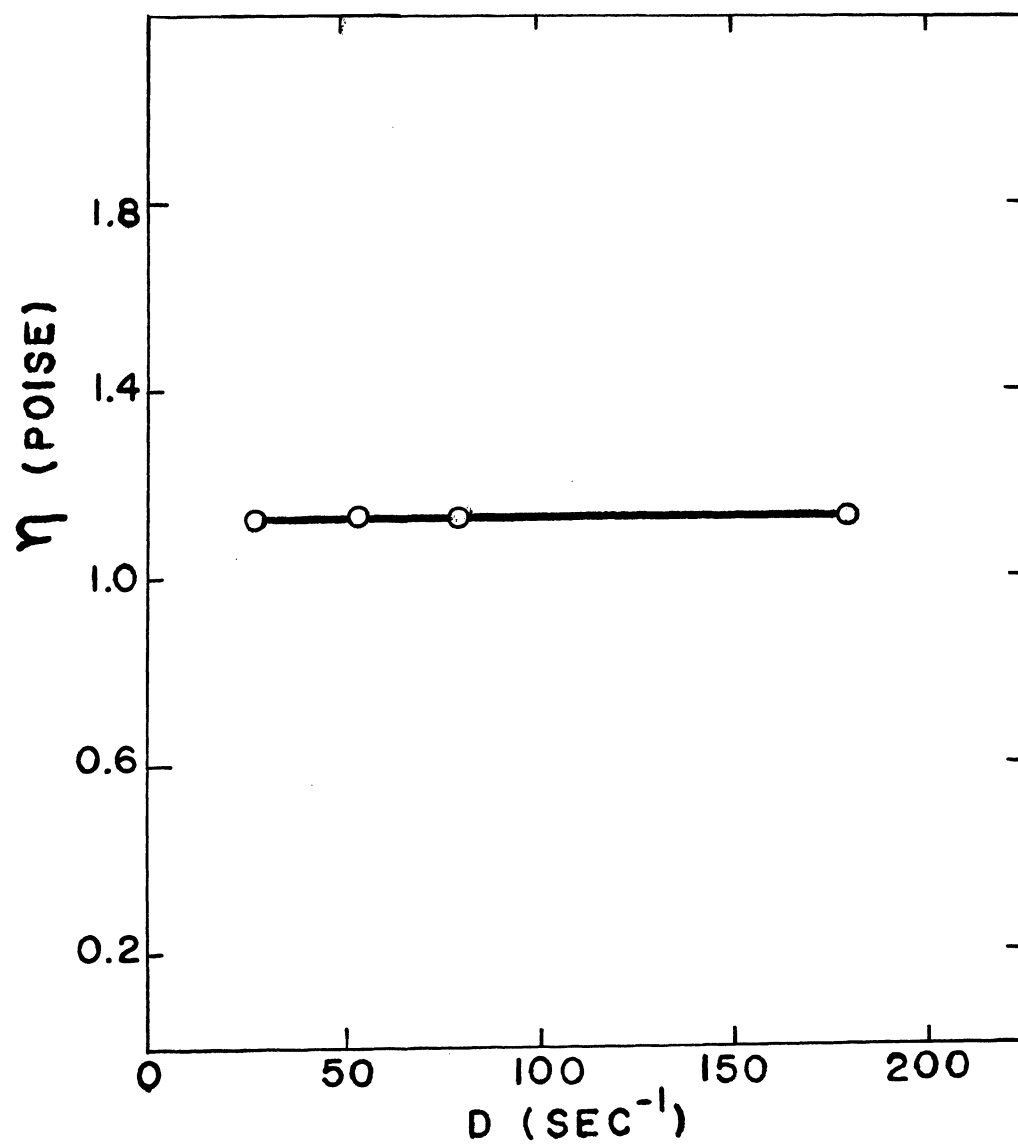
Figure 24. Steady Shear Viscosity Measurements;
Silicon Base Oil at 25°C
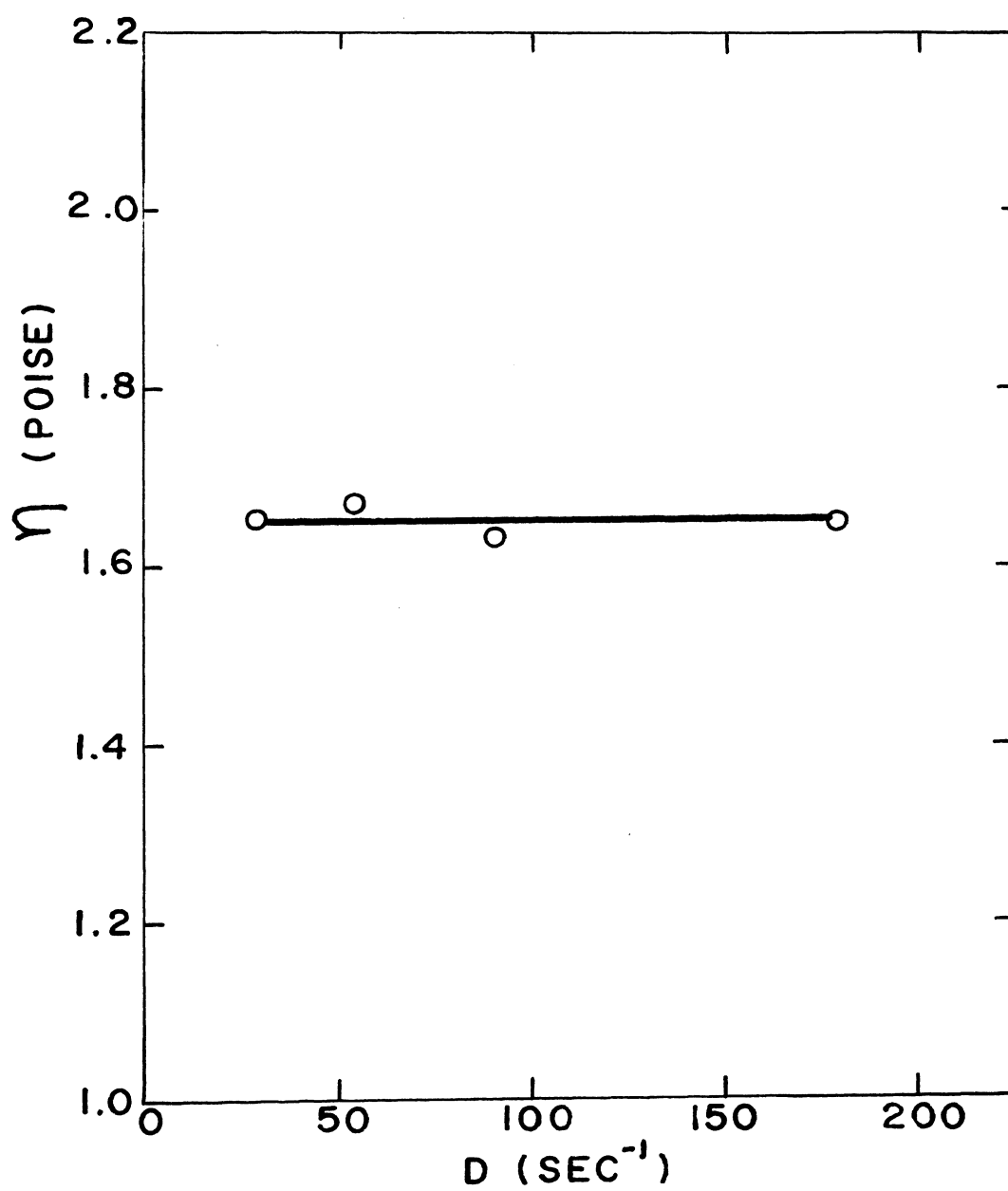
Figure 25. Steady Shear Viscosity Measurements;
NLGI Oil at 25°C

TABLE 6

Steady Shear Viscosity for PIB L-80 25°C

Conc.	U	S	D (sec^{-1})	η (poise)
3 g/Dl	54	7.10	9.2	2.86
	27	13.7	18.4	2.76
	18	20.3	27.6	2.72
	9	40.0	55.2	2.69
	6	59.5	83.6	2.66
5 g/Dl	162	16.0	3.07	19.4
	81	30.5	6.14	18.45
	54	45.0	9.2	18.1
	27	87.6	18.4	17.7

TABLE 7

Steady Shear Viscosity for NLGI Grease at 25°C

Conc.	U	S	D (sec^{-1})	η (poise)
17%	162	32.5	3.07	39.3
	81	39.9	6.14	24.1
	54	45.7	9.2	18.4
	27	62.2	18.4	12.5
	18	73.8	27.6	9.92

TABLE 8

Steady Shear Viscosity for Mobilgrease 24 at 25° C

Conc.	U	S	D (sec^{-1})	η (poise)
25%	162	5.5	3.07	6.66
	81	9.1	6.14	5.50
	54	11.8	9.2	5.15
	27	22.8	18.4	4.60
	18	32.0	27.6	4.30
	9	54.0	55.2	3.8
	6	78.6	83.6	3.4

TABLE 9

Steady Shear Viscosity for Silicon Base Oil at 25°C

U	S	D $(\sec^{-1})$	η (poise)
18	8.3	27.6	1.12
9	17.0	55.2	1.14
6	25.4	83.6	1.13
3	51.0	187.2	1.14

TABLE 10

Steady Shear viscosity for NLGI Oil at $25^{\circ}C$

U	S	D (sec^{-1})	η (poise)
18	12.3	27.6	1.65
9	25.0	55.2	1.67
6	36.5	83.6	1.63
3	73.5	187.2	1.65
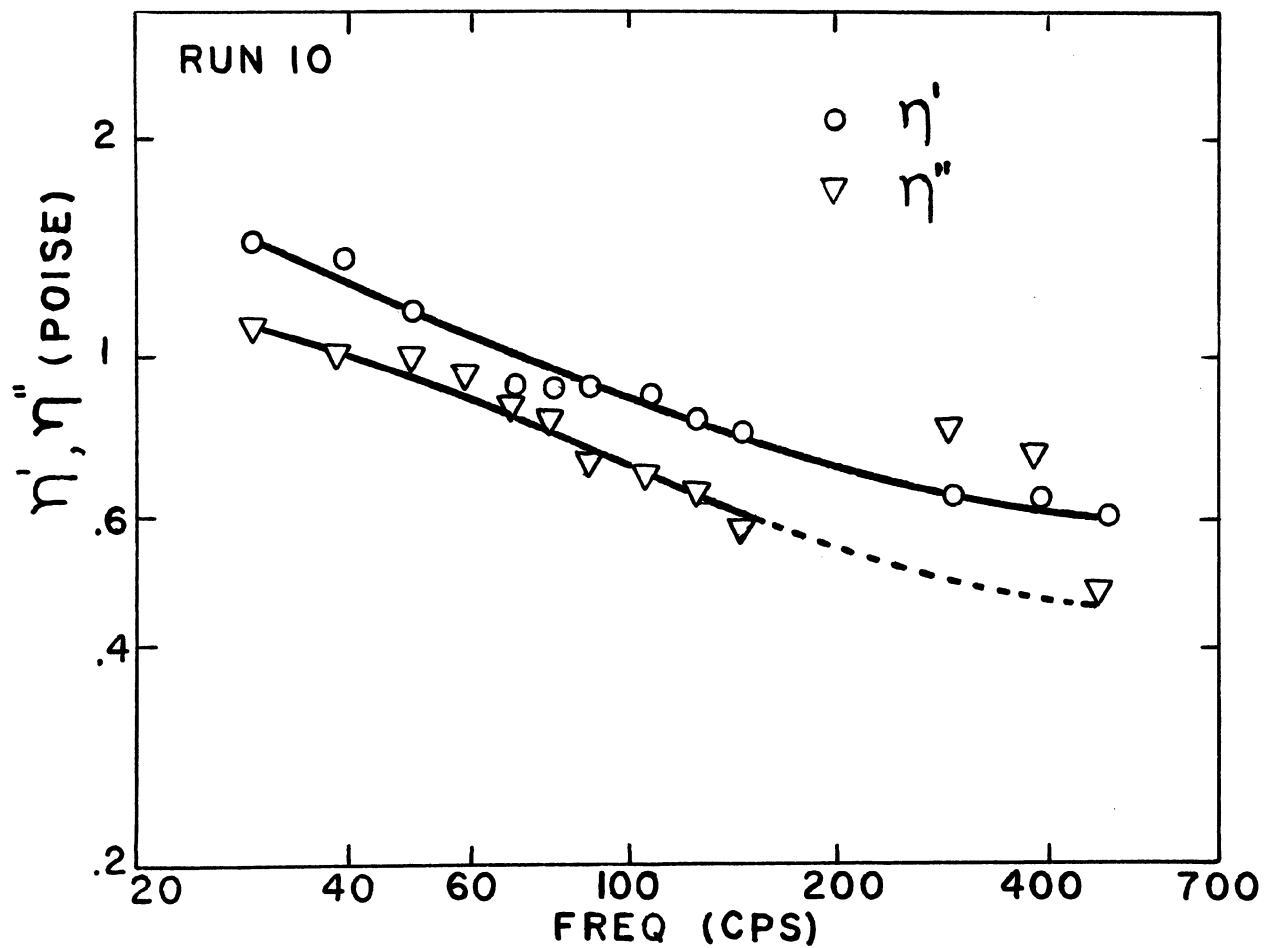
Figure 26. Complex Viscosity Measurements; 3 g/Dl PIB L-80 at 25°C
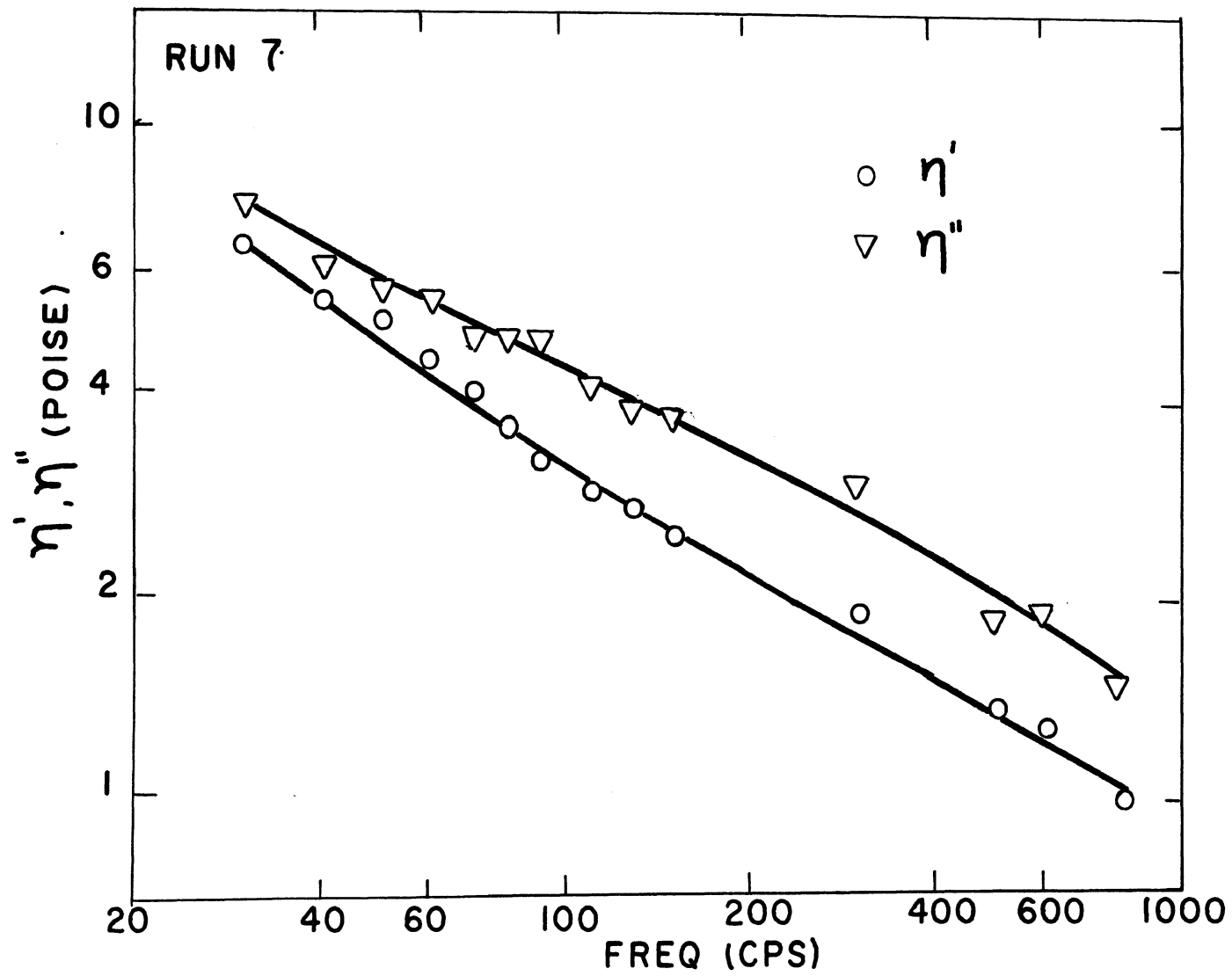
Figure 27. Complex Viscosity Measurements; 5 g/Dl PIB L-80 at 20.2°C
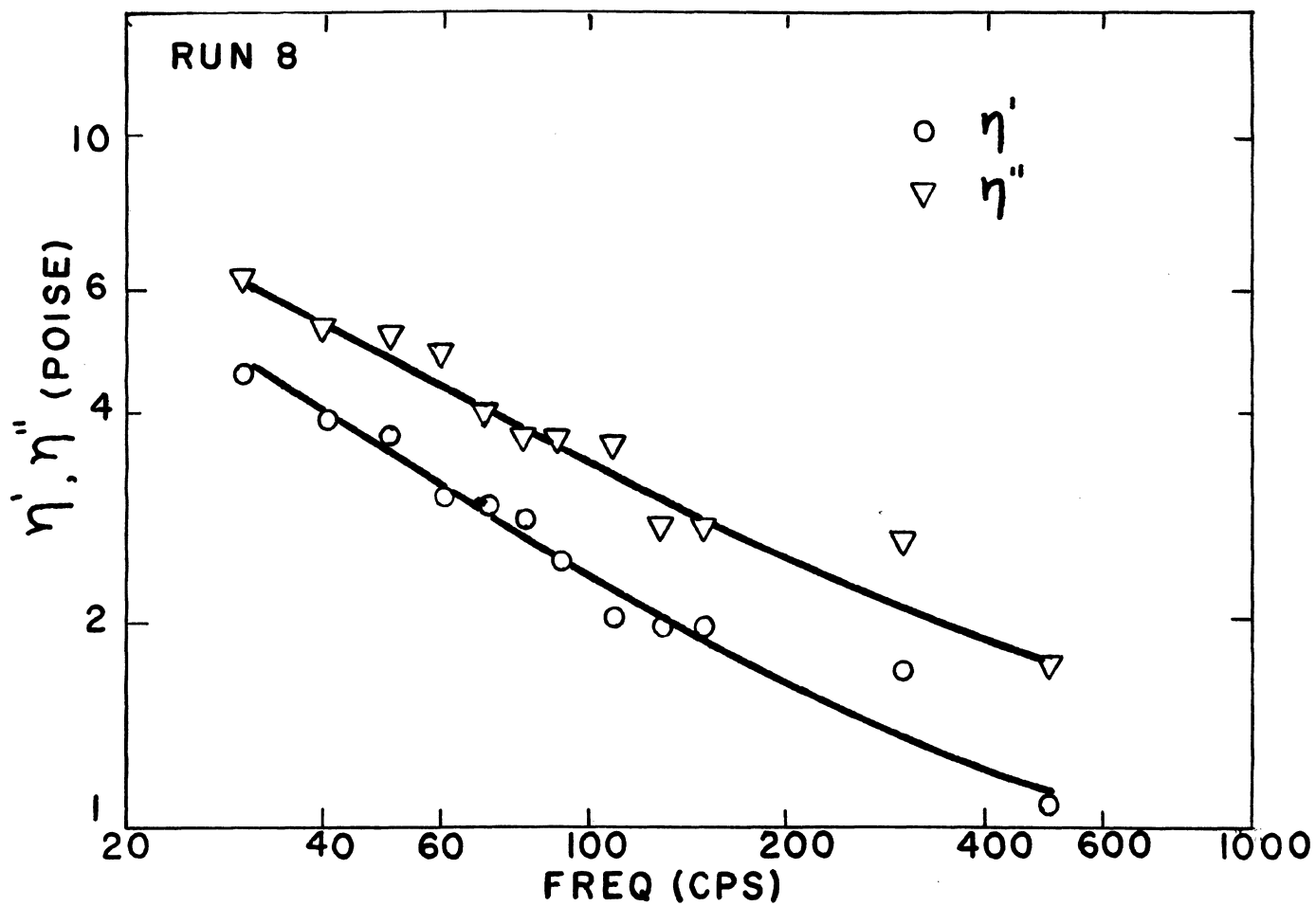
Figure 28. Complex Viscosity Measurements; 5 g/Dl PIB L-80 at 25°C
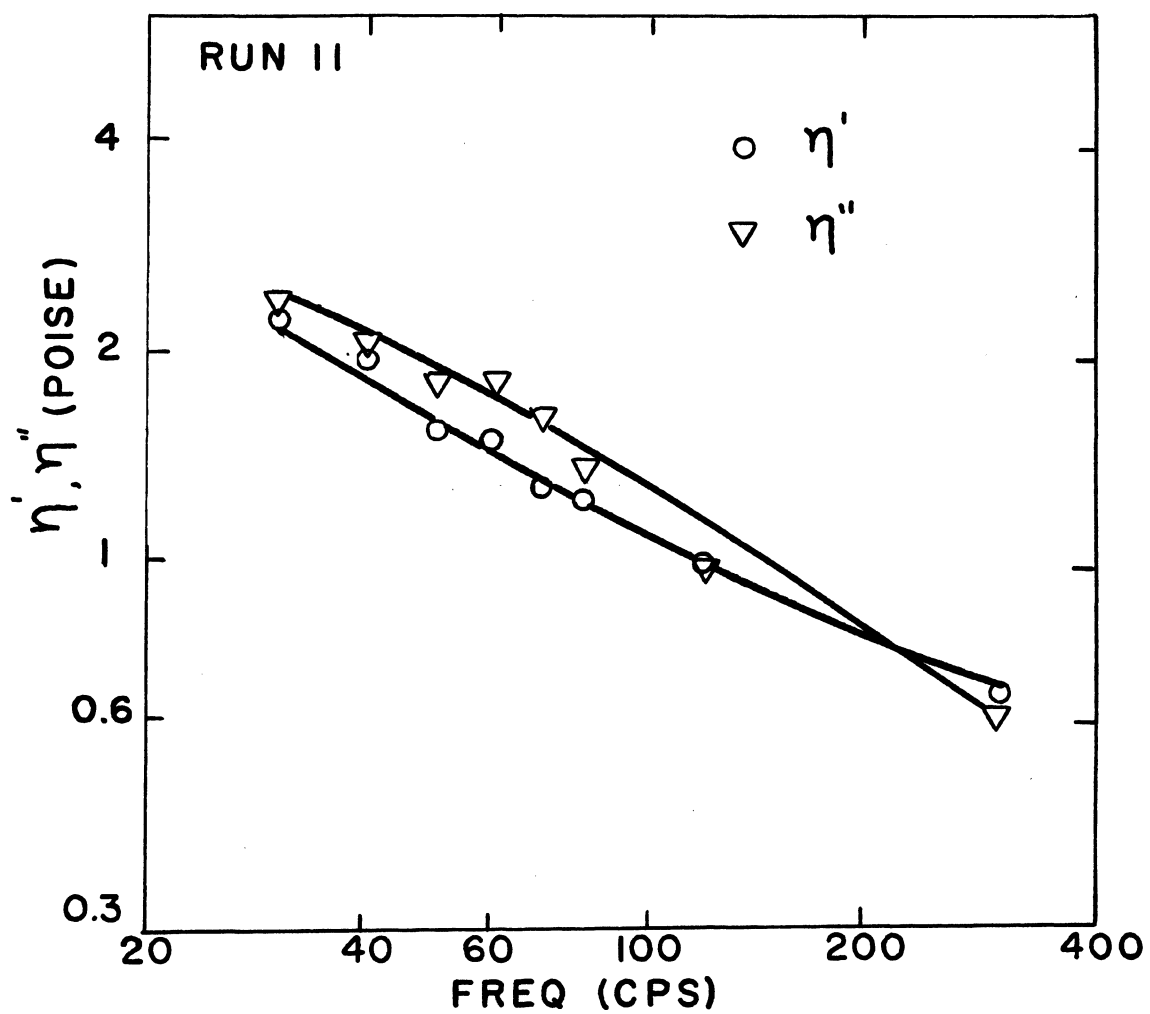
Figure 29. Complex Viscosity Measurements;

2 g/Dl PIB L-200 at 25°C
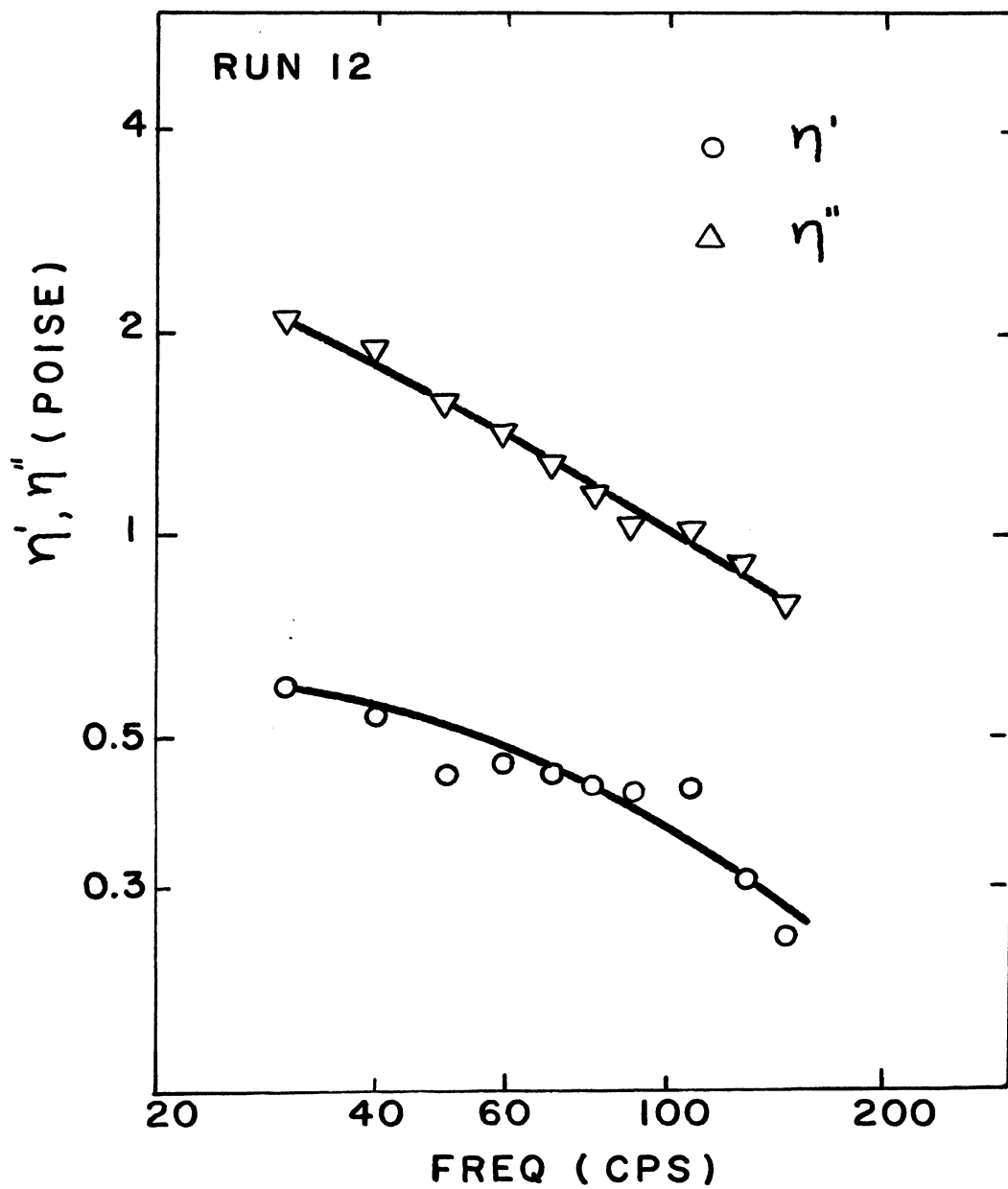
Figure 30. Complex Viscosity Measurements;
2.5 g/Dl SR 130 at 25°C
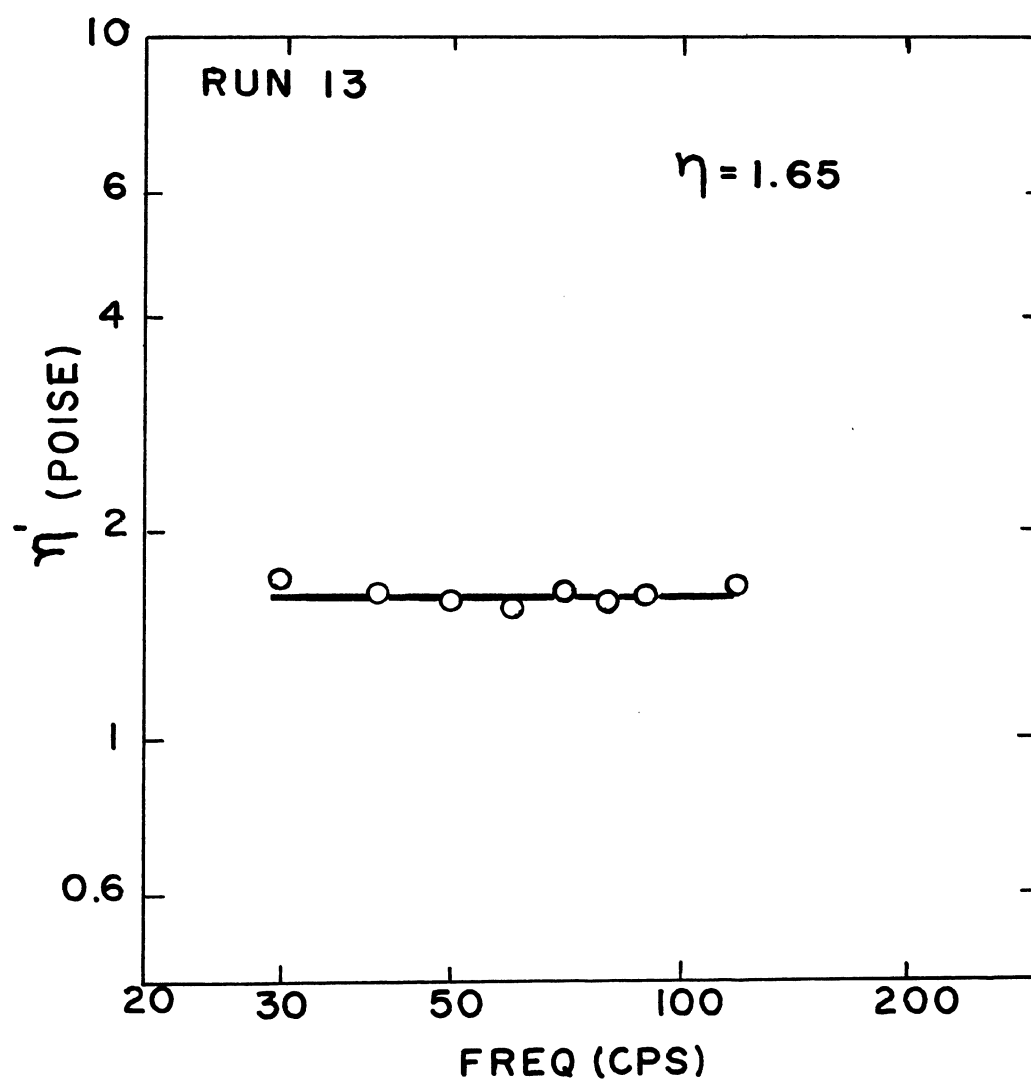
Figure 31. Complex Viscosity Measurements;
NLGI Reference Oil at 25°C
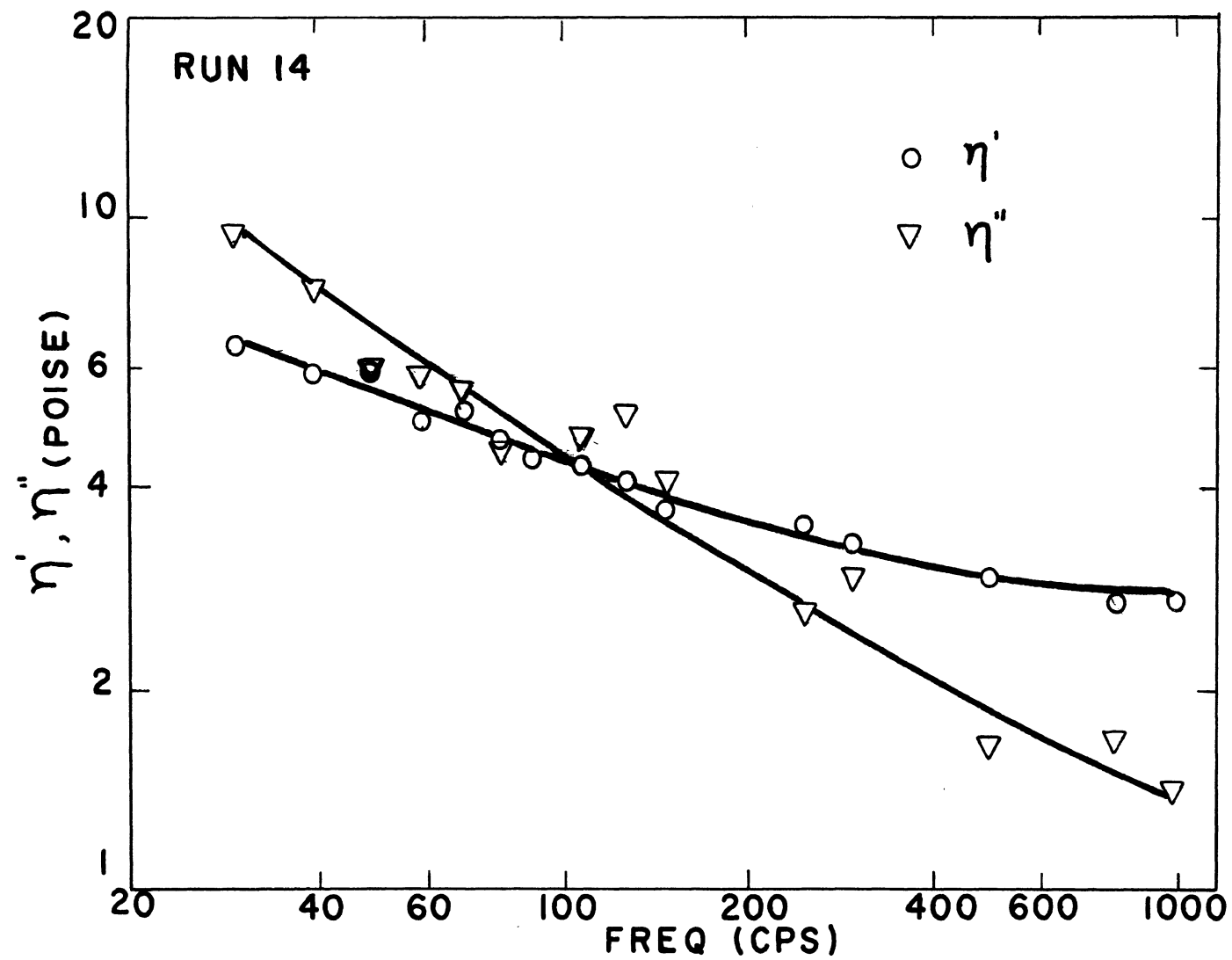
Figure 32. Complex Viscosity Measurements; 17% NLGI Grease at 25°C
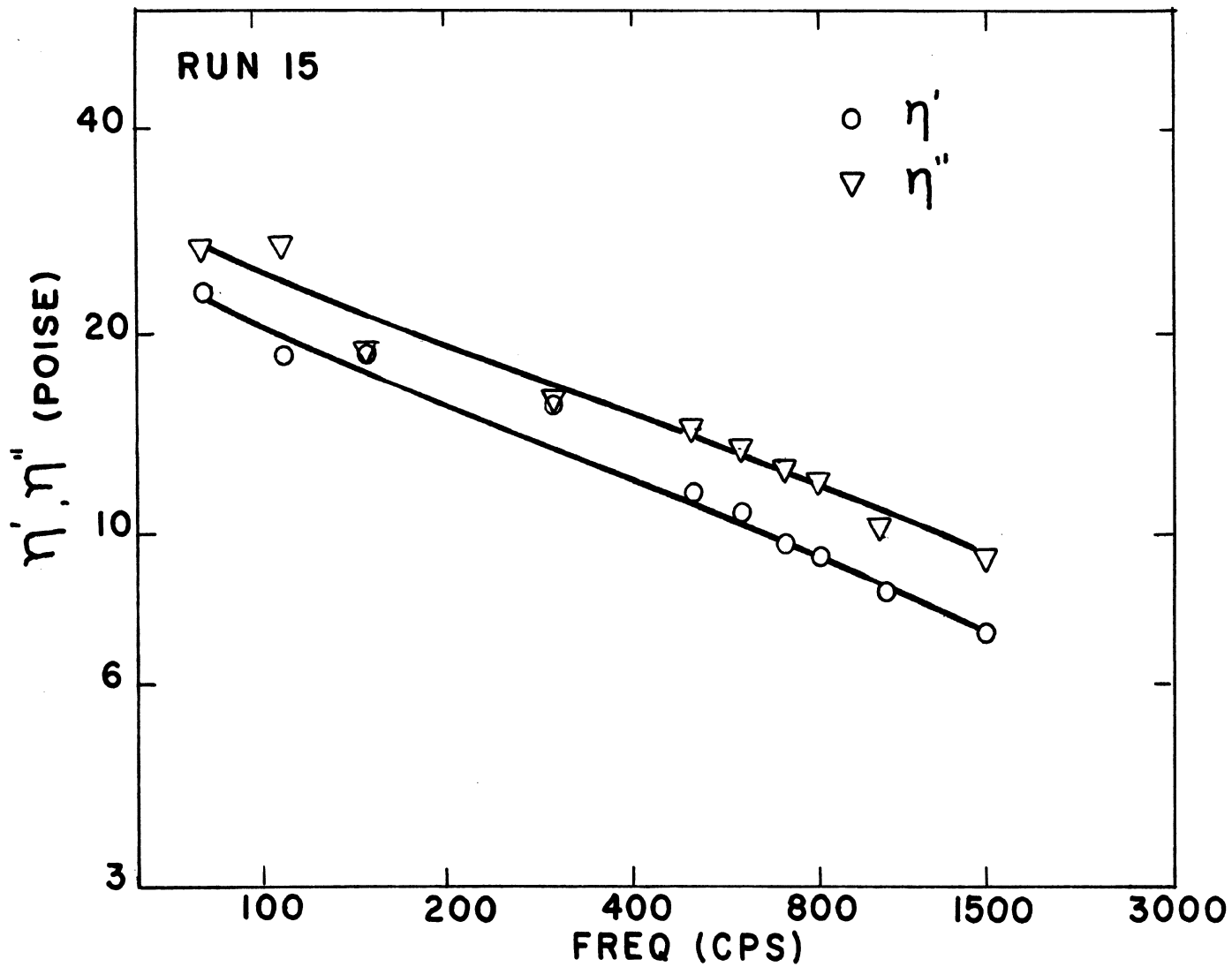
Figure 33. Complex Viscosity Measurements; 50% NLGI Grease at 25°C
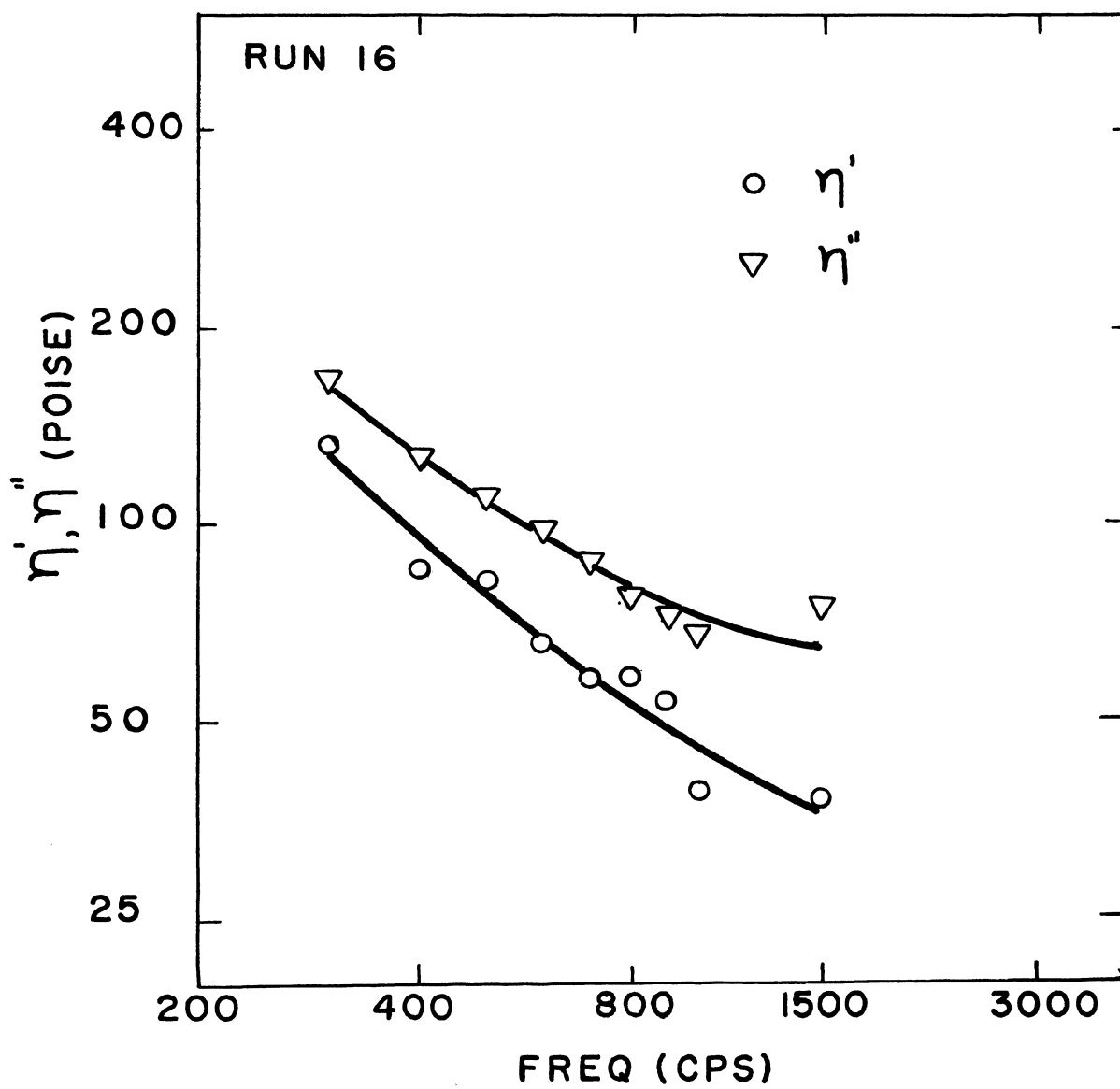
Figure 34. Complex Viscosity Measurements;
NLGI Grease at 25°C
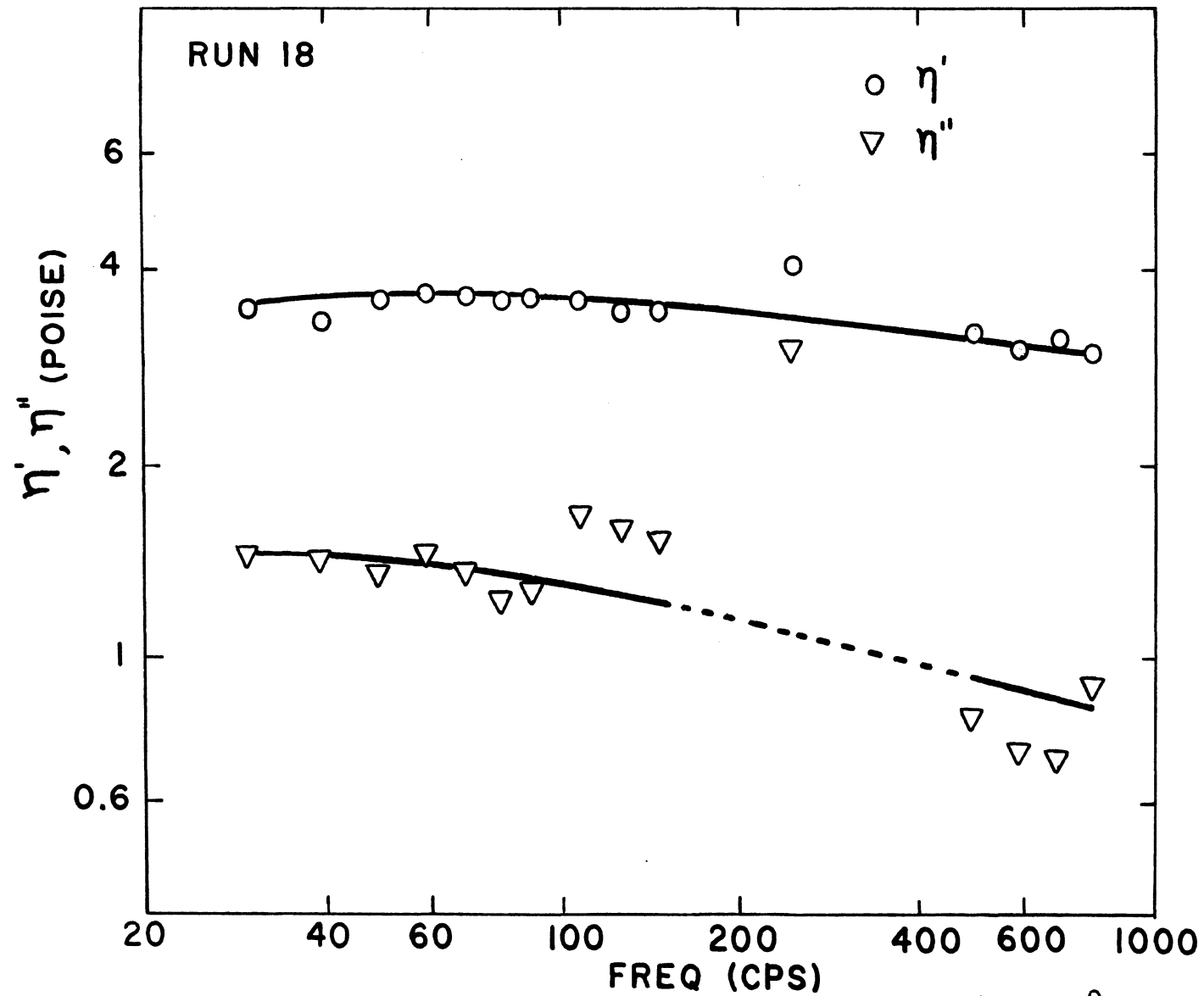
Figure 35. Complex Viscosity Measurements; 25% Mobilgrease 24 at 25°C
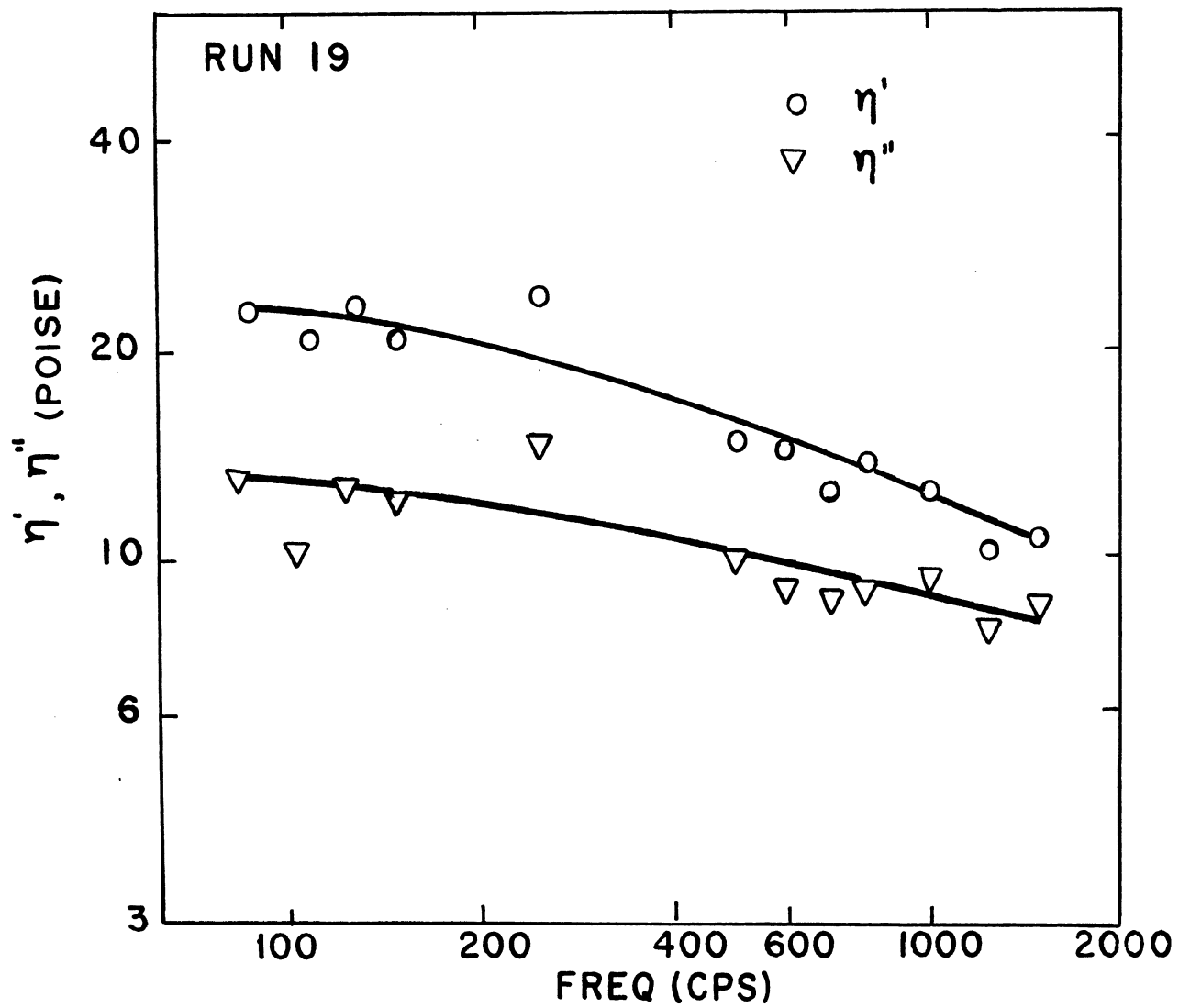
Figure 36. Complex Viscosity Measurements; 50% Mobilgrease 24 at 25°C

VII. DISCUSSION

A. Capability of the Instrument

All the instruments for dynamic measurements mentioned before were limited to very small strain amplitude, 10^{-4} - 10^{-6} cm, except Philippoff's. But Phillippoff's instrument was only suitable for extremely low frequencies, 3×10^{-5} to 10 Hz. The dynamic instrument described here has the capability for relatively large strain amplitude; it extends the measurement range from linear viscoelasticity to non-linear viscoelasticity. The equation for calculating strain amplitude of this instrument is

$$X_o = \frac{V_a}{\omega^2} \times 9.05 \times 10^3 \tag{73}$$

At 30 Hz the largest V_a value to be obtained was 0.5 volt. So the strain amplitude was 1.27×10^{-1} cm. Since the amplitude is inversely proportional to the square of frequency, only very small amplitude strains can be measured at high frequency.

The frequency range of this apparatus was 30 Hz - 1500 Hz. The low frequency limit was due to the force transducer which can maintain a linear piezoelectric effect only at higher frequencies. To extend the low frequency limit for this apparatus, another type force transducer would have to be developed, such as the force transducer used in the

Birnboim apparatus. The capacitive displacement transducer
is very suitable for the lower frequency range to measure
the displacement, and the phase angle measurement would
offer no difficulty.

The impedance of the force transducer itself is propor-
tional to the frequency, but the solution impedance is
proportional only to the square root of frequency. At
higher frequency, the impedance due to the solution is rela-
tively smaller than the impedance due to the mass of the
driving plate. This made the measurement inprecise and
limited the high frequency range. At 1000 cps, the un-
certainty can be up to $\pm 50\%$ for dynamic viscosity at the 5
poise level. This also limited the low viscosity that could
be measured by this apparatus. Elimination of the mass
effect on impedance could be obtained if two piezoelectric
crystals of the same sensitivity could be obtained. One
could be used for the transducer, and the other could be
mounted on the top of the force transducer with a weight of
the same mass as the driving plate glued on it. The output
terminals of the two crystals could be connected in such a
way as to cancel out the impedance due to the mass before
the output is amplified. In this case, when the force trans-
ducer vibrates in air, the output should be equal to zero
for all frequencies. It would also make measurements in
very dilute solutions with very low viscosity possible.

From equation 40, the real part of velocity is[31]

$$U = U_o \, e^{-\beta Z} \cos(\omega t - \beta Z) \tag{74}$$

This represents a wave of transverse vibrations propagated from the boundary with the velocity ω/β. The wave length, λ, is

$$\lambda = \frac{\omega}{f\beta} = \frac{2\pi}{\beta} \tag{75}$$

where

$$\beta = \left(\frac{\omega \rho}{2\eta}\right)^{\frac{1}{2}}$$

Since the basic equation used for calculating the dynamic properties of solution in this work was found with the assumption that the wave length was smaller than or equal to the distance between the driving plate and the sample beaker wall, the highest dyanmic viscosity that can be measured for each frequency is shown in figure 37. With a larger sample beaker the measuring range would include higher viscosities.

The dynamic functions refer to isothermal changes of states, and the control of constant temperature is an important feature of all measurements. It is evident, however, that the measurement must be adiabatic rather than isothermal, because of failure to reach thermal equilibrium within the period of deformation. Ferry[16] mentioned that the thermal equilibrium with the surrounding medium cannot be obtained when the frequency exceeds the order of $K/C_p \rho X^2$, where K
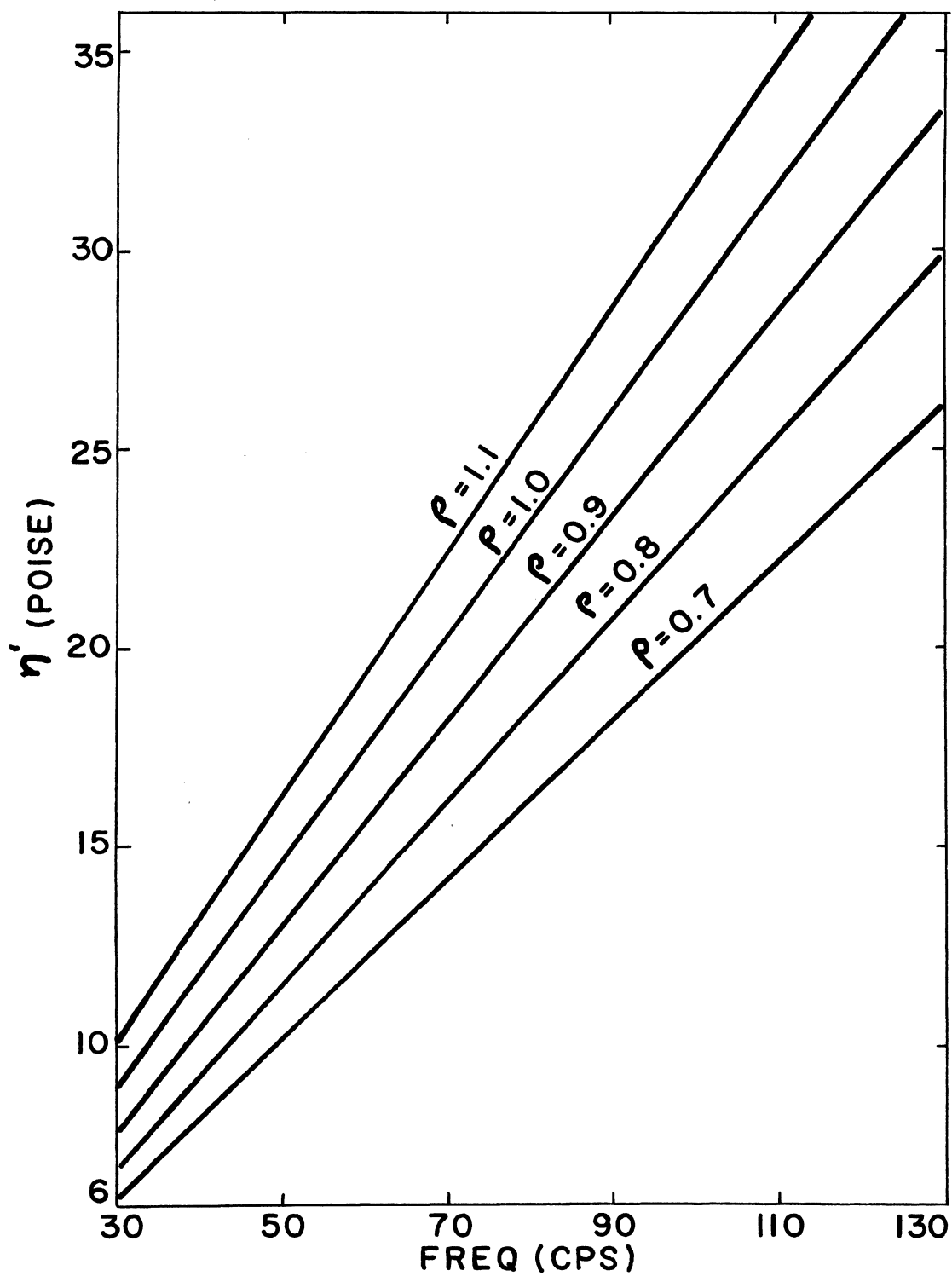
Figure 37. The Relation Between Highest Viscosity and Lowest Frequency That Can Be Measured by the Dynamic Apparatus

is the thermal conductivity, and C_p the heat capacity per
mass at constant pressure, and X the thickness of the sample.
For a polymer solution, K is of the order of 4×10^{-4} cal
$cm^{-1} deg^{-1} sec^{-1}$, and C_p is of the order of 0.4 cal deg^{-1}
g^{-1}. Since the damping was so severe, the X was of the
order of 0.3 cm. In this case, the critical frequency is of
the order 0.01 Hz, so the measurements were indeed adiabatic
as are the measurements with most other dynamic instruments.
However, this distinction can usually be ignored, because
the difference between the adiabatic and isothermal quanti-
ties is negligible for the strain magnitudes limited by the
conditions of linear viscoelastic behavior[16]. An analysis
of viscoelasticity by the methods of irreversible thermo-
dynamics[56,57] shows that under adiabatic conditions the
relaxation spectrum is composed of slightly shorter times
than under isothermal conditions.

B. Dynamic Properties of Polymer Solutions

The complex viscosities of all polymer solutions de-
creased with increasing frequency as shown in figures 26-30.
This was predicted by all the phenomenological and molecular
theories. From figures 27, 28, 29, 30, η'' greater than η'
was observed. According to molecular theories, η' is always
greater than η''. This difference was due to the concentra-
tions of the solutions, which were above the dilute range.
Using Sprigg's constitutive equation[58], a relationship may
be obtained between the concentration and the dependence of

complex viscosity on frequency using a parameter α . The result is shown in figure 38. Comparing figures 27 and 28 with figure 38, it is evident that for both concentrations of the polymer solultions $\alpha > 2$. For polyisobutylene with weight-average molecular weight 1.56×10^6 and a broad molecular weight distribution, the same kind of dynamic data result was obtained by Ferry[59] et al., Berge[60], and Philip-poff[61]. When the concentration of the PIB L-80 solution decreased to 3 g/Dl (see figure 26), the η' was greater than η'', hence for that concentration $\alpha \leqslant 2$.

For a concentrated polymer solution, the Rouse theory was modified[62] and the results obtained were:

$$G' = (\rho RT/M) \sum_{p=1}^{N} \frac{\omega^2 \tau_p^2}{(1 + \omega^2 \tau_p^2)} \tag{76}$$

$$G'' = (\rho RT/M) \sum_{p=1}^{N} \frac{\omega \tau_p}{(1 + \omega^2 \tau_p^2)} \tag{77}$$

$$\tau_p = \frac{6 \eta M}{\pi^2 p^2 \rho RT} \tag{78}$$

The effect of a change of temperature from T_0 to T is to multiply the factor before the summation sign by $\rho T / \rho_0 T_0$ and to multiply each τ_p by a_T, where $a_T = (\eta/\rho)_T T_0 / (\eta/\rho)_{T_0} T$, as though ω were multiplied by a_T. In other words, G' and G'' measured at frequency ω and temperature T is, except for the relatively small difference of the factor in front, equivalent to G' and G'' measured at frequency ωa_T and
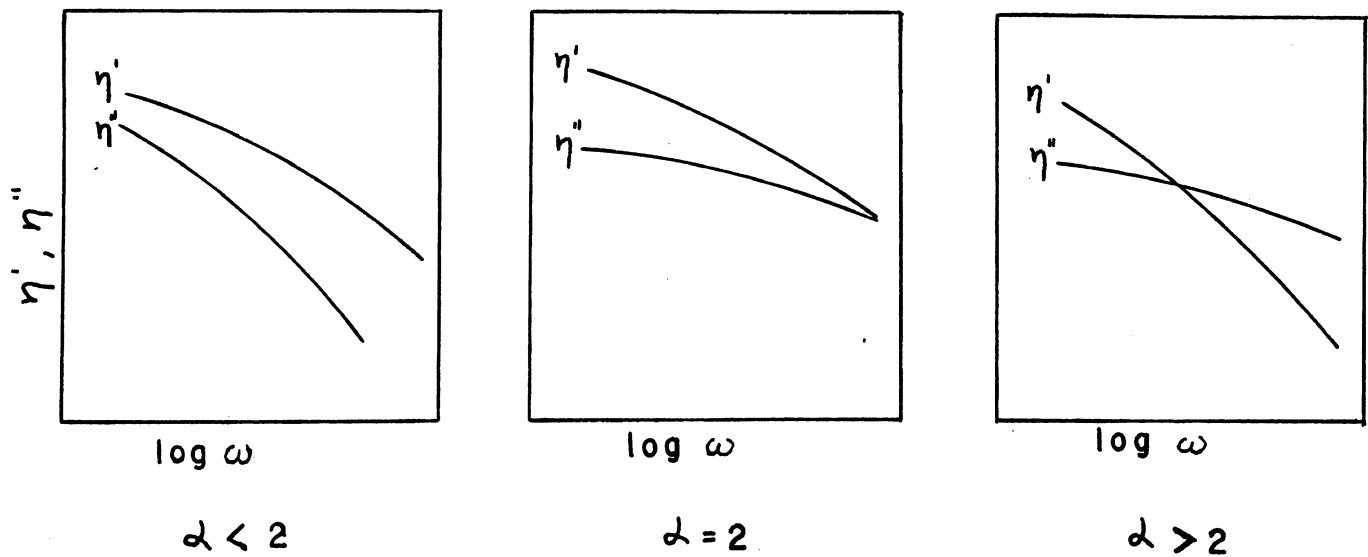
Figure 38. The Shape of Complex Viscosity Dependence on Frequency,
Concentration and the Parameter from the Sprigg's
Constitutive Equation

temperature T_o. It follows that measurement at a variety of temperatures, if plotted as G' $\rho_o T_o / \rho T$ against ωa_T, will all correspond to measurements at T_o and form a single composite curve. The measurements of G' and G'' at three different temperatures are shown in figures 39 and 40. The master curve is shown in figures 41 and 42.

C. Dynamic Properties of Grease

The frequency dependence of dynamic properties of the two greases was studied at different concentrations. From figure 32 it can be seen that η' becomes larger than η'' at higher frequencies. This indicates that the viscous response of this grease at lower concentration increases in importance and predominates at higher frequencies. But for the NLGI grease at higher concentrations, elastic response predominated. (See figures 33, 34). The η' of Mobilgrease 24 is about 1.5 times η''. This means that at the same level of viscous dissipation (η' is the measure of heat production in the grease) the NLGI grease will exhibit about two times the elastic response of the Mobilgrease 24. Since the elastic response may be an indication of the load bearing properties of the grease, this would mean greater load bearing capacity for the NLGI grease at the same heat dissipation rate. Several authors, among them Philip-poff[34,62], Forster and Kolfenbach[35], Bondi[63], Metzner[30], and Appeldoorn[64] have concluded that increased viscoelastic effects would increase load carrying capacity.
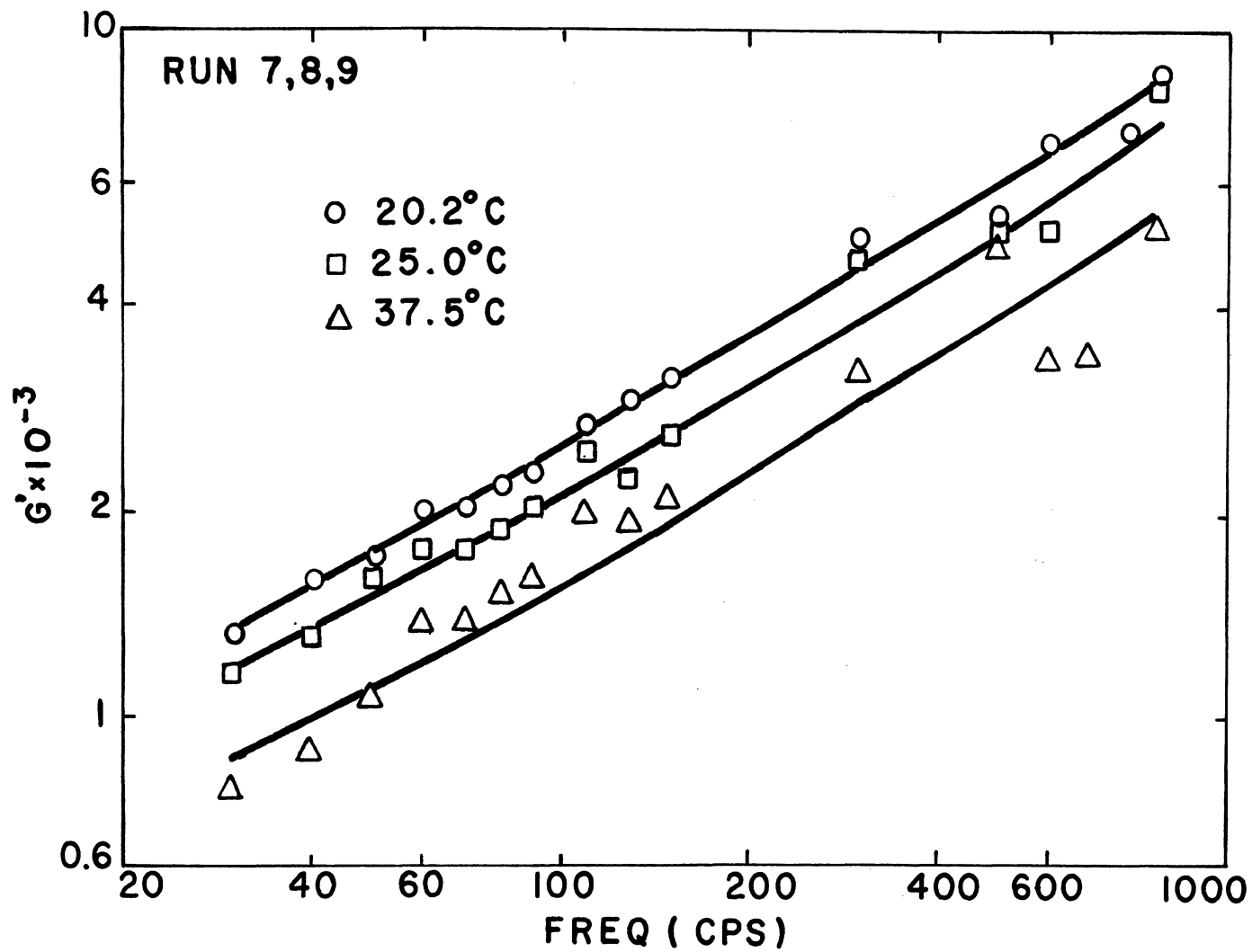
Figure 39. Real Part of Complex Modulus Measurements; 5 g/Dl PIB L-80 at 20.2°C, 25.0°C and 37.5°C
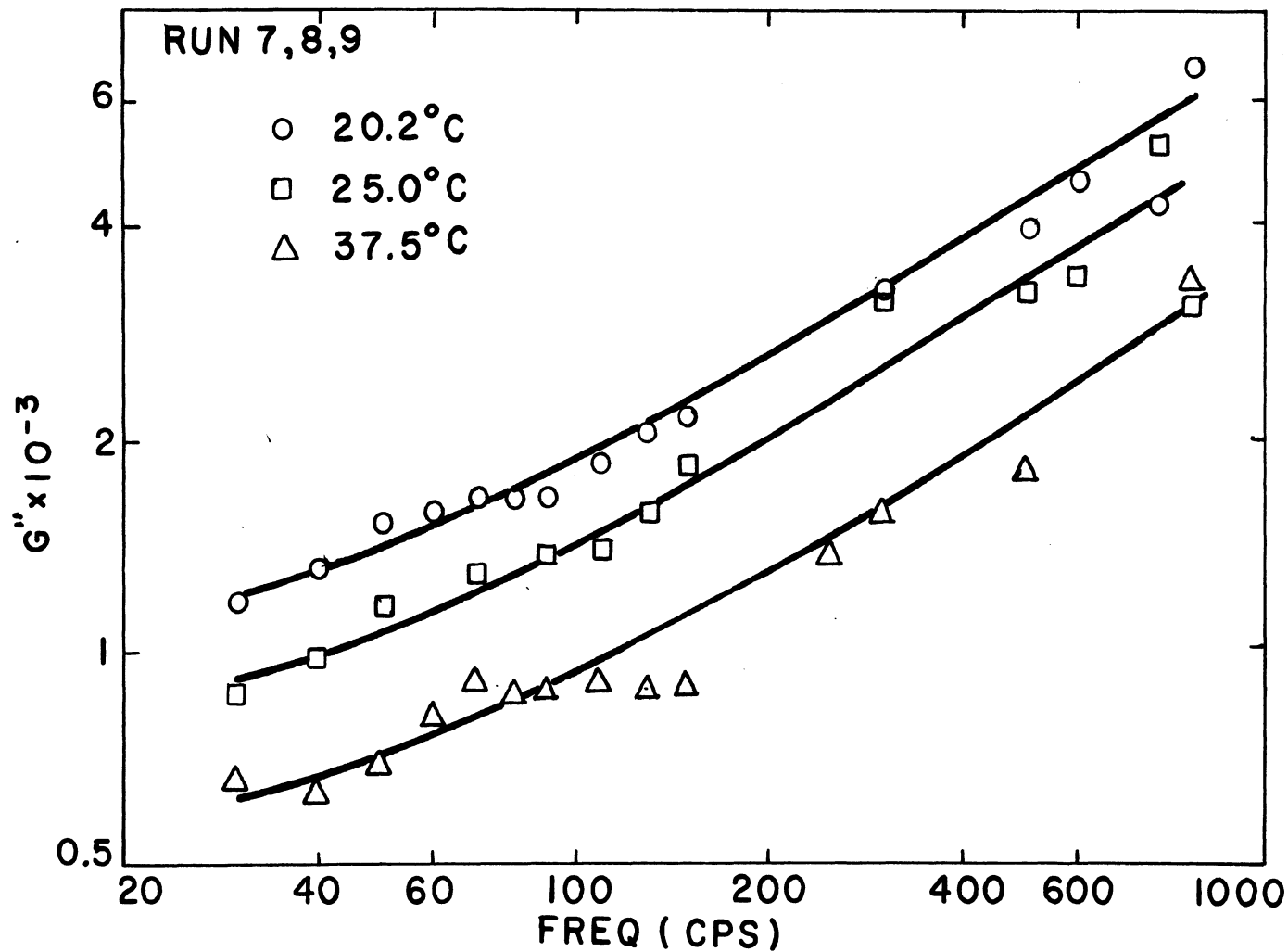
Figure 40. Imaginary Part of Complex Modulus Measurements; 5 g/Dl PIB L-80 at $20.2^\circ C$, $25.0^\circ C$ and $37.5^\circ C$
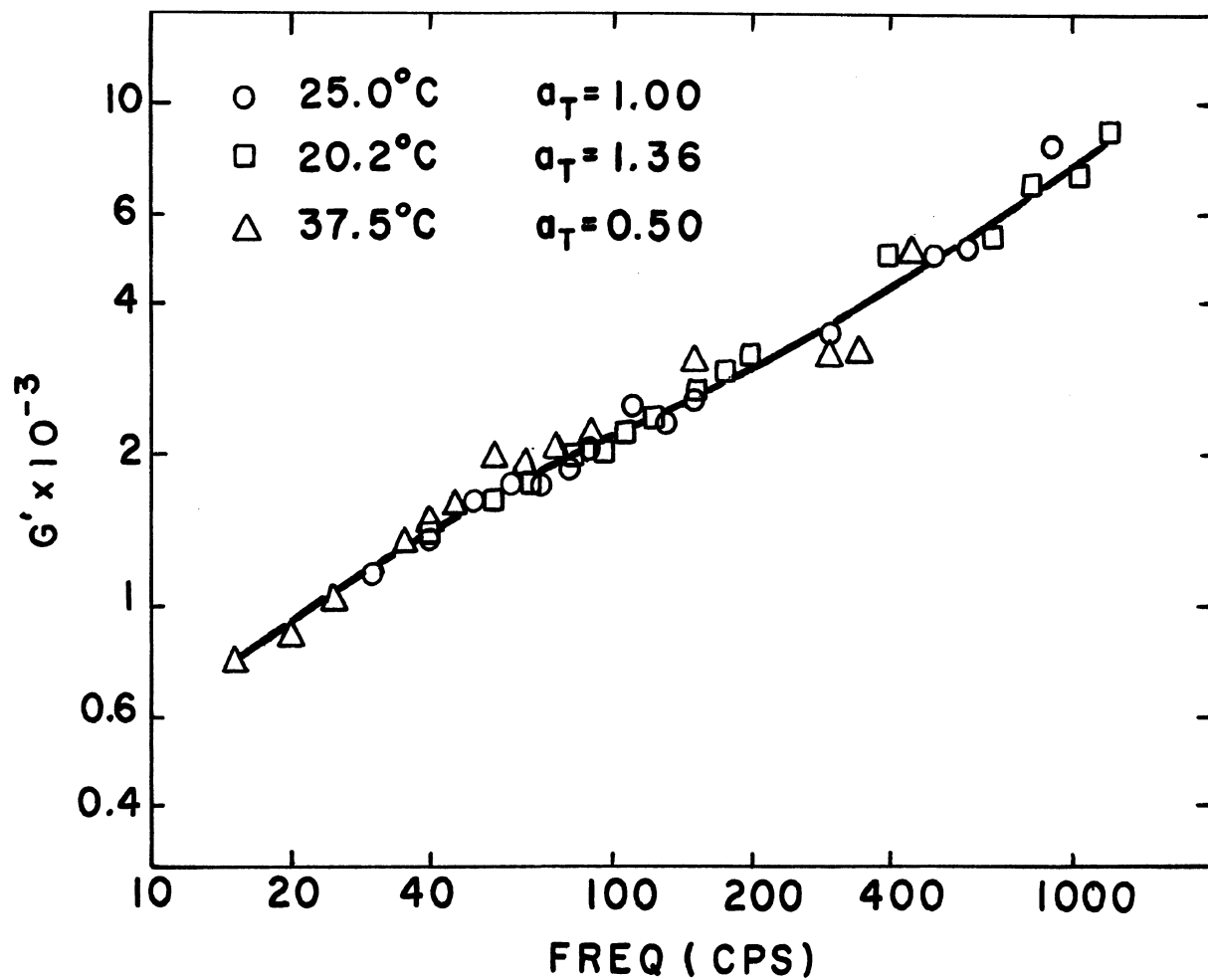
Figure 41. Master Curve for G' of 5 g/Dl PIB L-80 at 20.2°C, 25.0°C and 37.5°C
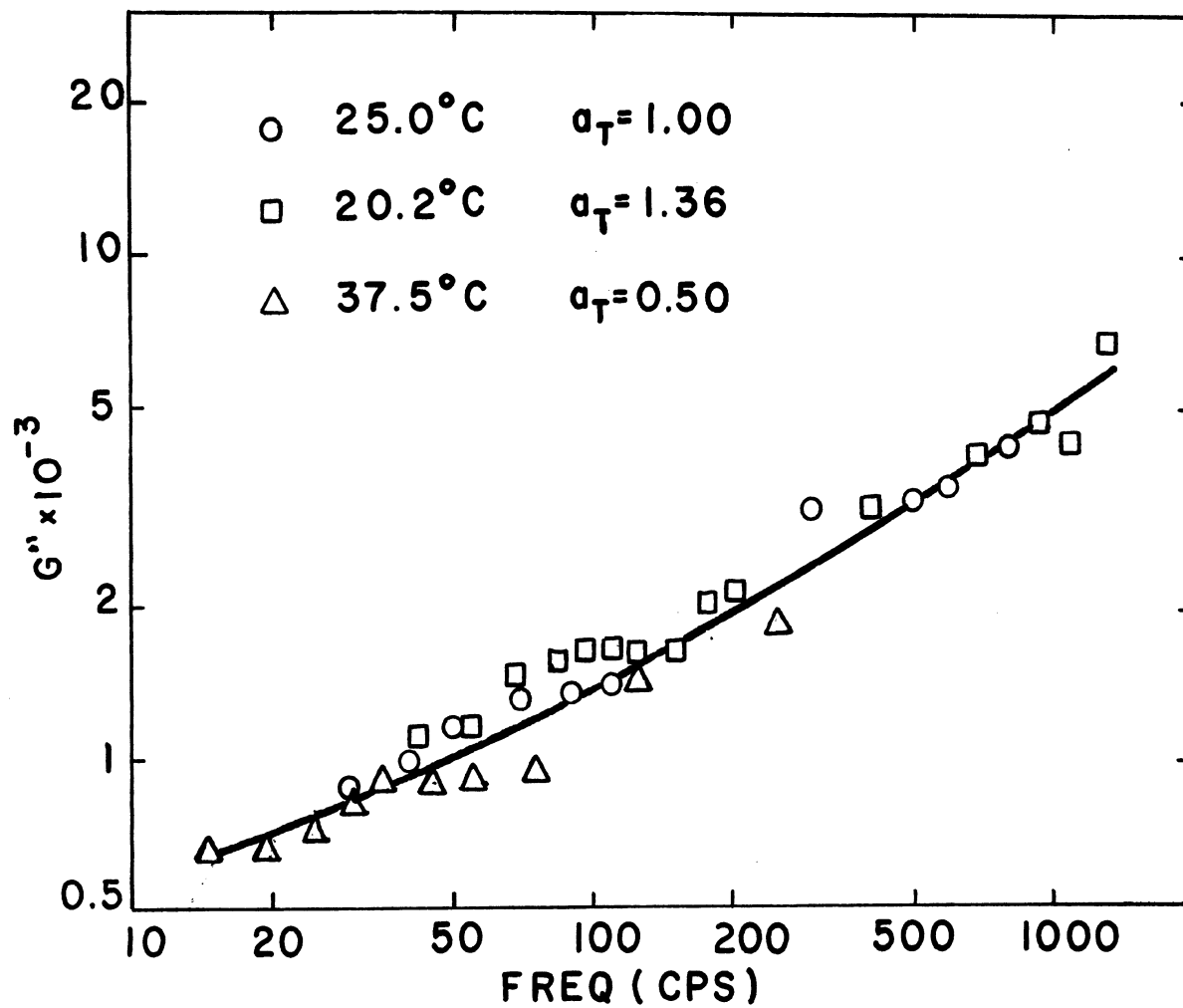
Figure 42. Master Curve for G" of 5 g/Dl PIB L-80 at 20.2°C, 25.0°C and 37.5°C

The η' and η'' of Mobilgrease 24 decrease slowly with frequency. Forster and Kolfenbach[35] investigated two types of grease and they also found that the elastic and loss moduli changed relatively little with frequency (by a factor of 10 over a range of frequencies that changed by a factor of 10,000). This indicates the shear-thinning effect is small and it will have good load carrying capacity at high shear rate. The η' and η'' of NLGI grease dropped off a little faster than Mobilgrease 24 with increasing frequency. These differences could be related to the higher thickener content of the NLGI grease and/or to the differences in base fluid-thickener interactions for the two greases. The Mobilgrease 24 was not used undiluted because the fluid tended to separate from the thickener during vibration of the plate.

The loss tangent $\tan \delta = \eta'/\eta''$ can be used to obtain $\sin \delta$ (which is a measure of the ratio of energy dissipated to total energy in a cyclic deformation), of the 17% NLGI grease shown in figure 43. It increased constantly with increasing frequency. For 50% NLGI grease and Mobilgrease 24, the loss tangent was almost independent of frequency. The loss tangent for 50% NLGI grease was about 0.8, and for 50% Mobilgrease 24 was about 1.3.

The energy dissipated during one cycle is

$$W = \int T d\gamma = \pi G'' \gamma_0^2 = \pi \gamma_0 \gamma_0 \sin \delta \tag{79}$$
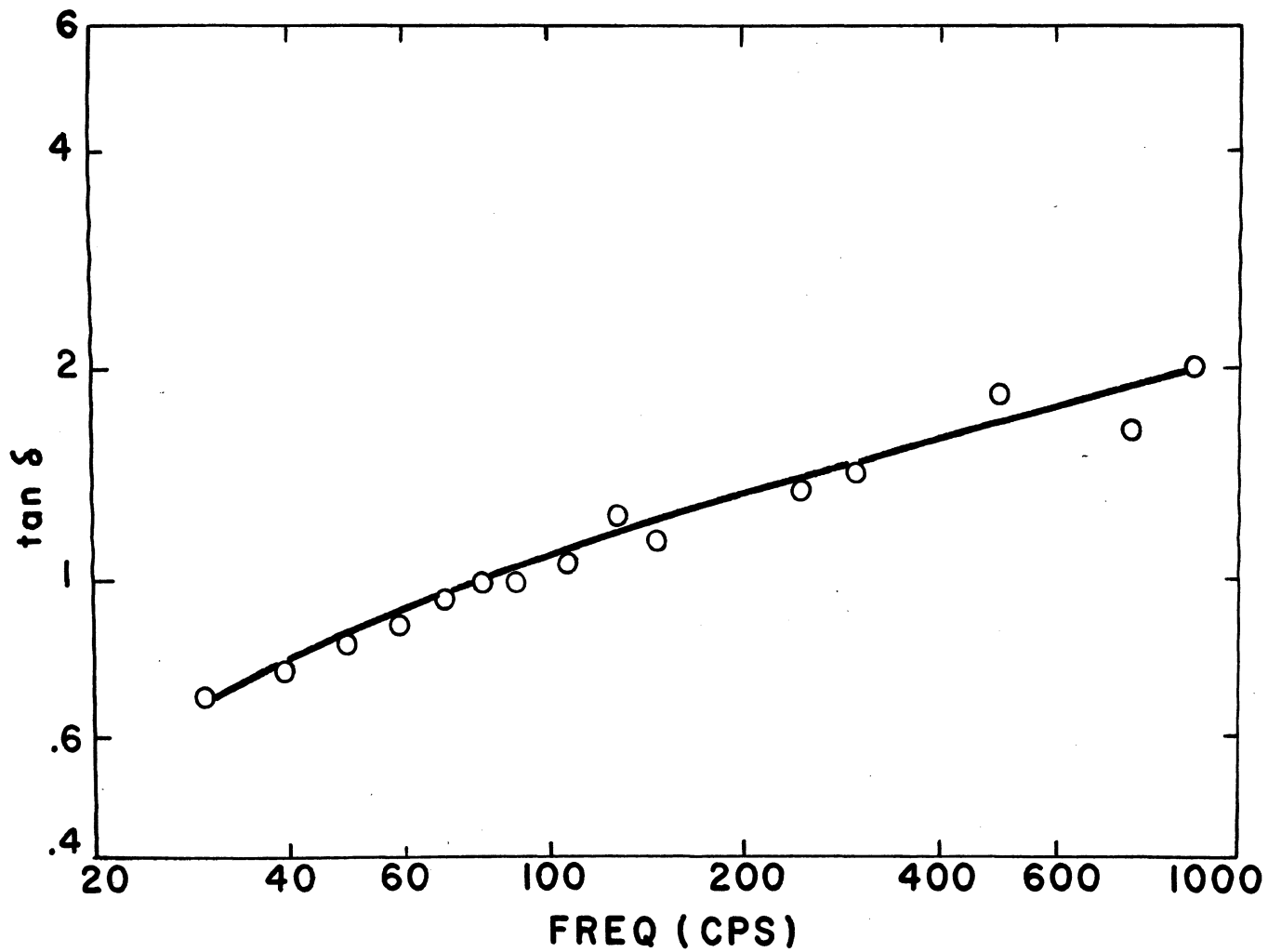
Figure 43. Loss Tangent of 17% NLGI Grease

where the total energy expended during one cycle, E, is given by

$$E = \pi \eta_0 \gamma_0 \qquad (80)$$

It can be obtained that about 60% of the total energy was dissipated under experimental conditions for 50% NLGI grease. This means that about 40% of the total energy has been stored in a reversible fashion. This energy can be stored by stretching bonds, changing bond angles, coiling or uncoiling of molecular aggregates or just simply displacing molecules or molecular aggregates from their equilibrium position. After the deforming stresses have been released, these displacements and molecular changes will be reversed within a definite time interval. For 50% Mobilgrease 24, about 80% of energy was dissipated under experimental conditions.

D. Amplitude Dependence

The amplitude dependence of PIB L-80 5 g/Dl solution was examined. The result is shown in figures 44 and 45. From figure 44, it can be seen that when X_0 was over 0.060 cm the η' decreased gradually. It can be seen that the η' was unaffected by amplitude below this line. Above this line, η' decreased with amplitude.

So the conclusion can be made that η' will show linear viscoelasticity when the vibration amplitude is smaller than
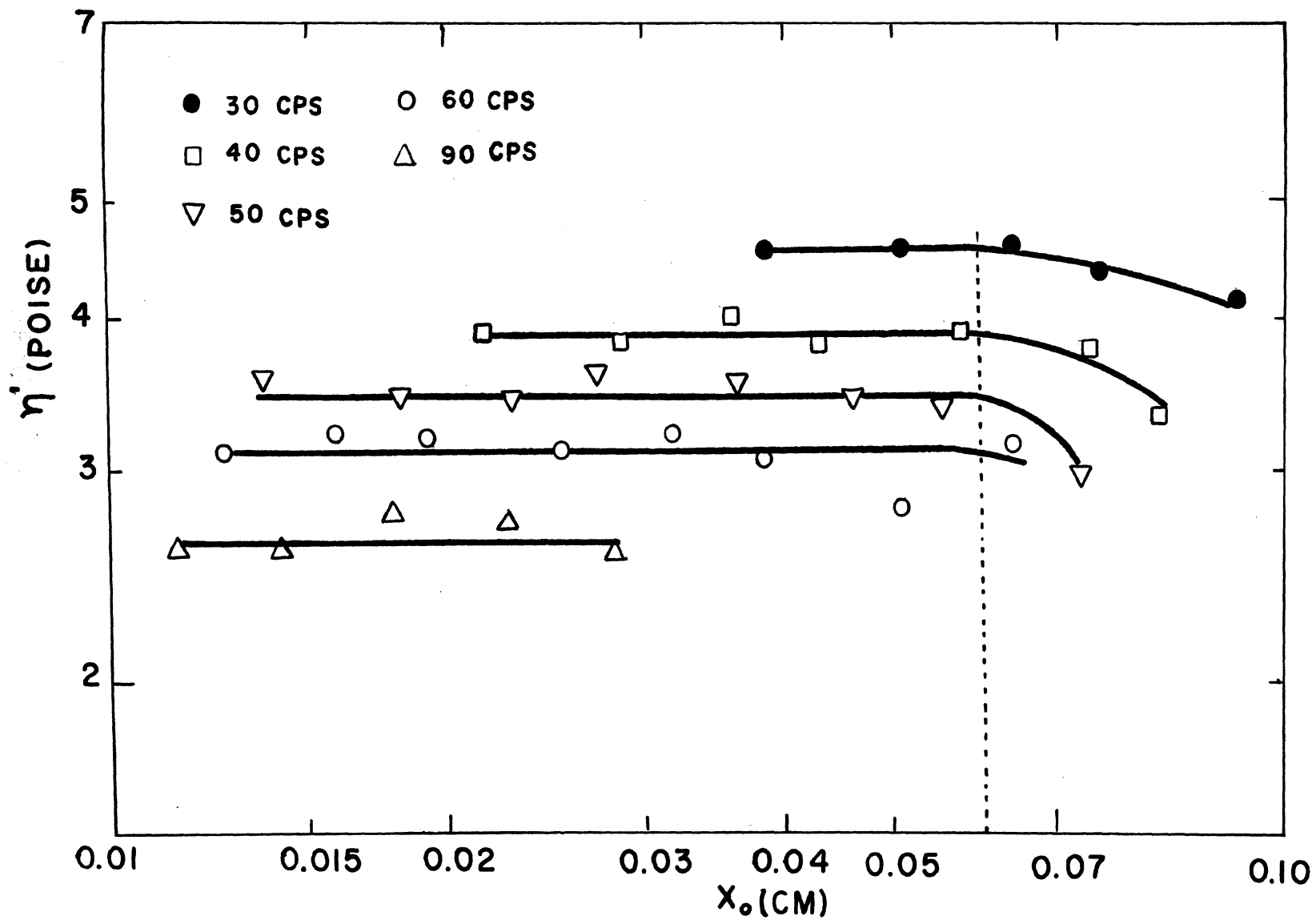
Figure 44. The Dependence of η' on Amplitude; 5 g/Dl PIB L-80 at 25°C
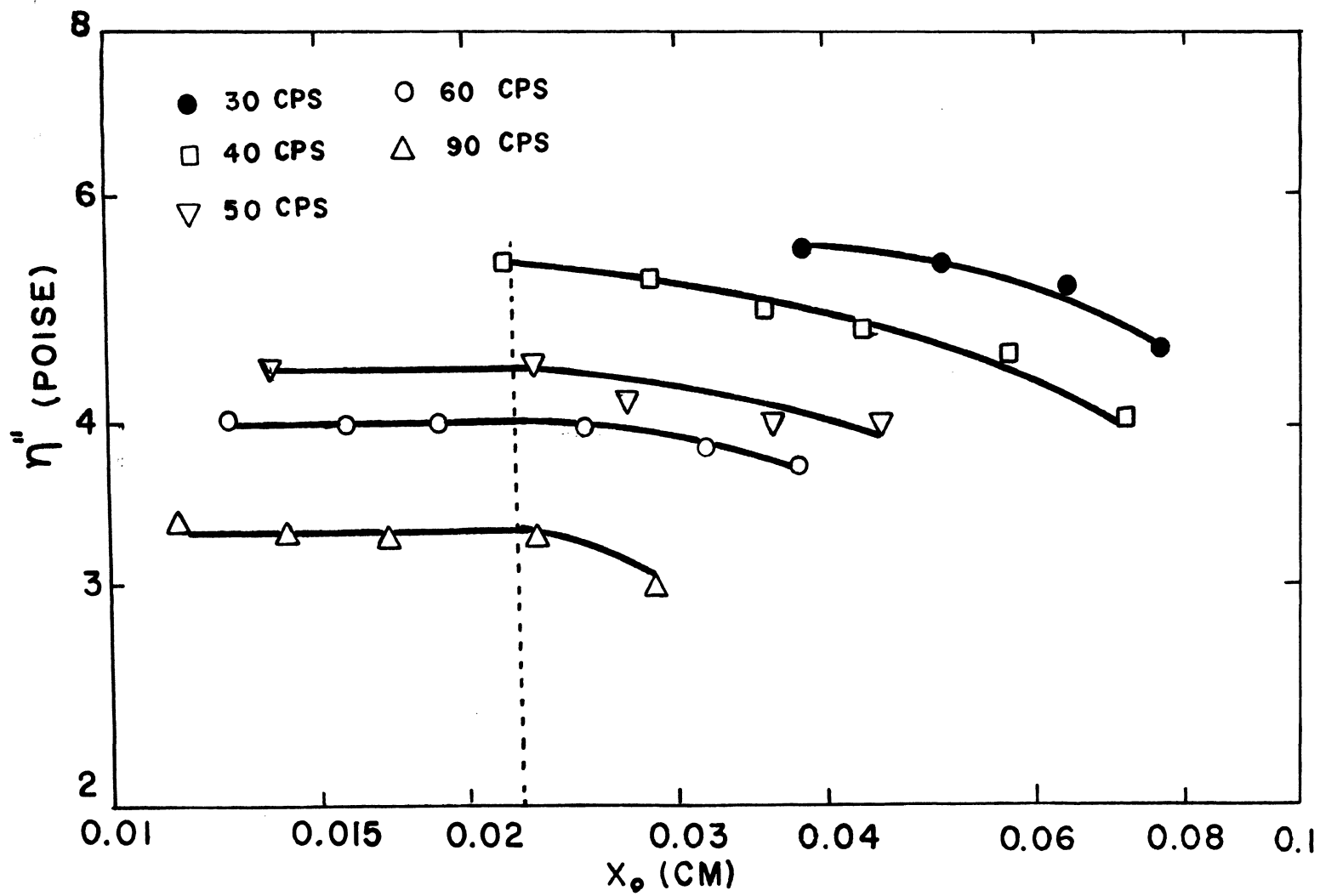
Figure 45. The Dependance of η" on Amplitude; 5 g/Dl PIB L-80 at 25°C

0.060 cm. If the sinusoidal shear displacement wave is represented by

$$X = X_o \sin \frac{2\pi Z}{\lambda}$$

then

$$\left(\frac{dX}{dZ}\right)_{Z=0} = X_o \frac{2\pi}{\lambda} = X_o \sqrt{\frac{\pi f \rho}{\eta}} \quad (\% \text{ strain})$$

For 5 g/Dl PIB L-80 at 30 cps and wave length λ equal to 1.5 cm, the strain corresponding to 0.060 cm vibration amplitude is 25%. For the imaginary part, η'', it can be seen from figure 45 that η'' starts to change at much smaller amplitude than η'. Philippoff[21] studied the influence of the shear amplitude on dynamic behavior of polymer solution at very low frequency range, 0.2 to 5 sec^{-1}. He found that at amplitudes < 100% strain, the dynamic viscosity remained constant, but the storage modulus G' decreased considerably. The same trend was obtained here. A dotted line was also drawn for equal amplitude in figure 45 for an amplitude of 0.022 cm. So the limitation for the validity of the theory of linear viscoelasticity is that the amplitude should be smaller than 0.022 cm. This corresponded to a strain of 9.5% at λ = 1.5 cm. For 5 g/Dl PIB L-80 at 30 cps, the maximum shear stress per unit area is 139.4 dyne/cm^2.

Forster et al.[35] investigated the amplitude dependence for two greases at frequency range 10^{-4}- 10 cps, they found that the region of non-linearity seems to extend from very

low shear strains of about 0.3% to about 5% and the η'' was decreased in magnitude more rapidly than η'.

MacDonald et al.[65] also studied the dependence of the complex viscosity of four viscoelastic fluids on strain amplitude with a Weissenberg Rheogoniometer at the frequencies 0.188, 1.88 and 5.95 sec^{-1}. They found that both the dynamic viscosity and the dynamic storage modulus decrease with increasing strain amplitude, with the latter showing a much larger decrease and the relative decrease in both functions was only slightly dependent on the fluid and the frequency of oscillation. Two models (the Bird-Carreau model and the modified OWFS model) were tested and neither of them was able to predict the data adequately.

E. Comparisons of Dynamic Viscosity and Steady Shear Viscosity

Because of the low frequency limitation of this apparatus, the comparisons of dynamic viscosity and steady shear viscosity are qualitive rather than quantitative. Comparing the shapes of the steady shear viscosity and the dynamic viscosity of PIB L-80 (3 g/Dl and 5 g/Dl) in figures 46 and 47, it is seen that none of them can be shifted into coincidence. They have a trend toward agreement with equation 22, and for vanishingly small values of ω the η' will equal η at zero shear rate.
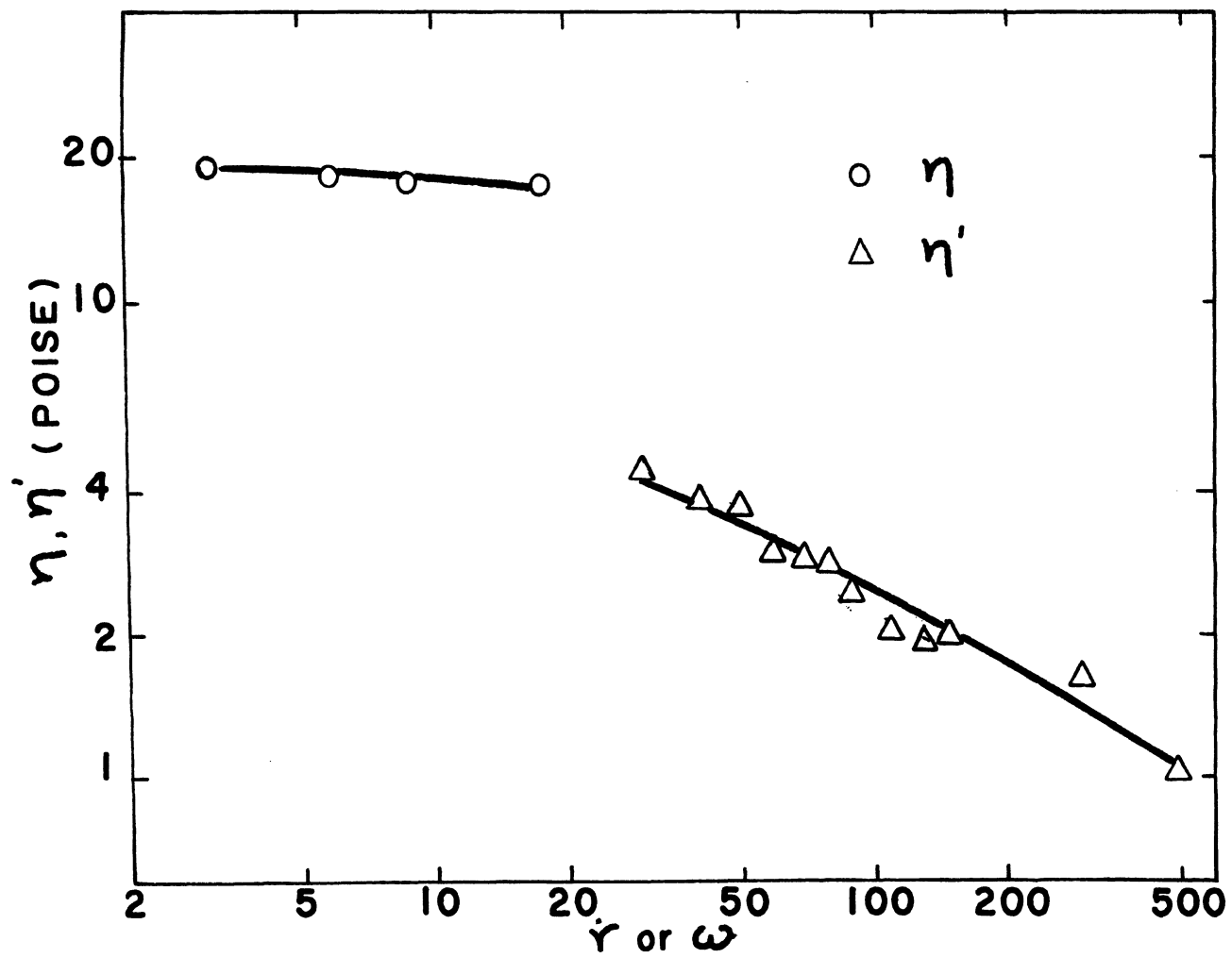
Figure 46. Comparisons of Dynamic Viscosity and Steady Shear Viscosity;
5 g/Dl PIB L-80
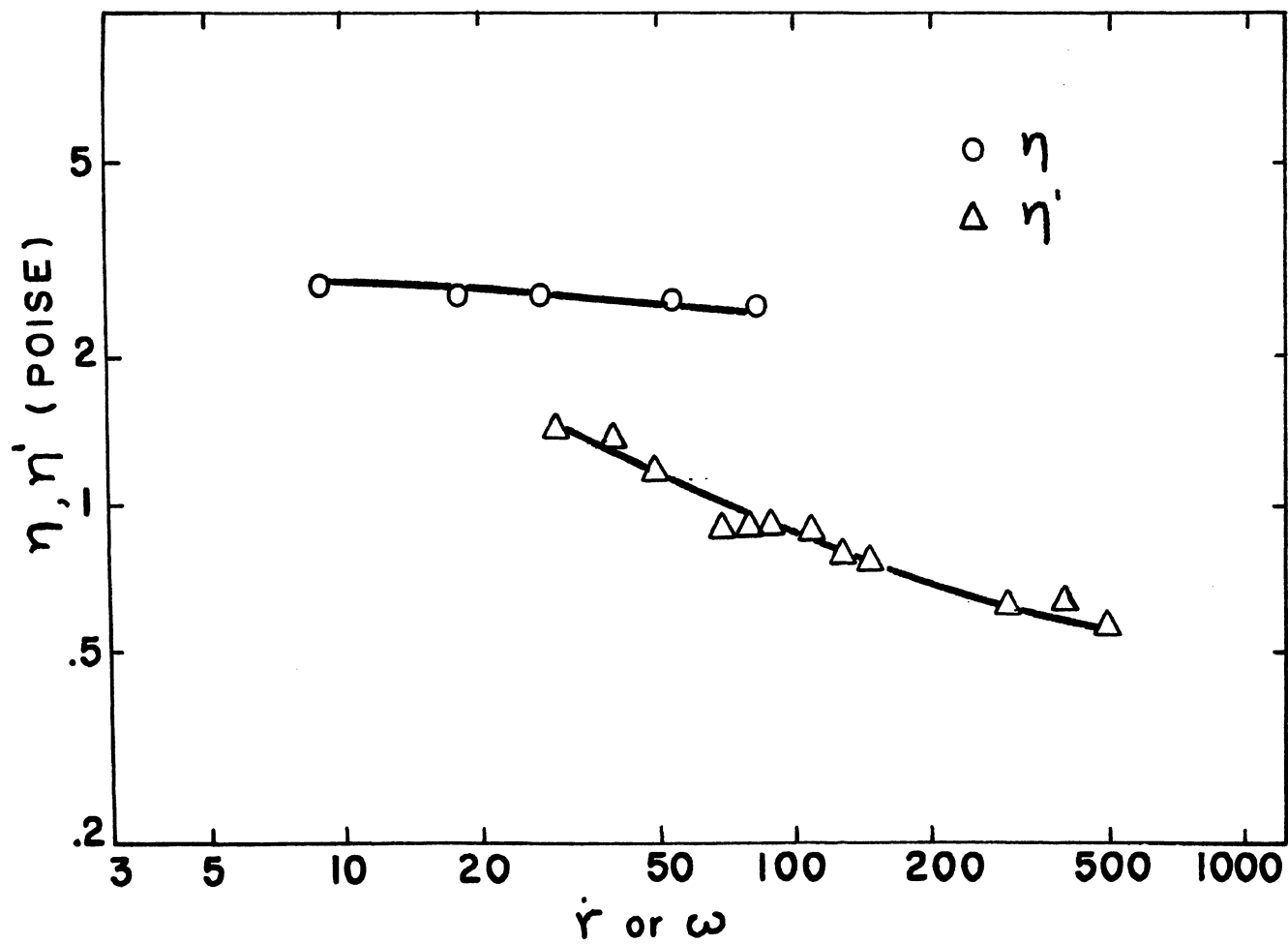
Figure 47. Comparisons of Dynamic Viscosity and Steady Shear Viscosity;
3 g/Dl PIB L-80

For 17% NLGI grease and 25% Mobilgrease 24, η' and η have similar shapes, (see figures 48 and 49). If a shift factor of 2 is applied to η', it seems that η' and η can be shifted into coincidence along the $\dot{\gamma} - \omega$ axis. This is in agreement with Sprigg's prediction.
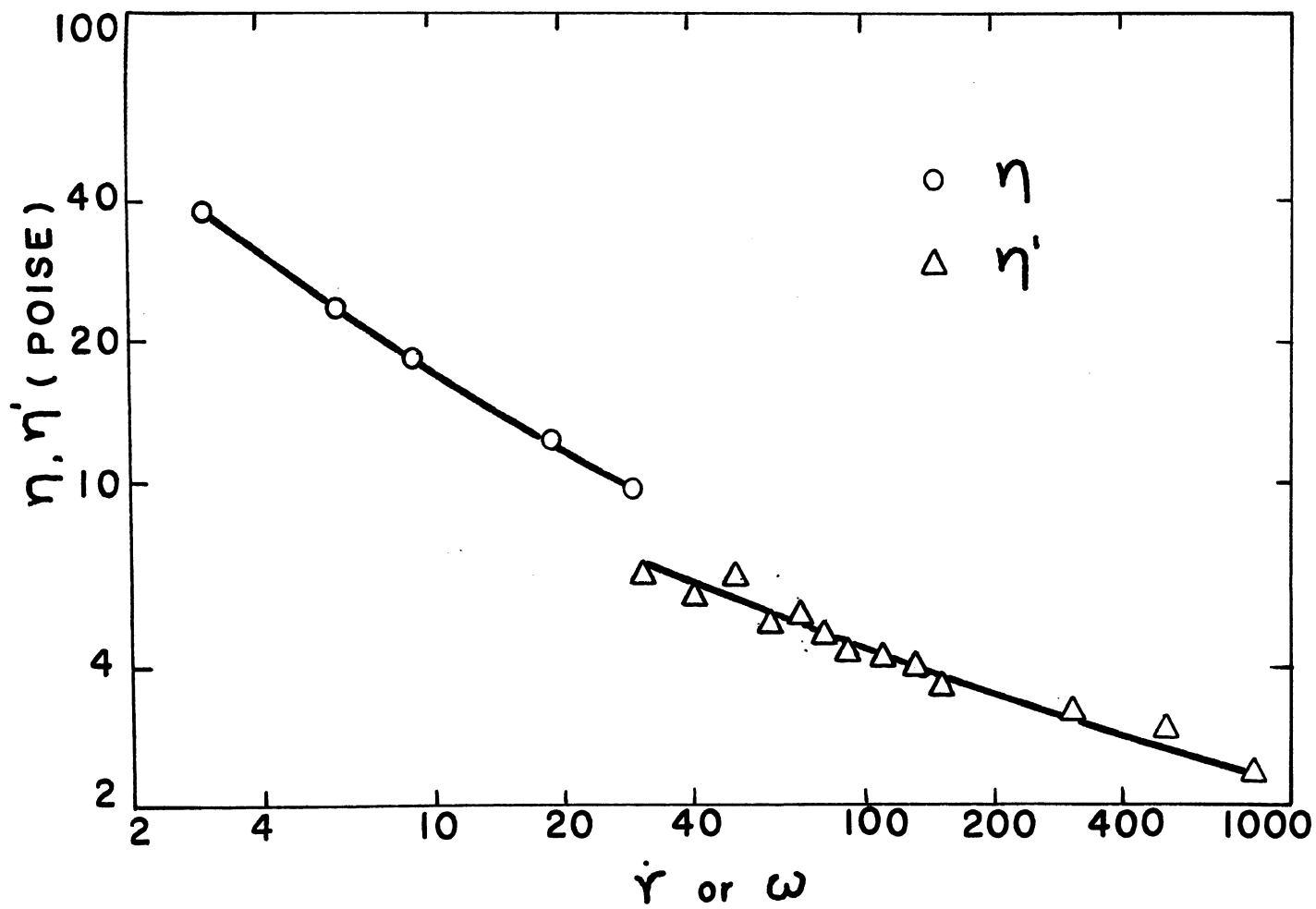
Figure 48. Comparisons of Dynamic Viscosity and Steady Shear Viscosity;
17% NLGI Grease
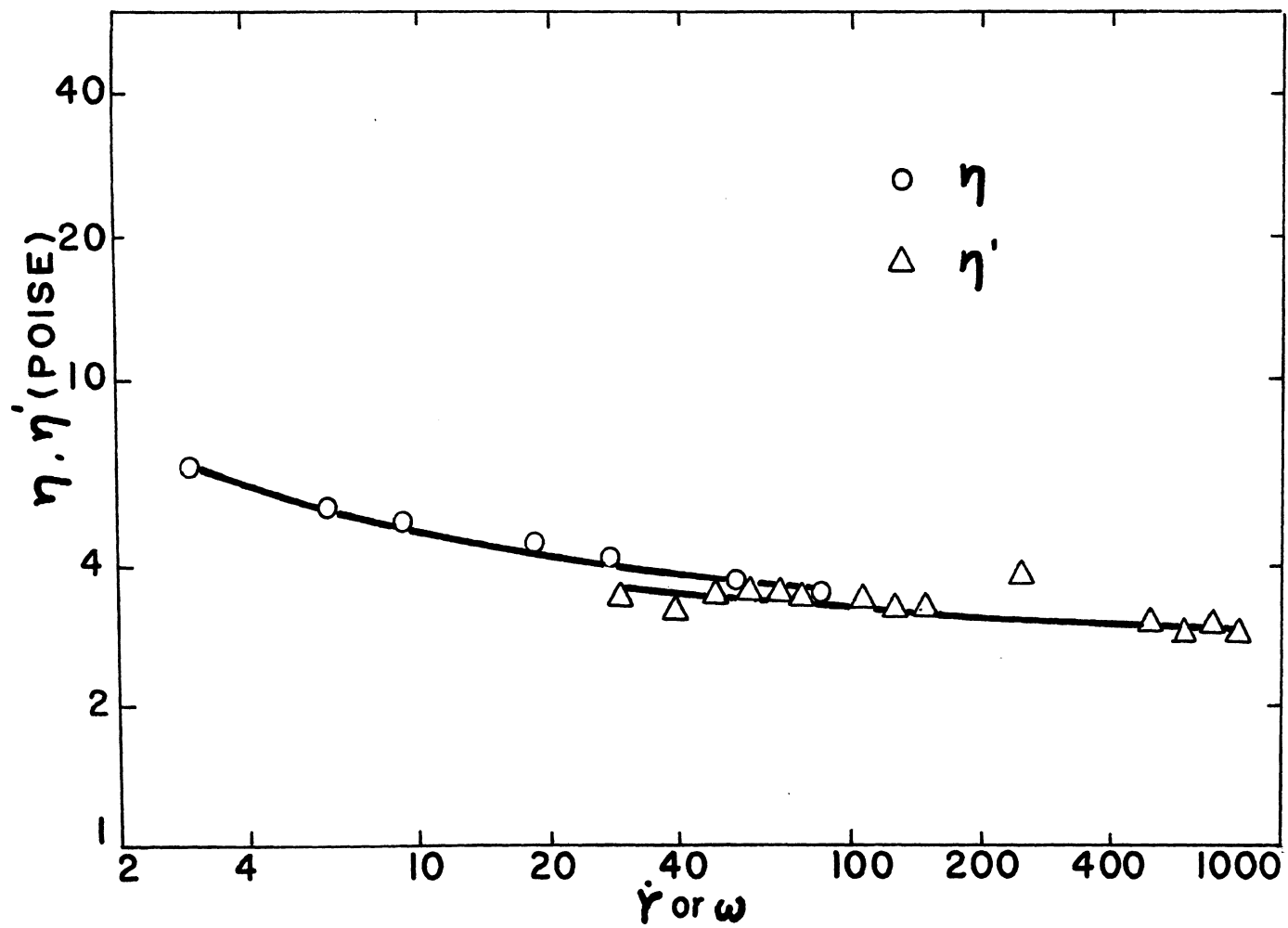
Figure 49. Comparisons of Dynamic Viscosity and Steady Shear Viscosity;
25% Mobilgrease 24

VIII. CONCLUSIONS

A dynamic apparatus was built for making measurements of characteristic impedance in solutions. Large amplitudes can be obtained with this apparatus. The largest amplitude used was 1.27×10^{-1} cm. The frequency range was 30 Hz - 1500 Hz and the lowest dynamic viscosity to be measured was 0.5 poise.

The dependence of complex viscosity on amplitude was investigated. Both η' and η'' decrease with increasing amplitude when amplitude is beyond a limit; the η'' was more sensitive to amplitude. That means that the dynamic storage modulus data are more critical than dynamic viscosity data in determining the limitation on amplitude for linear visco-elasticity. When wave length equaled to 1.5 cm, the limitation on shear strain for linear viscoelasticity was 9.5% for a 5 g/Dl PIB L-80 solution.

Comparison of results for NLGI grease and Mobilgrease 24 showed that at the same level of η' the NLGI grease had twice the elastic response of Mobilgrease 24. For NLGI grease about 60% of the total energy input was dissipated under the experimental conditions. About 80% of the total energy input was dissipated for Mobilgrease 24.

BIBLIOGRAPHY

1. Papazian, H. S., Engr. Experiment Bulletin 192, 17 (1962).

2. Flory, P. J., Principles of Polymer Chemistry, Cornell University Press, Ithaca, N. Y. (1953).

3. Cerf, R., Adv. Poly. Sci., 1, 382 (1959).

4. Benoit, H., J. Poly. Sci., 3, 376 (1948).

5. Rouse, P. E., J. Chem. Phys., 21, 1272 (1953).

6. Zimm, B. H., J. Chem. Phys., 24, 269 (1956).

7. Tschoegl, N. W., J. Chem. Phys., 39, 149 (1963).

8. Spriggs, T. W., Chem. Eng. Sci., 20, 931 (1965).

9. Oldroys, J. G., Quart. J. Mech. Appl. Math., 4, 271 (1951).

10. Oldroyd, J. G., Proc. Roy. Soc. (London), A 245, 278 (1958).

11. Bernstein, B., Kearsley, E., and Zapas, L., Trans. Soc. Rheol., 7, 391 (1963).

12. Zapas, L., and Craft, T., J. Res. Natl. Bur. Std., 69 A 541 (1965).

13. Tanner, R. I., A. I. Ch. E. J., 15, 177 (1969).

14. Lodge, A. S., Elastic Liquids, Academic Press, New York (1964).

15. Lodge, A. S., Trans. Faraday Soc., 52, 210 (1956).

16. Ferry, J. D., Viscoelastic Properties of Polymer, John Wiley, New York (1961).

17. Macdonald, I. F., and Bird, R. B., J. Phys. Chem., 70, 2068 (1966).

18. Lighthill, M. J., *Fourier Series and Generalised Functions*, Cambridge University Press, Cambridge (1958).

19. Bogue, D. C., and Doughty, J. O., Ind. Eng. Chem. Fund. 5, 243 (1966).

20. Spriggs, T. W., Huppler, J. D., and Bird, R. B., Trans. Soc. Rheol., 10:1, 191 (1966).

21. Philippoff, W., Trans. Soc. Rheol., 10:1, 317 (1966).

22. Noll, W., Arch. Rat. Mech. Anal., 2, 197 (1958).

23. Coleman, B. D., and Noll, W., Arch. Rat. Mech. Anal., 3, 289 (1959).

24. Osaki, K., Tamura, M., Kotaka, T., and Katsuhisa, M., J. Phys. Chem., 69, 3642 (1965).

25. Lamb, J., *Symposium on Rheology*, ASME Pub., New York, 1 (1965).

26. Onogi, S., Hamana, I., and Hirai, H., J. Appl. Phys., 29, 1053 (1958).

27. Dewitt, T. W., Markovitz, H., Padden, F. J., and Zapas, L. J., J. Colloid Sci., 10, 174 (1955).

28. Markovitz, H., and Williamson, R. B., Trans. Soc. Rheol., 1, 25 (1957).

29. Markovitz, H., Trans. Faraday Soc., 52, 120 (1956).

30. Metzner, A. B., J. Lub. Tech., July, 531 (1965).

31. Appeldoorn, J. K., ASLE Trans., 18, 182 (1965).

32. Astarita, G., Ind. Eng. Chem. Fund., 6, 257 (1967).

33. Jaeger, J. C., Elasticity, Fracture and Flow, Methuen (1956).

34. Philippoff, W., J. of Lub. Tech., July, 543 (1968).

35. Forster, E. O., and Kolfenbach, J. J., A. S. L. E. Preprint, Lubrication Conference, Oct. 13-15 (1958).

36. Miles, D. O., and Knollman, G. C., J. Appl. Phys.,33, 1422 (1962).

37. Miles, D. O., and Knollman, G. C., J. Appl. Phys.,35, (1964).

38. Weissenberg Rheogoniometer Instruction Manual, Farol Research Engineer, Ltd.

39. Birnboim, M. H., and Ferry, J. D., J. Appl. Phys., 32, 2305 (1961).

40. Markovitz, H., J. Appl. Phys., 23, 1070 (1952).

41. Philippoff, W., J. Appl. Phys., 24, 685 (1953).

42. Philippoff, W., J. Appl. Phys., 25, 1102 (1954).

43. Morrison, T. E., Zapas, L. J., and Dewitt, T. W., Rev. Sci-Instr. 26, 357 (1955).

44. Horio, M., Fujii, T., and Onogi, S., J. Phys. Chem., 68, 778 (1964).

45. Mason, W. P., Trans A. S. M. E., 69, 359 (1947).

46. Konno, A., Makio, S., and Kaneko, M., Jap. J. Appl. Phys., 7, 89 (1969).

47. Sittel, K., Rouse, P. E., Jr., and Bailey, E. D., J.

Appl. Phys., 25, 1312 (1954).

48. Birnboim, M. H., and Elyash, L. J., Bull. Amer. Phys. Soc., Ser. II, 11, 165 (1966).

49. DeMallie, R. B.,,Jr., Birnboim, M. H., Frederick, J. E., Tschoegl, N. W., and Ferry, J. D., J. Phys. Chem., 66, 536 (1962).

50. Frederick, J. E., Tschoegl, N. W., and Ferry, J. D., J. Phys. Chem., 68, 1974 (1964).

51. Tschoegl, N. W., J. Chem. Phys., 40, 473 (1964).

52. Harrison, G., Lamb, J., and Matheson, A. J., J. Phys. Chem., 68, 1072 (1964).

53. Sakanish, A., J. Chem. Phys., 48, 3850 (1968).

54. O'Reilly, J. M., and Prest, W. M., General Electric Report N. 66-C-272 (1966).

55. Simmons, J. M., J. Sci. Instr., 43, 887 (1966).

56. Meixner, J., Z. Naturd., 4a, 594 (1949).

57. Meixner, J., Z. Naturd., 9a, 654 (1954).

58. Spriggs, T. W., Ph. D. thesis, University of Wisconsin, 1966.

59. Fitzgerald, E. R., Grandine, L. D., Jr., and Ferry J. D., J. Appl. Phys., 24, 659 (1953); 24, 911 (1953).

60. Plazek, D. J., Vrancken, M. N., and Berge, J. W., Trans. Soc. Rheol., 2, 39 (1958).

61. Philippoff, W., J. Appl. Phys., 24, 685 (1953).

62. Tao, F. F., and Philippoff, W., A. S. L. E. Trans. 10, 302 (1967).

63. Bondi, A., Mech. Eng., <u>81</u>, 98 (1959).

64. Appeldoorn, J. K., J. Lub. Tech., July, 526 (1968).

65. Macdonald, I. F., Marshand, B. D., and Ashare, E.,
Chem. Eng. Sci. <u>24</u>, 1615 (1969).

VITA

Kuo-Shein Shen, son of T'se and Wen-I Shen, was born on January 4, 1939, in San-Si, China.

He attended elementary school in Taiwan, China. He received the Bachelor of Science in Chemical Engineering from the Chung-Yung College of Science and Engineering in June, 1963, and the Master of Science in Chemical Engineering from the University of Missouri-Rolla in August, 1967.

On September 20, 1969, he married Miss Po-I Yang, daughter of Wen-Ta and Ya-Ping Yang, at Rolla, Missouri. A daughter was born on October 1, 1970.

He has been awarded a National Science Foundation Research Fellowship and a Research Assistantship in the Department of Chemical Engineering. He also been a part-time Graduate Assistant in the Department of Chemical Engineering.

APPENDIX A
Materials

The solvents and polymers used in this investigation, their properties, and suppliers are as follows:

Mineral Oil

light mineral seal oil

A. P. I. gravity: -32.5

Saybolt seconds at 100°F: 37.8 -38.2

maximum pouring point: -85°F

flash point (minimum): 200°F

color ASTM (D1500): 1.0

donated by Mobil Oil Company

Polyisobutylene (PIB) L-80

Enjay MM Vistanex

grade L-80

molecular weight approximately 720,000

distribution unknown

color, slightly yellow

donated by Enjay Corporation, Baton Rouge, Louisiana

Polyisobutylene (PIB) L 200

Enjay HM Vistanex

grade L-200

viscosity average molecular weight 4,000,000-4,700,000

distribution unknown

color, white

obtained from Enjay Corporation, Baton Rouge, Louisiana

Polydimethyl Siloxane SR 130

Viscosity average molecular weight 13×10^6

color, white

donated by General Electric Company, Waterford, New York.

APPENDIX B

Tabulated Data and Results

1. Complex impedance data and results

The computer printouts showing data and results for Castor oil at various levels in Runs 1-4 constitute Table 11.

2. Force transducer calibration data and results

Table 12 shows the data and numerical results for force transducer calibration in Runs 5 and 6.

3. Complex viscosity data and results

Table 13 shows the data and results for complex viscosity and complex modulus in Runs 7-19.

4. Amplitude dependence data and results

Table 14 contains the data and results for complex viscosity of 5 g/Dl PIB L-80 at various amplitudes in runs 20-28.

TABLE 11

Complex Impedance Data and Results

The table contains information identified by the
following symbols for each run:

FREQ   Frequency in cycles per second

VOLA   Output voltage in volts from accelerometer

VOLF   Output voltage in volts from force transducer

PHA   Phase angle in degrees

R   Resistance of the complex impedance

X   Reactance of the complex impedance

RUN   1

SOLUTION LEVEL = 1.00   DENSITY=   0.973

FREQ	VOLA	VOLF	PHA	R	X
30.00	0.150	0.184	14.00	55.9374	224.3528
40.00	0.150	0.180	14.50	75.5126	291.9861
50.00	0.200	0.231	13.00	81.6241	353.5532
60.00	0.200	0.220	12.00	86.2188	405.6277
70.00	0.200	0.215	11.20	91.8356	463.8044
80.00	0.200	0.210	11.00	100.7063	518.0898
90.00	0.200	0.200	10.60	104.0217	555.8359
100.00	0.300	0.324	7.00	82.6983	673.5251
120.00	0.300	0.310	9.00	121.8801	769.5217
140.00	0.300	0.292	7.50	111.7547	848.8623
250.00	0.300	0.363	9.20	303.8794	1876.2110
300.00	0.300	0.362	9.60	379.3164	2242.6570
400.00	0.400	0.290	3.50	111.2378	1818.7220
600.00	0.600	0.541	3.20	189.7482	3393.8980
800.00	0.800	0.865	4.80	454.7837	5415.8820

RUN 2

SOLUTION LEVEL= 1.40   DENSITY=   0.973

FREQ	VOLA	VOLF	PHA	R	X
30.00	0.150	0.214	20.00	91.9759	252.7021
40.00	0.150	0.205	18.80	110.6919	325.1555
50.00	0.200	0.258	17.20	119.8399	387.1406
60.00	0.200	0.247	17.00	136.1232	445.2393
70.00	0.200	0.236	15.40	137.8209	500.3562
80.00	0.200	0.230	14.00	139.8434	560.8818
90.00	0.200	0.222	14.10	152.9144	608.7786
100.00	0.300	0.349	9.90	125.6701	720.0586
120.00	0.300	0.332	12.00	173.4826	816.1721
140.00	0.300	0.315	10.30	165.1463	908.7427
250.00	0.300	0.382	11.80	409.0210	1957.8760
300.00	0.300	0.381	11.60	481.3577	2344.9950
400.00	0.400	0.305	6.50	216.9389	1904.0500
600.00	0.600	0.560	4.60	282.1858	3507.2460
800.00	0.800	0.895	6.70	656.0896	5595.0350

RUN   3

SOLUTION LEVEL= 2.00   DENSITY=   0.973

FREQ	VOLA	VOLF	PHA	R	X
30.00	0.150	0.258	24.00	131.8687	296.1821
40.00	0.150	0.240	23.50	160.3462	368.7715
50.00	0.200	0.296	22.00	174.1750	431.0989
60.00	0.200	0.280	20.00	180.5135	495.9573
70.00	0.200	0.270	19.30	196.2461	560.3914
80.00	0.200	0.259	18.00	201.1504	619.0781
90.00	0.200	0.248	17.60	212.0224	668.3796
100.00	0.300	0.390	13.80	194.8370	793.2351
120.00	0.300	0.369	15.60	249.3950	893.2334
140.00	0.300	0.349	13.80	244.0956	993.7803
250.00	0.300	0.410	14.50	537.5032	2078.3720
300.00	0.300	0.410	15.10	671.0854	2487.1560
400.00	0.400	0.330	9.40	338.6475	2045.6070
600.00	0.600	0.585	7.40	473.4075	3645.0420
900.00	0.800	0.935	8.30	848.0581	5813.2340

RUN   4

SOLUTION LEVEL= 2.50   DENSITY=   0.973

FREQ	VOLA	VOLF	PHA	R	X
30.00	0.150	0.289	25.80	158.0618	326.9666
40.00	0.150	0.266	25.00	188.3552	403.9294
50.00	0.200	0.328	23.50	205.4435	472.4880
60.00	0.200	0.310	21.50	214.1594	543.6758
70.00	0.200	0.296	21.40	237.5116	606.0588
80.00	0.200	0.283	20.80	252.5716	664.8999
90.00	0.200	0.269	20.50	266.3599	712.4128
100.00	0.300	0.430	16.80	260.2983	862.1506
120.00	0.300	0.400	18.30	315.6589	954.4653
140.00	0.300	0.370	16.60	309.9414	1039.6780
250.00	0.300	0.428	15.10	583.7898	2163.6240
300.00	0.300	0.420	14.90	678.5557	2550.2030
400.00	0.400	0.360	12.00	470.2842	2212.5150
600.00	0.600	0.609	9.30	618.3687	3776.1570
800.00	0.800	0.955	9.00	938.6731	5926.5540

TABLE 12

Force Transducer Calibration Data and Results

The table contains information identified by the following symbols:

SOL. 1	Solution level 1 in inches
VOLA 1	Output voltage in volts from accelerometer at solution level 1
VOLF 1	Output voltage in volts from force transducer at solution level 1
PHA 1	Phase angle in degrees at solution level 1
SOL 2	Solution level 2 in inches
VOLA 2	Output voltage in volts from accelerometer at solution level 2
VOLF 2	Output voltage in volts from force transducer at solution level 2
PHA 2	Phase angle in degrees at solution level 2
R	Resistance of the complex impedance
X	Reactance of the complex impedance
KF	Calibration constant for force transducer
CXV 1	Real part, η', of the complex viscosity
CXV 2	Imaginary part, η'', of the complex viscosity
CXM 1	Real part, G', of the complex modulus
CXM 2	Imaginary part, G'', of the complex modulus

RUN   5

SOL. L1= 1.00   SOL. L2= 2.50

FREQ	VOLA1	VOLF1	PHA1	VOLA2	VOLF2	PHA2
30.00	0.150	0.184	14.00	0.150	0.289	25.80
40.00	0.150	0.180	14.50	0.150	0.266	25.00
50.00	0.200	0.231	13.00	0.200	0.328	23.50
60.00	0.200	0.220	12.00	0.200	0.310	21.50
70.00	0.200	0.215	11.20	0.200	0.296	21.40
80.00	0.200	0.210	11.00	0.200	0.283	20.80
90.00	0.200	0.200	10.60	0.200	0.269	20.50
100.00	0.300	0.324	7.00	0.300	0.430	16.80
120.00	0.300	0.310	9.00	0.300	0.400	18.30
140.00	0.300	0.292	7.50	0.300	0.370	16.60
250.00	0.300	0.363	9.20	0.300	0.428	15.10
300.00	0.300	0.362	9.60	0.300	0.420	14.90
400.00	0.400	0.290	3.50	0.400	0.360	12.00
600.00	0.600	0.541	3.20	0.600	0.609	9.30
800.00	0.800	0.865	4.80	0.800	0.955	9.00

RUN   5

FREQ	R*1000	X*1000	KF
30.00	0.0332	0.0334	875.3374
40.00	0.0367	0.0364	920.6169
50.00	0.0403	0.0387	953.4668
60.00	0.0416	0.0449	954.2256
70.00	0.0474	0.0463	950.8984
80.00	0.0494	0.0477	980.1252
90.00	0.0528	0.0509	973.6414
100.00	0.0578	0.0613	894.2454
120.00	0.0630	0.0601	946.9294
140.00	0.0645	0.0621	995.5835
250.00	0.0910	0.0935	912.0718
300.00	0.0973	0.1000	934.1577
400.00	0.1168	0.1281	871.0952
600.00	0.1394	0.1243	991.6367
800.00	0.1574	0.1661	931.1919

RUN   6

SOL. L1= 1.00   SOL. L2= 2.50

FREQ	VOLA1	VOLF1	PHA1	VOLA2	VOLF2	PHA2
30.00	0.150	0.165	14.00	0.150	0.234	24.20
40.00	0.150	0.162	13.40	0.150	0.220	24.00
50.00	0.200	0.210	12.20	0.200	0.274	22.20
60.00	0.200	0.200	11.90	0.200	0.262	20.90
70.00	0.200	0.195	10.50	0.200	0.251	18.90
80.00	0.200	0.192	9.60	0.200	0.243	18.00
90.00	0.200	0.188	8.40	0.200	0.235	16.20
100.00	0.300	0.295	6.70	0.300	0.365	14.90
120.00	0.300	0.283	7.70	0.300	0.345	15.80
140.00	0.300	0.273	6.80	0.300	0.333	14.30
250.00	0.300	0.343	9.00	0.300	0.388	13.90
300.00	0.300	0.339	8.40	0.300	0.382	13.00
400.00	0.400	0.280	3.80	0.400	0.318	10.50
600.00	0.600	0.528	3.10	0.600	0.572	7.30
800.00	0.800	0.841	3.80	0.800	0.900	7.20

RUN   6

FREQ	CXV1	CXV2	CXM1	CXM2
30.00	5.0590	0.2470	0.46554820E 02	0.95358980E 03
40.00	5.0390	0.9201	0.23124440E 03	0.12789930E 04
50.00	4.5484	0.9154	0.28759300E 03	0.14289210E 04
60.00	4.8816	0.3053	0.11510980E 03	0.18403000E 04
70.00	4.6525	0.0035	0.15404440E 01	0.20462810E 04
80.00	4.5731	0.1376	0.69145640E 02	0.22987020E 04
90.00	4.3211	-0.1763	-0.99715920E 02	0.24435490E 04
100.00	5.0113	-0.0258	-0.16183620E 02	0.31486720E 04
120.00	4.8875	0.4099	0.30906860E 03	0.36850840E 04
140.00	5.0904	-0.1681	-0.14788720E 03	0.44777380E 04
250.00	5.2834	0.2309	0.36264250E 03	0.82992030E 04
300.00	5.6799	-0.0677	-0.12765770E 03	0.1070638CE 05
400.00	4.1645	0.7044	0.17702760E 04	0.10466440E 05
600.00	3.7494	0.3560	0.13419500E 04	0.14134760E 05
800.00	4.8700	0.2913	0.14642250E 04	0.24479340E 05

TABLE 13

Complex Viscosity Data and Results

The table contains information identified by the following symbols for each run:

FREQ   Frequency in cycles per second

SOL. 1   Solution level 1 in inches

VOLA 1   Output voltage in volts from accelerometer at solution level 1

VOLF 1   Output voltage in volts from force transducer at solution level 1

PHA 1   Phase angle in degrees at solution level 1

SOL. 2   Solution level 2 in inches

VOLA 2   Output voltage in volts from accelerometer at solution level 2

VOLF 2   Output voltage in volts from force transducer at solution level 2

PHA 2   Phase angle in degrees at solution level 2

CXV 1   Real part, η', of the complex viscosity

CXV 2   Imaginary part, η'', of the complex viscosity

CXM 1   Real part, G', of the complex modulus

CXM 2   Imaginary part, G'', of the complex modulus

RUN   7

SOL. L1= 1.00   SOL. L2= 2.50

FREQ	VOLA1	VOLF1	PHA1	VOLA2	VOLF2	PHA2
30.00	0.150	0.161	23.00	0.150	0.244	40.80
40.00	0.150	0.156	21.00	0.150	0.220	37.80
50.00	0.200	0.202	17.00	0.200	0.270	33.00
60.00	0.200	0.194	15.10	0.200	0.250	31.00
70.00	0.200	0.190	13.60	0.200	0.237	28.20
80.00	0.200	0.189	12.40	0.200	0.229	26.80
90.00	0.200	0.186	12.00	0.200	0.221	25.80
110.00	0.200	0.183	9.50	0.200	0.211	21.90
130.00	0.200	0.181	8.50	0.200	0.205	19.80
150.00	0.200	0.176	6.80	0.200	0.196	17.80
300.00	0.300	0.304	6.70	0.300	0.321	13.00
500.00	0.500	0.434	2.70	0.500	0.450	7.50
600.00	0.600	0.545	2.70	0.600	0.562	7.00
800.00	0.800	0.724	2.10	0.800	0.739	5.40
900.00	0.900	0.790	2.10	0.900	0.810	5.50

RUN   7

FREQ	CXV1	CXV2	CXM1	CXM2
30.00	6.2337	7.0627	0.13312950E 04	0.11750280E 04
40.00	5.2496	6.4106	0.16111500E 04	0.13193630E 04
50.00	4.8549	5.5029	0.17287990E 04	0.15252170E 04
60.00	4.2017	5.3637	0.20220610E 04	0.15840080E 04
70.00	3.7820	4.5813	0.20149490E 04	0.16633900E 04
80.00	3.2944	4.6896	0.23572400E 04	0.16559310E 04
90.00	2.9248	4.5044	0.25471590E 04	0.16539580E 04
110.00	2.7043	3.8646	0.26710050E 04	0.18690970E 04
130.00	2.5529	3.5141	0.28703750E 04	0.20852130E 04
150.00	2.3050	3.4492	0.32507650E 04	0.21724160E 04
300.00	1.7629	2.7248	0.51361950E 04	0.33229670E 04
500.00	1.2836	1.7338	0.54468350E 04	0.40323980E 04
600.00	1.2703	1.8280	0.68915150E 04	0.47887460E 04
800.00	0.8708	1.4108	0.70916870E 04	0.43772530E 04
900.00	1.2059	1.5391	0.87035740E 04	0.68191910E 04

RUN   8

SOL. L1= 1.00   SOL. L2= 2.50

FREQ	VOLA1	VOLF1	PHA1	VOLA2	VOLF2	PHA2
30.00	0.150	0.158	22.90	0.150	0.230	40.70
40.00	0.150	0.155	20.80	0.150	0.210	36.80
50.00	0.200	0.200	17.10	0.200	0.260	33.10
60.00	0.200	0.195	15.50	0.200	0.243	30.80
70.00	0.200	0.190	13.70	0.200	0.231	27.50
80.00	0.200	0.186	13.10	0.200	0.222	26.20
90.00	0.200	0.185	11.80	0.200	0.216	24.40
110.00	0.200	0.182	9.50	0.200	0.206	21.50
130.00	0.200	0.180	9.10	0.200	0.201	19.10
150.00	0.200	0.175	6.50	0.200	0.193	16.50
300.00	0.300	0.303	7.50	0.300	0.320	13.60
500.00	0.500	0.432	2.80	0.500	0.446	7.50
600.00	0.600	0.542	2.60	0.600	0.556	6.30
800.00	0.800	0.713	2.00	0.800	0.730	5.40
1000.00	1.000	0.860	1.00	1.000	0.870	4.00

RUN   8

FREQ	CXV1	CXV2	CXM1	CXM2
30.00	4.5977	6.3097	0.11893510E 04	0.86664470E 03
40.00	3.9542	5.3653	0.13484350E 04	0.99379100E 03
50.00	3.7454	5.2453	0.16478540E 04	0.11766360E 04
60.00	3.0527	4.8623	0.18330420E 04	0.11508500E 04
70.00	2.9620	4.0099	0.17636650E 04	0.13027500E 04
80.00	2.7230	3.7780	0.18990330F 04	0.13687430E 04
90.00	2.4414	3.6466	0.20621200E 04	0.13805780F 04
110.00	2.0553	3.5663	0.24648720E 04	0.14205140E 04
130.00	1.9994	2.7296	0.22295350E 04	0.16331170E 04
150.00	1.9833	2.7890	0.26285360F 04	0.18692310E 04
300.00	1.7081	2.6166	0.49322140F 04	0.32197010E 04
500.00	1.0736	1.7070	0.53626010E 04	0.33727380E 04
600.00	0.9191	1.3533	0.51018390E 04	0.34650810F 04
800.00	1.0509	1.4517	0.72972100E 04	0.52824020E 04
1000.00	0.4947	1.3669	0.85884290F 04	0.31083280E 04

RUN   9

SOL. L1= 1.00   SOL. L2= 2.50

FREQ	VOLA1	VOLF1	PHA1	VOLA2	VOLF2	PHA2
30.00	0.150	0.160	22.60	0.150	0.219	37.40
40.00	0.150	0.157	20.50	0.150	0.199	34.00
50.00	0.200	0.204	17.00	0.200	0.249	30.90
60.00	0.200	0.195	15.40	0.200	0.234	29.00
70.00	0.200	0.191	13.70	0.200	0.224	26.00
80.00	0.200	0.187	13.10	0.200	0.215	25.00
90.00	0.200	0.186	11.80	0.200	0.210	23.10
110.00	0.200	0.180	9.40	0.200	0.200	20.40
130.00	0.200	0.180	9.10	0.200	0.195	19.40
150.00	0.200	0.176	6.50	0.200	0.188	15.40
250.00	0.200	0.202	6.10	0.200	0.210	12.30
300.00	0.300	0.298	7.00	0.300	0.309	12.00
500.00	0.500	0.429	2.70	0.500	0.438	7.10
600.00	0.600	0.540	2.80	0.600	0.548	5.80
700.00	0.700	0.638	2.80	0.700	0.643	5.40
800.00	0.800	0.710	2.20	0.800	0.718	4.30
900.00	0.900	0.775	2.20	0.900	0.788	4.80

RUN   9

FREQ	CXV1	CXV2	CXM1	CXM2
30.00	3.5142	4.1404	0.78043890E 03	0.66241960E 03
40.00	2.5165	3.5521	0.89273550E 03	0.63246630E 03
50.00	2.2223	3.7796	0.11873800E 04	0.69815840E 03
60.00	2.1623	3.7088	0.13981930E 04	0.81517260E 03
70.00	2.0498	3.1381	0.13802010E 04	0.90154900E 03
80.00	1.7308	3.0704	0.15433250E 04	0.86997360E 03
90.00	1.5533	2.9110	0.16461450E 04	0.87834930E 03
110.00	1.5358	2.9475	0.20371870E 04	0.10614950E 04
130.00	1.1007	2.3740	0.19391060F 04	0.89907320E 03
150.00	1.0073	2.2606	0.21305910E 04	0.94931270E 03
250.00	0.8822	2.2924	0.36009480E 04	0.13857590E 04
300.00	0.8450	1.7260	0.32534070F 04	0.15926970E 04
500.00	0.5824	1.5626	0.49090930E 04	0.18297260E 04
600.00	0.3960	0.9434	0.35566250E 04	0.14927590E 04
700.00	0.1710	0.8546	0.37585010F 04	0.75225210E 03
800.00	0.3031	0.5824	0.29275560F 04	0.15235710E 04
900.00	0.6097	0.9297	0.52572890E 04	0.34477930E 04

RUN 10

SOL. L1= 1.00				SOL. L2= 2.50		
FREQ	VOLA1	VOLF1	PHA1	VOLA2	VOLF2	PHA2
30.00	0.150	0.149	11.00	0.150	0.180	22.50
40.00	0.150	0.148	9.40	0.150	0.173	19.50
50.00	0.200	0.194	8.50	0.200	0.220	17.80
60.00	0.200	0.188	8.50	0.200	0.210	17.10
70.00	0.200	0.184	7.50	0.200	0.203	15.40
80.00	0.200	0.183	6.60	0.200	0.200	14.00
90.00	0.200	0.180	6.00	0.200	0.196	12.80
110.00	0.200	0.176	5.40	0.200	0.190	11.70
130.00	0.200	0.177	4.70	0.200	0.189	10.40
150.00	0.200	0.174	4.40	0.200	0.185	9.50
250.00	0.200	0.200	4.30	0.200	0.209	8.40
300.00	0.300	0.300	4.10	0.300	0.309	7.70
400.00	0.400	0.330	2.50	0.400	0.340	6.20
500.00	0.500	0.429	2.90	0.500	0.441	5.60
600.00	0.600	0.540	1.80	0.600	0.552	4.35
700.00	0.700	0.631	1.70	0.700	0.640	3.50
800.00	0.800	0.715	1.50	0.800	0.718	3.20
900.00	0.900	0.785	1.10	0.900	0.800	3.00
1000.00	1.000	0.850	1.00	1.000	0.860	2.40

RUN 10

FRFQ	CXV1	CXV2	CXM1	CXM2
30.00	1.4888	1.1343	0.21380590E 03	0.28063960E 03
40.00	1.4033	1.0240	0.25735960E 03	0.35269260E 03
50.00	1.1692	1.0148	0.31880170E 03	0.36732610F 03
60.00	1.0374	0.9659	0.36414080E 03	0.39108050E 03
70.00	0.9574	0.8643	0.38013860E 03	0.42110300E 03
80.00	0.9248	0.8231	0.41375240E 03	0.46487840E 03
90.00	0.9242	0.7111	0.40210830E 03	0.52261320E 03
110.00	0.9016	0.6917	0.47810130E 03	0.62313910E 03
130.00	0.8335	0.6597	0.53887470E 03	0.68080830E 03
150.00	0.7969	0.5547	0.52283170E 03	0.75104190E 03
250.00	0.9793	0.8084	0.12697730F 04	0.15383220E 04
300.00	0.6397	0.8022	0.15120740F 04	0.17058710E 04
400.00	0.6402	0.7390	0.18572530E 04	0.16089440E 04
500.00	0.6139	0.4765	0.14969330E 04	0.19285120E 04
600.00	0.6106	0.5814	0.21916360E 04	0.23017850E 04
700.00	0.3238	0.3433	0.15098360F 04	0.14241700E 04
800.00	0.0782	0.3891	0.19557830E 04	0.39311130F 03
900.00	0.5763	0.3986	0.22542100E 04	0.32588890E 04
1000.00	0.2735	0.2484	0.15608840E 04	0.17187580E 04

RUN 11

SOL. L1= 1.00   SOL. L2= 2.50

FREQ	VOLA1	VOLF1	PHA1	VOLA2	VOLF2	PHA2
30.00	0.150	0.176	30.10	0.150	0.136	15.10
40.00	0.150	0.165	25.00	0.150	0.135	11.50
50.00	0.200	0.205	22.50	0.200	0.175	10.20
60.00	0.200	0.198	19.10	0.200	0.173	7.10
70.00	0.200	0.192	16.10	0.200	0.172	5.30
80.00	0.200	0.189	13.80	0.200	0.171	4.20
90.00	0.200	0.188	13.00	0.200	0.171	4.20
100.00	0.300	0.287	11.50	0.300	0.270	3.70
120.00	0.300	0.270	12.30	0.300	0.250	5.50
140.00	0.300	0.259	9.70	0.300	0.246	3.50
300.00	0.300	0.309	6.50	0.300	0.300	3.40

RUN 11

FREQ	CXV1	CXV2	CXM1	CXM2
30.00	2.2255	2.3633	0.44546750E 03	0.41949430E 03
40.00	1.9789	2.0571	0.51701680E 03	0.49734100E 03
50.00	1.5342	1.8441	0.57934860E 03	0.48199480E 03
60.00	1.5136	1.8605	0.70138200E 03	0.57061980E 03
70.00	1.3009	1.6102	0.70820330E 03	0.57216890E 03
80.00	1.2761	1.3427	0.67491670E 03	0.64141400E 03
90.00	1.2758	1.2313	0.69628320E 03	0.72147480E 03
100.00	0.7864	1.2092	0.75977270E 03	0.49408830E 03
120.00	1.0082	0.9067	0.68359930E 03	0.76017130E 03
140.00	0.6546	0.8486	0.74642400E 03	0.57579100E 03
300.00	0.6512	0.5991	0.11293210E 04	0.12274220E 04

RUN 12

SOL. L1= 1.00   SOL. L2= 2.50

FREQ	VOLA1	VOLF1	PHA1	VOLA2	VOLF2	PHA2
30.00	0.150	0.134	12.40	0.150	0.156	28.40
40.00	0.150	0.134	10.00	0.150	0.150	23.90
50.00	0.200	0.177	7.50	0.200	0.192	19.40
60.00	0.200	0.177	7.00	0.200	0.190	17.50
70.00	0.200	0.174	6.00	0.200	0.185	15.50
80.00	0.200	0.174	6.40	0.200	0.184	14.80
90.00	0.200	0.174	6.00	0.200	0.183	13.50
110.00	0.200	0.171	3.00	0.200	0.178	10.10
130.00	0.200	0.171	2.50	0.200	0.176	8.70
150.00	0.200	0.169	2.00	0.200	0.173	7.50

RUN 12

FRFQ	CXVl	CXV?	CXM1	CXM2
3C.CO	0.5996	2.1024	0.39628710E 03	0.11303040E C3
40.CO	0.5378	1.9118	0.48049140E 03	0.13515230E C3
50.00	0.4449	1.5810	C.49669580E 03	0.13975740E 03
6C.CO	0.4595	1.4430	0.54401220F 03	0.17323350F 03
7C.00	0.4455	1.2950	0.56955020E 03	0.19592330E 03
90.CO	0.4286	1.1494	0.57776290E 03	0.21545610E C3
90.00	0.4214	1.0135	C.57309740F 03	0.23828570F 03
110.CO	0.4272	1.0197	C.70479760E 03	0.29528580F C3
130.00	0.3046	0.9053	0.73947970E 03	C.24882910E 03
150.CO	0.2558	0.7934	0.74778540E C3	0.24109210E 03

RUN 13

SOL. L1= 1.00   SOL. L2= 2.50

FREQ	VOLA1	VOLF1	PHA1	VOLA2	VOLF2	PHA2
30.00	0.150	0.147	6.20	0.150	0.183	14.80
40.00	0.150	0.146	5.90	0.150	0.176	13.60
50.00	0.200	0.191	6.00	0.200	0.226	13.10
60.00	0.200	0.190	5.50	0.200	0.222	11.80
70.00	0.200	0.189	4.10	0.200	0.218	10.80
80.00	0.200	0.188	4.00	0.200	0.214	10.50
90.00	0.200	0.188	3.90	0.200	0.214	9.60
120.00	0.300	0.265	4.50	0.300	0.299	9.90
140.00	0.300	0.263	3.60	0.300	0.289	7.90

RUN 13

FREQ	CXV1	CXV2	CXM1	CXM2
30.00	1.7093	0.0046	0.85939190E 00	0.32219010E 03
40.00	1.6342	0.0337	0.84766600E 01	0.41072770E 03
50.00	1.5897	0.0566	0.17784720E 02	0.49942080E 03
60.00	1.5502	-0.0558	-0.21029460E 02	0.58441740E 03
70.00	1.6532	0.1071	0.47109710E 02	0.72712860E 03
80.00	1.5972	0.1979	0.99488580E 02	0.80283640E 03
90.00	1.6290	-0.0377	-0.21342360E 02	0.92116690E 03
120.00	1.6718	0.0137	0.10356030E 02	0.12605010E 04
140.00	1.1577	-0.0280	-0.24658460E 02	0.10183730E 04

RUN 14

SOL. L1= 1.50   SOL. L2= 2.50

FREQ	VOLA1	VOLF1	PHA1	VOLA2	VOLF2	PHA2
30.00	0.150	C.185	26.60	0.150	0.243	39.50
40.00	0.150	0.176	24.30	0.150	0.221	35.80
50.00	0.200	0.225	22.00	0.200	0.276	31.90
60.00	0.200	C.220	19.50	0.200	0.261	29.20
70.00	0.200	0.214	17.20	0.200	0.251	26.70
80.00	0.200	0.210	16.30	0.200	0.242	24.80
90.00	0.200	0.206	14.20	0.200	0.234	22.80
110.00	0.200	0.205	14.40	0.200	0.230	22.40
130.00	0.200	0.201	11.80	0.200	0.222	19.90
150.00	0.200	0.194	10.70	0.200	0.212	17.90
250.00	0.200	0.225	8.70	0.200	0.238	12.90
300.00	0.300	C.338	9.00	0.300	0.355	13.00
500.00	0.500	0.465	4.70	0.500	0.485	7.90
800.00	0.800	0.760	3.90	0.800	0.783	6.40
1000.00	1.000	0.903	3.40	1.000	0.930	5.70
1500.00	1.500	1.495	3.50	1.500	1.530	5.20

RUN 14

FREQ	CXV1	CXV2	CXM1	CXM2
30.00	6.4822	9.5284	0.17960610E 04	0.12218620E 04
40.00	5.8424	7.8474	0.19722770E 04	0.14683560E 04
50.00	6.0689	6.0020	0.18855870E 04	0.19065870E 04
60.00	5.0735	5.7222	0.21572000E 04	0.19126560E 04
70.00	5.2648	5.5251	0.24300550E 04	0.23155850E 04
80.00	4.7347	4.5525	0.22883180E 04	0.23799000E 04
90.00	4.4378	4.6789	0.26458430E 04	0.25095110E 04
110.00	4.3584	4.8350	0.33416790E 04	0.30122830E 04
130.00	4.1213	5.2046	0.42512070E 04	0.33663400E 04
150.00	3.7259	4.1755	0.39352840E 04	0.35115430E 04
250.00	3.5101	2.6178	0.41120850E 04	0.55135970E 04
300.00	3.3293	2.9795	0.56161830E 04	0.62755270E 04
500.00	2.9728	1.6201	0.50897810E 04	0.93394170E 04
800.00	2.7139	1.6711	0.83998000E 04	0.13641610E 05
1000.00	2.8575	1.4283	0.89744410E 04	0.17954110E 05
1500.00	3.0535	1.2839	0.12100560E 05	0.28778560E 05

RUN 15

SOL. L1= 0.70   SOL. L2= 1.70

FREQ	VOLA1	VOLF1	PHA1	VOLA2	VOLF2	PHA2
90.00	0.200	0.196	17.30	0.200	0.270	34.30
110.00	0.200	0.190	17.00	0.200	0.251	34.00
150.00	0.200	0.185	11.00	0.200	0.230	25.50
300.00	0.300	0.319	11.10	0.300	0.362	20.00
500.00	0.500	0.442	4.20	0.500	0.479	12.90
600.00	0.600	0.551	4.20	0.600	0.589	11.60
700.00	0.700	0.648	3.60	0.700	0.685	10.20
800.00	0.800	0.758	2.50	0.800	0.795	8.50
1000.00	1.000	0.912	1.90	1.000	0.950	7.10
1250.00	1.250	1.144	2.90	1.250	1.189	7.00
1500.00	1.500	1.470	1.20	1.500	1.510	5.00

RUN 15

FREQ	CXV1	CXV2	CXM1	CXM2
90.00	23.4061	26.1107	0.14765230E 05	0.13235830E 05
110.00	18.9930	27.5621	0.19049550E 05	0.13126980E 05
150.00	19.1666	19.5817	0.18455330E 05	0.19064060E 05
300.00	17.4171	16.2368	0.30605640E 05	0.32830420E 05
500.00	11.9636	14.6527	0.46032830E 05	0.37584770E 05
600.00	11.0233	13.7402	0.51799190E 05	0.41556780E 05
700.00	9.7562	12.6634	0.55696420E 05	0.42909940E 05
800.00	9.4427	12.1325	0.60984730E 05	0.47464380E 05
1000.00	8.3986	10.2244	0.64241520E 05	0.52769950E 05
1250.00	8.0786	7.6027	0.59711150E 05	0.63449020E 05
1500.00	7.1720	9.2257	0.86950560E 05	0.67594750E 05

RUN 16

SOL. L1= 1.00   SOL. L2= 2.00

FREQ	VOLA1	VOLF1	PHA1	VOLA2	VOLF2	PHA2
300.00	0.300	0.449	36.80	0.300	0.620	46.80
400.00	0.400	0.380	27.00	0.400	0.530	42.00
500.00	0.500	0.484	20.60	0.500	0.630	35.00
600.00	0.600	0.592	16.60	0.600	0.725	30.20
700.00	0.700	0.688	14.50	0.700	0.815	27.10
800.00	0.800	0.790	12.90	0.800	0.920	24.30
900.00	0.900	0.840	14.10	0.900	0.975	25.00
1000.00	1.000	0.960	10.60	1.000	1.070	21.00
1500.00	1.500	1.500	10.40	1.500	1.630	19.20

RUN 16

FREQ	CXV1	CXV2	CXM1	CXM2
300.00	135.8928	167.5209	0.31576920E 06	0.25615170E 06
400.00	86.4151	129.2220	0.32476990E 06	0.21718460CE 06
500.00	82.6639	111.6910	0.35088730E 06	0.25969600F 06
600.00	66.3233	99.3619	0.37458520E 06	0.2500326CE 06
700.00	58.0120	88.4534	0.38903780E 06	0.25514950E 06
800.00	59.3848	77.7000	0.39056230E 06	0.29850010E 06
900.00	54.5589	72.9837	0.41271270F 06	0.30852260E 06
1000.00	39.2811	68.2007	0.42851700E 06	0.24681010F 06
1500.00	38.8428	75.8445	0.71481730E 06	0.36608450F 06

RUN 17

SOL. L1= 1.00   SOL. L2= 2.50

FREQ	VOLA1	VOLF1	PHA1	VOLA2	VOLF2	PHA2
30.00	0.150	0.149	7.00	0.150	0.179	14.60
40.00	0.150	0.150	6.70	0.150	0.176	13.00
50.00	0.200	0.195	5.50	0.200	0.226	11.90
60.00	0.200	0.193	5.00	0.200	0.216	11.40
70.00	0.200	0.186	5.00	0.200	0.211	10.30
80.00	0.200	0.186	4.50	0.200	0.209	10.10
90.00	0.200	0.186	4.50	0.200	0.206	9.70
110.00	0.200	0.179	1.80	0.200	0.200	6.80
130.00	0.200	0.182	3.80	0.200	0.200	8.10
150.00	0.200	0.177	3.30	0.200	0.192	7.80

RUN 17

FREQ	CXV1	CXV2	CXM1		CXM2	
30.00	1.2631	0.0789	0.14868420E	02	0.23809080E	03
40.00	1.2264	-0.0232	-0.58425140E	01	0.30823070E	03
50.00	1.3087	0.0415	0.13042320E	02	0.41113030E	03
60.00	1.0483	0.3019	0.11381710E	03	0.39519040E	03
70.00	1.1651	-0.0421	-0.1851298OE	02	0.51243940E	03
80.00	1.2443	0.1014	0.50947540E	02	0.62547680E	03
90.00	1.1067	0.1465	0.82842360E	02	0.62581270E	03
110.00	1.3557	-0.1168	-0.80754250E	02	0.93701020E	03
130.00	1.1920	-0.0210	-0.17154370E	02	0.97365720E	03
150.00	1.1157	0.1797	0.16936910E	03	0.10515510E	04

RUN 18

SOL. L1= 1.00   SOL. L2= 2.50

FREQ	VOLA1	VOLF1	PHA1	VOLA2	VOLF2	PHA2
30.00	0.150	0.155	11.30	0.150	0.202	23.70
40.00	0.150	0.151	11.20	0.150	0.192	22.50
50.00	0.200	0.196	10.10	0.200	0.246	20.90
60.00	0.200	0.195	9.00	0.200	0.240	19.50
70.00	0.200	0.194	8.30	0.200	0.235	18.20
80.00	0.200	0.192	8.20	0.200	0.230	17.40
90.00	0.200	0.189	8.00	0.200	0.225	17.00
110.00	0.200	0.190	7.30	0.200	0.221	16.20
130.00	0.200	0.190	6.20	0.200	0.217	14.40
150.00	0.200	0.182	6.00	0.200	0.208	13.30
250.00	0.200	0.216	8.40	0.200	0.237	15.00
500.00	0.500	0.445	3.40	0.500	0.478	7.70
600.00	0.600	0.550	3.30	0.600	0.585	7.00
700.00	0.700	0.650	3.10	0.700	0.688	6.60
800.00	0.800	0.742	2.50	0.800	0.780	5.90
1000.00	1.000	0.898	1.50	1.000	0.921	4.50
1250.00	1.250	1.130	1.25	1.250	1.160	3.90
1500.00	1.500	1.410	0.90	1.500	1.440	4.10

RUN 1R

FREQ	CXV1	CXV2	CXM1	CXM2
30.00	3.2658	1.4579	0.27480270E 03	0.61559320F 03
40.00	3.3570	1.4198	0.35684270F 03	0.84370990E 03
50.00	3.5950	1.3632	0.42824650E 03	0.11293890E 04
60.00	3.6588	1.4579	0.54962150E 03	0.13793430E 04
70.00	3.6319	1.3845	0.60895360F 03	0.15974100F 04
80.00	3.5628	1.2380	0.62231000E 03	0.17908440E 04
90.00	3.6370	1.2733	0.72002000E 03	0.20566560E 04
110.00	3.5841	1.6936	0.11705460E 04	0.24771190E 04
130.00	3.3836	1.5802	0.12906990E 04	0.27637990E 04
150.00	3.3846	1.0202	0.96152680E 03	0.31898760E 04
250.00	4.1479	2.9918	0.46995270E 04	0.65154760E 04
500.00	3.2447	0.8028	0.25219890E 04	0.10193440E 05
600.00	3.0467	0.7008	0.26421280E 04	0.11485730E 05
700.00	3.1548	0.7796	0.34290180E 04	0.13875600E 05
800.00	3.0207	0.9965	0.50088320E 04	0.15183690E 05
1000.00	1.4588	1.4311	0.89920540E 04	0.91660070E 04
1250.00	1.7499	1.2758	0.10020480E 05	0.13743370E 05
1500.00	2.0860	2.8401	0.26767420E 05	0.19660100E 05

RUN 19

SOL. L1= 0.50   SOL. L2= 1.50

FREQ	VOLA1	VOLF1	PHA1	VOLA2	VOLF2	PHA2
90.00	0.200	0.186	6.50	0.200	0.246	22.60
110.00	0.200	0.189	7.70	0.200	0.241	21.00
130.00	0.200	0.187	6.10	0.200	0.236	20.00
150.00	0.200	0.183	5.20	0.200	0.225	18.40
250.00	0.200	0.216	6.10	0.200	0.250	16.00
500.00	0.500	0.441	2.60	0.500	0.483	10.20
600.00	0.600	0.550	2.50	0.600	0.595	9.00
700.00	0.700	0.640	2.40	0.700	0.684	8.30
900.00	0.800	0.748	2.00	0.800	0.798	7.60
1000.00	1.000	0.890	1.20	1.000	0.940	6.50
1250.00	1.250	1.125	1.60	1.250	1.175	5.90
1500.00	1.500	1.421	3.90	1.500	1.480	7.70

RUN 19

FREQ	CXV1	CXV2	CXM1	CXM2
90.00	23.1443	13.4374	0.75986830E 04	0.13087800E 05
110.00	20.9398	10.4883	0.72489960E 04	0.14472550E 05
130.00	23.4428	13.0051	0.10622770E 05	0.19148390E 05
150.00	21.1087	12.3256	0.11616550E 05	0.19894470E 05
250.00	24.2724	15.0948	0.23710870E 05	0.38127010E 05
500.00	15.0999	10.1960	0.32031530E 05	0.47437590E 05
600.00	14.5540	9.1384	0.34450810E 05	0.54867420E 05
700.00	12.7174	8.9264	0.39260500E 05	0.55933900E 05
800.00	14.2747	9.1462	0.45973700E 05	0.71752500E 05
1000.00	12.9236	9.5207	0.59820410E 05	0.80572810E 05
1250.00	10.4600	7.9838	0.62704600E 05	0.82152810E 05
1500.00	10.9752	8.7545	0.82508870E 05	0.10343900E 06

TABLE 14

Amplitude Dependence Data and Results

The table contains information identified by the following symbols for each run:

FREQ   Frequency in cycles per second

SOL. 1   Solution level 1 in inches

VOLA 1   Output voltage in volts from accelerometer at solution level 1

VOLF 1   Output voltage in volts from force transducer at solution level 1

PHA 1   Phase angle in degrees at solution level 1

SOL. 2   Solution level 2 in inches

VOLA 2   Output voltage in volts from accelerometer at solution level 2

VOLF 2   Output voltage in volts from force transducer at solution level 2

PHA 2   Phase angle in degrees at solution level 2

CXV 1   Real part, η', of the complex viscosity

CXV 2   Imaginary part, η'', of the complex modulus

CXM 1   Real part, G', of the complex modulus

CXM 2   Imaginary part, G'', of the complex modulus

RUN 20

SOL. L1 = 1.00   SOL. L2= 2.50

FREQ	VOLA1	VOLF1	PHA1	VOLA2	VOLF2	PHA2
30.00	0.150	0.161	20.20	0.150	0.233	38.10
40.00	0.150	0.156	18.00	0.150	0.212	35.30
50.00	0.150	0.151	16.00	0.150	0.196	31.60
60.00	0.150	0.147	14.00	0.150	0.184	29.00
70.00	0.150	0.143	12.60	0.150	0.175	27.30
80.00	0.150	0.141	11.50	0.150	0.169	25.00
90.00	0.150	0.140	10.30	0.150	0.165	23.20
110.00	0.150	0.139	9.00	0.150	0.159	19.90
130.00	0.150	0.135	8.00	0.150	0.151	18.00
150.00	0.150	0.132	7.70	0.150	0.146	17.20

RUN 20

FREQ	CXV1	CXV2	CXM1	CXM2
30.00	4.6294	5.4802	0.10330010E 04	0.87261910E 03
40.00	3.9754	5.3301	0.13395890E 04	0.99912010E 03
50.00	3.6099	4.4161	0.13873530E 04	0.11340810E 04
60.00	3.1948	4.1384	0.15601330E 04	0.12043970E 04
70.00	2.9725	4.0887	0.17982920E 04	0.13073880E 04
80.00	2.8190	3.5827	0.18008670E 04	0.14169950E 04
90.00	2.7152	3.4272	0.19380580E 04	0.15353830E 04
110.00	2.3604	2.6823	0.18538420E 04	0.16314220E 04
130.00	1.9507	2.3924	0.19541330E 04	0.15933900E 04
150.00	1.7963	2.3379	0.22034040E 04	0.16929910E 04

RUN 21

SOL. L1= 1.00   SOL. L2= 2.50

FREQ	VOLA1	VOLF1	PHA1	VOLA2	VOLF2	PHA2
30.00	0.200	0.216	20.20	0.200	0.312	37.80
40.00	0.200	0.209	18.00	0.200	0.282	35.10
50.00	0.200	0.202	16.00	0.200	0.262	32.60
60.00	0.200	0.196	14.00	0.200	0.245	28.90
70.00	0.200	0.192	12.60	0.200	0.233	27.20
80.00	0.200	0.188	11.50	0.200	0.225	24.90
90.00	0.200	0.187	10.00	0.200	0.220	23.10
110.00	0.200	0.185	9.00	0.200	0.212	19.80
130.00	0.200	0.180	8.00	0.200	0.202	17.90
150.00	0.200	0.176	7.70	0.200	0.195	17.10

RUN 21

FREQ	CXV1	CXV2	CXM1	CXM2
30.00	4.6786	5.3491	0.10082780E 04	0.88190400E 03
40.00	3.8048	5.1869	0.13036140E 04	0.95624680E 03
50.00	3.4625	5.0366	0.15822980E 04	0.10877700E 04
60.00	3.1598	4.0723	0.15352020E 04	0.11912240E 04
70.00	2.7412	4.0388	0.17763620E 04	0.12056200E 04
80.00	2.7757	3.5196	0.17691380E 04	0.13951960E 04
90.00	2.6915	3.5260	0.19938890E 04	0.15220290E 04
110.00	2.4097	2.6143	0.18068800E 04	0.16654830E 04
130.00	2.0531	2.3333	0.19058440E 04	0.16769680E 04
150.00	1.8490	2.2802	0.21490520E 04	0.17426720E 04

RUN 22

SOL. L1= 1.00   SOL. L2= 2.50

FREQ	VOLA1	VOLF1	PHA1	VOLA2	VOLF2	PHA2
30.00	0.250	0.271	20.20	0.250	0.391	37.40
40.00	0.250	0.260	18.10	0.250	0.355	34.60
50.00	0.250	0.252	16.30	0.250	0.326	32.00
60.00	0.250	0.245	14.00	0.250	0.307	28.90
70.00	0.250	0.239	12.60	0.250	0.292	27.10
80.00	0.250	0.235	11.50	0.250	0.281	24.90
90.00	0.250	0.233	10.30	0.250	0.275	23.10
110.00	0.250	0.232	9.00	0.250	0.265	20.20
130.00	0.250	0.226	8.00	0.250	0.254	17.90
150.00	0.250	0.220	7.70	0.250	0.243	17.10

RUN 22

FREQ	CXV1	CXV2	CXM1	CXM2
30.00	4.7458	5.1389	0.96865500E 03	0.8945534CE 03
40.C0	4.2545	4.9070	C.12332650E 04	0.10692610E C4
50.00	3.4465	4.4981	0.14131210E 04	0.10827410E 04
60.00	3.2413	4.0864	0.15405280E 04	0.1221931CE C4
70.00	2.9522	3.9846	0.17525370E 04	0.12984360E 04
80.00	2.7463	3.5166	0.17676280E 04	0.13804250E C4
90.00	2.7597	3.3614	0.19008200E 04	0.15605920E 04
110.00	2.3197	2.8635	C.19791170E 04	0.16032530E C4
130.00	2.1191	2.3516	C.19208200E 04	0.17308710E C4
150.00	1.7512	2.2837	0.21523200E 04	0.16504990E C4

RUN 23

SOL. L1= 1.00   SOL. L2= 2.50

FREQ	VOLA1	VOLF1	PHA1	VOLA2	VOLF2	PHA2
30.00	0.300	0.324	24.20	0.300	0.470	39.30
40.00	0.300	0.315	18.00	0.300	0.423	34.30
50.00	0.300	0.302	16.00	0.300	0.392	31.20
60.00	0.300	0.294	14.00	0.300	0.368	28.90
70.00	0.300	0.285	12.60	0.300	0.350	27.10
80.00	0.300	0.282	11.50	0.300	0.338	24.80
90.00	0.300	0.280	10.30	0.300	0.330	23.00
110.00	0.300	0.274	9.00	0.300	0.318	20.70
130.00	0.300	0.272	8.60	0.300	0.304	17.90
150.00	0.300	0.264	7.70	0.300	0.292	17.10

RUN 23

FREQ	CXV1	CXV2	CXM1	CXM2
30.00	4.5737	4.5846	0.86416910E 03	0.86211690E 03
40.00	3.8146	4.7209	C.11864960E 04	0.95870670E 03
5C.00	3.6567	4.1816	0.13136870E 04	0.11487900E 04
6C.00	3.2050	4.0801	0.15381740E 04	0.12082540E 04
70.00	3.0879	3.9605	0.17419280E 04	0.13581350E 04
80.00	2.8303	3.4665	0.17424290E 04	0.14226560E 04
90.00	2.7227	3.3091	C.18712330E 04	0.15396270E 04
110.00	2.7778	2.7657	C.19114830E 04	0.19198840E 04
130.00	1.9533	2.3732	C.19384620E 04	0.15954710E 04
150.00	1.7946	2.2823	0.21510250E 04	0.16913650E 04

RUN 24

SOL. L1= 1.00   SOL. L2= 2.50

FREQ	VOLA1	VOLF1	PHA1	VOLA2	VOLF2	PHA2
30.00	0.400	0.429	25.80	0.400	0.620	40.10
40.00	0.400	0.420	18.20	0.400	0.565	34.10
50.00	0.400	0.403	16.00	0.400	0.521	31.00
60.00	0.400	0.392	14.00	0.400	0.490	28.90
70.00	0.400	0.382	12.60	0.400	0.466	27.10
80.00	0.400	0.376	11.50	0.400	0.450	24.80
90.00	0.400	0.374	10.30	0.400	0.439	23.00
110.00	0.400	0.370	9.00	0.400	0.425	20.00
130.00	0.400	0.361	8.00	0.400	0.405	17.80
150.00	0.400	0.352	7.70	0.400	0.390	17.20

RUN 24

FREQ	CXV1	CXV2	CXM1	CXM2
30.00	4.2935	4.2879	0.80825360E 03	0.80741520E 03
40.00	3.9000	4.5313	0.11388310E 04	0.98018110E 03
50.00	3.5508	4.0480	0.12717230E 04	0.11155190E 04
60.00	3.1598	4.0723	0.15352000E 04	0.11912230E 04
70.00	2.8950	3.9683	0.17453440E 04	0.12732960E 04
80.00	2.7813	3.4619	0.17401450E 04	0.13980310E 04
90.00	2.5962	3.3123	0.18730510E 04	0.14680980E 04
110.00	2.4904	2.7280	0.18854560E 04	0.17212550E 04
130.00	2.0520	2.2914	0.18716320E 04	0.16761350E 04
150.00	1.8512	2.3362	0.22017880E 04	0.17447300E 04

RUN 25

SOL. L1= 1.00   SOL. L2= 2.50

FREQ	VOLA1	VOLF1	PHA1	VOLA2	VOLF2	PHA2
40.00	0.500	0.525	18.00	0.500	0.705	34.00
50.00	0.500	0.504	16.00	0.500	0.649	31.00
60.00	0.500	0.490	14.20	0.500	0.614	28.80
70.00	0.500	0.476	12.60	0.500	0.584	27.10
80.00	0.500	0.471	11.50	0.500	0.564	24.80
90.00	0.500	0.469	10.30	0.500	0.550	22.90
110.00	0.500	0.464	9.00	0.500	0.530	19.90
130.00	0.500	0.451	8.00	0.500	0.505	17.80
150.00	0.500	0.440	7.70	0.500	0.485	17.00

RUN 25

FREQ	CXV1	CXV2	CXM1	CXM2
40.00	3.8589	4.5476	0.11429230E 04	0.96984470E 03
50.00	3.4252	4.0279	0.12654000E 04	0.10760640E 04
60.00	3.2421	3.9347	0.14833320E 04	0.12222320E 04
70.00	3.0684	3.9725	0.17472070E 04	0.13495330E 04
80.00	2.8110	3.4783	0.17484010E 04	0.14129530E 04
90.00	2.5858	3.2733	0.18509790E 04	0.14622440E 04
110.00	2.3200	2.6905	0.18595450E 04	0.16034760E 04
130.00	1.9395	2.2919	0.18720560E 04	0.16250280E 04
150.00	1.6853	2.2309	0.21025430E 04	0.15883260E 04

RUN 26

SOL. L1= 1.00   SOL. L2= 2.50

FREQ	VOLA1	VOLF1	PHA1	VOLA2	VOLF2	PHA2
40.00	0.600	0.630	22.00	0.600	0.845	37.10
50.00	0.600	0.604	16.60	0.600	0.778	31.60
60.00	0.600	0.586	14.30	0.600	0.731	28.70
70.00	0.600	0.572	12.80	0.600	0.695	27.00
80.00	0.600	0.565	11.60	0.600	0.675	24.70
90.00	0.600	0.558	10.30	0.600	0.660	22.90
110.00	0.600	0.555	9.00	0.600	0.636	19.80
130.00	0.600	0.542	8.00	0.600	0.607	17.80
150.00	0.600	0.527	7.70	0.600	0.584	17.00

RUN 26

FREQ	CXV1	CXV2	CXM1	CXM2
40.00	3.3348	4.5331	0.11392910E 04	0.83812790E 03
50.00	3.3408	4.0899	0.12848890E 04	0.10495440E 04
60.00	3.0786	3.7820	0.14257700E 04	0.11605860E 04
70.00	2.7543	3.7817	0.16632940E 04	0.12113830E 04
80.00	2.7317	3.3638	0.16908240E 04	0.13730760E 04
90.00	2.8264	3.2327	0.18280370E 04	0.15982730E 04
110.00	2.4097	2.6143	0.18068800E 04	0.16654830E 04
130.00	2.0008	2.2984	0.18773780E 04	0.16342770E 04
150.00	1.8453	2.2160	0.20885070E 04	0.17391850E 04

RUN 27

SOL. L1= 1.00   SOL. L2= 2.50

FREQ	VOLA1	VOLF1	PHA1	VOLA2	VOLF2	PHA2
40.00	0.800	0.844	23.80	0.800	1.120	37.90
50.00	0.800	0.805	16.60	0.800	1.020	31.50
60.00	0.800	0.780	14.30	0.800	0.965	28.70
70.00	0.800	0.765	12.80	0.800	0.930	27.00
80.00	0.800	0.751	11.60	0.800	0.900	24.70
90.00	0.800	0.746	10.30	0.800	0.880	22.90
110.00	0.800	0.740	9.00	0.800	0.847	19.60
130.00	0.800	0.722	8.00	0.800	0.809	17.70
150.00	0.800	0.705	7.70	0.800	0.776	17.00

RUN 27

FREQ	CXV1	CXV2	CXM1	CXM2
40.00	2.9564	4.1291	0.10377670E 04	0.74303540E 03
50.00	2.8385	3.9165	0.12304000E 04	0.89173090E 03
60.00	2.8076	3.7248	0.14042010E 04	0.10584380E 04
70.00	2.7886	3.8077	0.16746930E 04	0.12264880E 04
80.00	2.8159	3.3517	0.16847410E 04	0.14154020E 04
90.00	2.7509	3.2461	0.18356080E 04	0.15556110E 04
110.00	2.3678	2.5022	0.17294110E 04	0.16365020E 04
130.00	2.0102	2.2387	0.18286320E 04	0.16419740E 04
150.00	1.6460	2.2382	0.21094970E 04	0.15513480E 04

RUN 28

SOL. L1= 1.00   SOL. L2= 2.50

FREQ	VOLA1	VOLF1	PHA1	VOLA2	VOLF2	PHA2
50.00	1.000	1.010	16.60	1.000	1.280	31.70
60.00	1.000	0.975	14.00	1.000	1.220	28.70
70.00	1.000	0.952	12.80	1.000	1.170	27.50
80.00	1.000	0.945	11.70	1.000	1.120	24.70
90.00	1.000	0.935	11.30	1.000	1.100	23.20
110.00	1.000	0.926	9.00	1.000	1.060	19.30
130.00	1.000	0.905	7.90	1.000	1.010	17.70
150.00	1.000	0.880	7.20	1.000	0.975	16.20

RUN 28

FRFQ	CXV1	CXV2	CXM1	CXM2
50.00	2.8393	4.0534	0.12734050E 04	0.89199950E 03
60.00	3.1806	3.9220	0.14785740E 04	0.11990520E 04
70.00	3.0302	4.1218	0.18128480E 04	0.13547360E 04
80.00	2.4873	3.3148	0.16661900E 04	0.12502740E 04
90.00	2.5377	2.9494	0.16678360E 04	0.14633220E 04
110.00	2.3481	2.3402	0.16174370E 04	0.16367430E 04
130.00	1.9068	2.3047	0.18824980E 04	0.15575280E 04
150.00	1.8722	2.0284	0.19117390E 04	0.17644750E 04

NOMENCLATURE

<u>Symbol</u>

A - contact area between the driving plate and solution

A - area of sensing surfaces for capacitance transducer

a - separation between surfaces for capacitance transducer

a_T - ratio of relaxation times at two different temperatures

B - constant in equation 16

B - flux density of the magnetic field

B - rate of shear factor

C - capacitance

C_0 - reference value of capacitance

C'- change in capacitance relative to C_0

$\bar{\bar{C}}$ - deformation tensor

C - concentration in g/cc

c - shift factor in equations 22, 23

D - rate of shear

F - force

f - frequency

G^*- complex shear modulus

G'- storage modulus

G"- loss modulus

h_1- contact length 1

h_2- contact length 2

Symbol

K - calibration constant for accelerometer

K_a - constant for accelerometer

K_d - calibration constant for the capacitive transducer

K_f - calibration constant for the force transducer

L - length of wire in coil

L - dimension of apparatus

M - molecular weight

m - mass

p - integer

R - ideal gas constant

R - real part of the total impedance

R_e - real part of the electrical impedance

R_o - real part of the electrical impedance when coil is firmly clamped

R_r - real part of the characteristic impedance

S - scale reading from the Haake Rotovisco

T - absolute temperature

T_o - reference temperature

U - speed factor for Haake Rotovisco

V - velocity

V_o - imposed velocity

V_a - output voltage from the accelerometer

V_d - output voltage from the capacitive transducer

V_f - output voltage from the force transducer

Symbol

W - width of the driving plate

X - imaginary part of the total impedance

X - displacement of the driving plate

X_o - imaginary part of the electrical impedance when coil

is firmly clamped

X_o - maximum amplitude of the displacement

X_e - imaginary part of the electrical impedance

X_r - imaginary part of the characteristic impedance

Z - total impedance

Z_e - electrical impedance

Z_r - characteristic impedance

α - constant in equation 11

β - constant in equation 16

γ - strain

γ_o - maximum strain

$\bar{\bar{\gamma}}$ - rate of deformation tensor

$\dot{\gamma}$ - strain rate

ϵ - dielectrical constant

η^* - complex viscosity

η' - real part of the complex viscosity

η'' - imaginary part of the complex viscosity

η_o - steady state viscosity

η_s - viscosity of the solvent

η_∞ - limiting viscosity at very high shear rate

Symbol

θ - phase angle

θ - relaxation time function in equation 24

λ - wave length

λ - constant in equation 11

λ_p - relaxation times

μ_1 - scalar function of time

ρ - density

τ - stress

$\bar{\bar{\tau}}$ - stress tensor

τ_1 - relaxation time corresponding to the first mode of
relaxation for the Zimm or Rouse model

ϕ - phase angle

ψ_{12} - normal stress coefficient

$\psi_{12}^{(o)}$ - zero shear normal stress coefficient

ω - frequency in rad/sec

$\mathcal{H}$ - convected derivative given by Spriggs